2008

Disruption of 8-hydroxy-2'-deoxyguanosine DNA Glycosylase (OGG1) Antioxidant Response Capacity by Sodium Arsenite

David Paul Cox
The University of Montana

DISRUPTION OF 8-HYDROXY-2'-DEOXYGUANOSINE DNA GLYCOSYLASE (OGG1) ANTIOXIDANT RESPONSE CAPACITY BY SODIUM ARSENITE

By

David Paul Cox

B.S. Biology, Central Washington University, Ellensburg, WA 2002

Dissertation

presented in partial fulfillment of the requirements
for the degree of

Doctor of Philosophy
in Toxicology

The University of Montana
Missoula, Montana

Summer 2007

Approved by:

Dr. David A. Strobel, Dean
Graduate School

Fernando Cardozo-Pelaez, Ph.D., Chairperson
Department of Biomedical and Pharmaceutical Sciences

Douglas Coffin, Ph.D.
Department of Biomedical and Pharmaceutical Sciences

Elizabeth Putnam, Ph.D.
Department of Biomedical and Pharmaceutical Sciences

Diana Lurie, Ph.D.
Department of Biomedical and Pharmaceutical Sciences

Kent Sugden, Ph.D.
Department of Chemistry

David Paul Cox Ph.D. 2007 Toxicology

Disruption of 8-hydroxy-2'-deoxyguanosine DNA Glycosylase (Ogg1) Antioxidant Response Capacity by Sodium Arsenite

Chairperson: Fernando Cardozo-Pelaez, Ph.D.

8-hydroxy-2'-deoxyguanosine DNA glycosylase is the first step and rate-limiting enzyme involved in the removal of 8-hydroxy-2'-deoxyguanosine via the base excision repair pathway. Transcriptional regulation of human Ogg1 is sensitive to redox changes via modulation of intracellular glutathione. In response to changes in glutathione, changes in hOgg1 transcription occur similar to genes regulated by the transcription factor Nrf2. It was determined that positions – 47 to – 44 in the hOgg1 promoter are necessary for basal transcription of Ogg1 determined by site-directed deletion. This region is capable of interacting with nuclear protein determined by binding assays. Furthermore, transcription factor Nrf2 is identified as binding to this region determined by parallel, and competition EMSA binding assays. Exposure to arsenic has also been associated with oxidative stress and damage to DNA, specifically oxo^{8}dG. This study identified significant increases in the cellular antioxidant glutathione, and alterations in superoxide dismutase activities subsequent to arsenite exposure in actively dividing and NGF treated PC12 cells. Assessment of Ogg1 activity and mRNA levels demonstrated a significant decrease for both measures subsequent to arsenite exposure. The effect seen was due in large part to alterations in gene transcription since direct testing revealed no effect by arsenite on Ogg1 activity. Levels of oxo^{8}dG did not significantly change subsequent to arsenite exposure, however increased trends were evident. Characterization of Sp1 binding revealed that treatment with sodium arsenite could decrease Sp1 binding at two unique Sp1 sites in the human Ogg1 promoter. In summary, transcription factor Nrf2 is an important factor in the inducible regulation of Ogg1. Transcriptional changes in Ogg1 are further dependent on the redox status of the cell. Despite the role of Nrf2 in response to oxidative stress, sodium arsenite disrupted both the transcription and activity of Ogg1 in PC12 cells. This disruption occurred despite the induction of cellular stress response via increases in GSH and Mn SOD activity. This suggests that arsenite is acting through other mechanisms potentially through disruption of the Sp1 transcription factor.

ACKNOWLEDGEMENTS

To my sons, James Patrick David and Rhiver David Cox, for their sacrifice and patience with their dad during my tenure at the University of Montana. My hopes and desires are that this degree, and life experience will provide them with bigger and better opportunities during their lives.

Foremost, I would like to thank the Center for Environmental Health Sciences and the Department of Biomedical and Pharmaceutical Sciences for providing me the educational opportunity and resources to complete this degree.

I would like to further thank the members of my dissertation committee for their input and efforts: Drs. Cardozo-Pelaez, Coffin, Lurie, Putnam and Sugden.

TABLE OF CONTENTS

LIST OF FIGURES

LIST OF TABLES

CHAPTER ONE

Introduction and Relevant Background

Redox Balance and Oxidative Stress

Maintenance of the cellular environment is one of the fundamental requirements for normal cellular physiology. Proper homeostasis of the cell's internal and external environment is essential for cell growth, proliferation and survival. Homeostasis is accomplished by robust and redundant balances of numerous components of the cell including but not limited to structural integrity, energy levels, nutrient/waste exchange, and the cellular redox state. Deficiencies in any of these can have detrimental effects on cell function or survival. However, redox alterations appear to be a convergent pathway associated with numerous pathologies. Redox state is simply defined as the balance of oxidants to reductants in the cellular environment and when that balance is disrupted conditions can shift to more oxidizing conditions. When this shift in redox balance leads to cellular dysfunction, it is referred to as oxidative stress (Halliwell 1999).

Oxidative stress can occur as a result of a variety of conditions ranging from exposure to toxic substances, xenobiotic metabolism, inflammatory response and alterations in normal cellular processes such as ATP synthesis. Cellular systems exist to prevent and reduce the impact of these conditions via different protective mechanisms. Some effects of oxidative stress can involve oxidation of important cellular macromolecules such as proteins, lipids, and DNA. In some instances damaged cellular macromolecules undergo a process of turnover where the oxidized components are broken down, eliminated, and replaced by newly synthesized components. In other

situations the cell needs to repair the damaged element due to the element having a more fixed or stable function in cellular organization.

Sources of cellular oxidation

As stated previously there are many potential sources for free radical production. This discussion will be limited to endogenously produced free radicals and some of the pathways capable of generating them. Antioxidant defenses are mentioned, however they will be covered in greater detail in the following section.

Superoxide anion is one of the major reactive oxygen species present in cellular systems. It is produced as a result of both normal and abnormal cellular processes. In mitochondria, it is produced as a byproduct of cellular respiration. This is facilitated by the single electron reduction of molecular oxygen by distinct components of the electron transport chain; a process that can be exacerbated by changes in the mitochondrial redox state and/or changes in endogenous defense systems (Giulivi, Boveris et al. 1995; Halliwell 1999; Cadenas and Davies 2000). In mitochondria, manganese superoxide dismutase (discussed later) readily converts superoxide to the less reactive H_2O_2, which is converted to H_2O and molecular oxygen via the activities of catalase and/or glutathione peroxidase (Gpx) (Fridovich 1995). However, under unique conditions, such as in the presence of transition metals, H_2O_2 can undergo a single electron reduction to produce hydroxyl radical.

Hydroxyl radical formation was first characterized as the Haber-Weiss reaction where it was described as the reaction of superoxide with H_2O_2 to produce hydroxyl radical (Haber 1934). It has since been adapted to biological systems as the Fenton reaction. The Fenton reaction is similar to the Haber-Weiss reaction in that it describes

the same single electron reduction of H_2O_2. The key difference is that the Fenton reaction occurs in the presence of a transition metal such as Cu^{+} or Fe^{2+} that is acting as the electron source instead of superoxide (Kehrer 2000). Due to the presence of intracellular reducing equivalents such as ascorbate, the transition metal can be readily oxidized and reduced allowing it to participate in the reaction multiple times.

Fenton Reaction: $Fe^{2+} + H_2O_2 \rightarrow Fe^{3+} + OH\bullet + OH^-$

Hydroxyl radical is considered the most detrimental free radical produced in biological systems because of its ability to react with and oxidize most cellular components. The ability of hydroxyl radical to damage cellular macromolecules is limited to the high reactivity and regional production limiting its effective range of damage to its immediate area of production. Included in the list of macromolecules that hydroxyl radical can damage are lipids, proteins and DNA; hydroxyl radical formation is therefore the focus of numerous studies (Halliwell 1999). Despite the large number of macromolecules that are targets of oxidative damage by free radicals, damage to DNA appears to be more detrimental to cellular function and will be discussed later in greater detail.

Antioxidant Defense

Cells have evolved concerted mechanisms to reduce hydroxyl radical formation. Integral components of cellular defense are antioxidant molecules and enzymes whose purpose is to react with, and remove different oxidative moieties like reactive oxygen species (ROS) and reactive nitrogen species (RNS); both commonly referred to as free radical compounds.

Molecules capable of directly interacting with, and negating free radicals, mainly via one-electron transfer, are a part of endogenous antioxidant systems. The antioxidant

glutathione (GSH) is composed of the amino acids L-glutamate, L-cysteine and L-glycine. Its main role in antioxidant defense is to protect protein thiol groups (SH) and scavenge free radicals such as hydroxyl radical and peroxynitrite (Kalyanaraman, Karoui et al. 1996). In its reduced form, the thiol functional group of cysteine is the active component in antioxidant defense as the sulfur atom is capable of accepting and donating electrons. Upon interaction with free radicals, reduced GSH accepts the free electron creating a transient thiyl radical (GS•). GS• then reacts with another GS• to produce the oxidized form of GSH (GSSG) (Halliwell 1999).

GSH oxidation: $GS\bullet + GS\bullet \rightarrow GSSG$

It is the balance between reduced and oxidized GSH that is commonly used as a marker for oxidative stress. Under normal conditions the typical molar ratio of GSH/GSSG is ten to one depending on species and tissue examined. That ratio however can rapidly shift in oxidizing conditions. It is at this point that cellular systems rely on *de novo* synthesis and recycling of GSH to replenish the reduced form.

As stated, a main function of GSH is participating in cellular defense against oxidative stress (Griffith 1999; Sies 1999) and changes in GSH have been regarded as an assessment for shifts in redox state. The first enzyme in the synthetic pathway is the rate-limiting component for GSH synthesis and involves glutamate cysteine ligase (GCL); a dimeric enzyme composed of a catalytic (GCLc) and modulatory (GCLm) subunit (Huang, Anderson et al. 1993). In this reaction, GCL catalyzes the coupling of L-glutamate to L-cysteine in an ATP dependent manner (Meister and Anderson 1983).

Glutamate-cysteine ligase: L-glutamate + L-cysteine → γ-L-glutamyl-L-cysteine

What is unique in this reaction is the creation of a peptide bond between the γ-carboxyl group of glutamate and the amine group of cysteine. Secondary in the pathway is glutathione synthetase (GS) that catalyzes the addition of glycine to γ-glutamylcysteine (Meister and Anderson 1983; Griffith 1999) producing the reduced and functional form of GSH.

Glutathione synthetase: L-γ-Glutamyl-L-cysteine + L-glycine → GSH

Glutathione reductase (GR) is an integral part in maintaining basal levels of reduced GSH. The role of GR is to convert the oxidized form of GSH (GSSG, see below) back to the reduced form. This reaction requires the cellular reductant NADPH (Kehrer and Lund 1994).

Glutathione Reductase: GSSG + 2 NADPH → 2 GSH + 2 NAD^+

Enzymatic defense systems are present in addition to GSH and are crucial elements in the clearance of ROS. Superoxide dismutase enzymes (SOD) are capable of scavenging the free radical superoxide (O_2•-) by converting it to hydrogen peroxide (H_2O_2) via enzymatic dismutation (Fridovich 1995). There are two main SOD enzymes; a cytosolic isoform and mitochondrial isoform; Copper/Zinc SOD (Cu/ZnSOD) and Manganese SOD (MnSOD) respectively. Cu/ZnSOD relies on the activity of the transition metal copper to react with O_2•- to produce H_2O_2 and O_2. The mitochondrial form manganese SOD (MnSOD) catalyzes the same reaction however utilizing manganese as the transition metal instead of copper. The interesting component of this

reaction is producing hydrogen peroxide via SOD activity, a substrate for hydroxyl radical formation is produced. Fortunately additional enzymes exist to clear hydrogen peroxide from cellular compartments.

Superoxide dismutase: $2\ O_2^{\bullet -} + 2\ H^+ \rightarrow H_2O_2 + O_2$

Involved in the clearance of H_2O_2, catalase and glutathione peroxidase enzymes rapidly convert H_2O_2 to water and molecular oxygen in a dismutation reaction similar to SOD (Lardinois 1995). Catalase, however ,utilizes iron as the transition metal ion. Glutathione peroxidase (Gpx) is similar to catalase in its activities and is responsible for the mitochondrial clearance of H_2O_2 (Chance, Sies et al. 1979). Gpx catalyzes dismutation of H_2O_2 to water and molecular oxygen and utilizes selenium as the transition metal.

Catalase, Glutathione peroxidase: $H_2O_2 \rightarrow H_2O + \frac{1}{2} O_2$

Antioxidants from dietary sources can also help counteract the damaging effects of free radicals; included in this group are ascorbic acid (vitamin C) and tocopherol compounds (vitamin E), most notable being α-tocopherol. The antioxidant capacity is facilitated in both molecules by scavenging unpaired electrons similar to the actions of GSH. The role of these antioxidant compounds is not characterized by their individual action but the combined activities of numerous systems.

In summary, the main role of antioxidant molecules and enzymes is the conversion of free radicals to less reactive constituents. It is important to acknowledge, however, that although discussed individually, it is the cumulative effort of the

aforementioned systems that maintain cellular antioxidant defense and redox homeostasis. In relation to DNA damage, these defense systems work concertedly to prevent hydroxyl radical formation and its subsequent deleterious effects on DNA. This is due in large part to the importance of genomic maintenance. Damage to DNA can lead to genetic mutation, blockage of gene transcription, and induction of apoptotic pathways.

Oxidative Damage to DNA; Formation of 8-hydroxy-2'-deoxyguanosine

Oxidative damage to DNA occurs from a variety of endogenous and environmental sources. Oxidative DNA damage has been found after exposure to ionizing radiation (Kasai, Crain et al. 1986; Breen and Murphy 1995; Hamilton, Guo et al. 2001; Jeong, Youn et al. 2004), genotoxic compounds including heavy metals such as Fe, Cu, Cr (Kehrer 2000; Qi, Reiter et al. 2000; Welch, Davis et al. 2002) and singlet oxygen, an additional ROS shown to induce DNA damage (Devasagayam, Steenken et al. 1991). Damage to DNA also occurs as a consequence of normal metabolic processes such as ATP synthesis where reactive oxygen species are produced as a byproduct of electron transfer (Giulivi, Boveris et al. 1995; Cadenas and Davies 2000). Although reports are varied as to the projected number, it has been proposed that there can be up to 10^3 oxidative attacks on DNA per day in human cells (Helbock, Beckman et al. 1998).

While multiple types of damage can occur to DNA, one specific form of DNA damage is the lesion 8-hydroxy-2'-deoxyguanosine (oxo^{8}dG) that is formed via purine oxidation of guanine. The reaction is facilitated by oxidative attack of hydroxyl radical at the C8 position of guanine generating a guanine-adduct radical. Further oxidation of the guanine-adduct radical forms oxo^{8}dG one of the final products in this reaction pathway (Figure 1) (Breen and Murphy 1995; Dizdaroglu, Jaruga et al. 2002). Recent evidence

has demonstrated that oxo^{8}dG can undergo further oxidation in both artificial and cellular systems. The relevance of these further oxidized guanine lesions is still being characterized. However, their production has been established in the presence of the metal chromium (VI) and cellular reductants, and presents an alternative hypothesis for chromium mediated genotoxicity (Hailer, Slade et al. 2005; Slade, Hailer et al. 2005). This suggests that oxo^{8}dG serves as an intermediate for further oxidative damage to DNA. However, in biological systems, oxo^{8}dG formation is the first event in this oxidative cascade, lending support to a need for understanding the role of oxo^{8}dG in pathological processes, and in the existing mechanisms of repair.

FIGURE 1

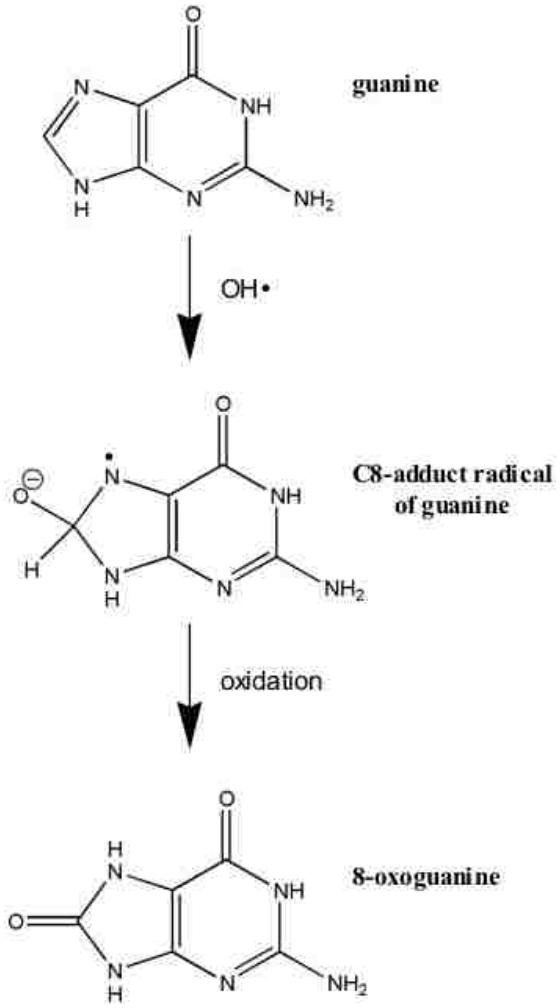

Adapted from (Breen and Murphy 1995; Dizdaroglu, Jaruga et al. 2002)

Figure 1

The reaction pathway for oxidation of guanine in DNA by hydroxyl radical producing oxo^{8}dG. Hydroxyl radical reacts with the C-8 position of guanine producing the C-8OH-adduct guanine radical. Further oxidation stabilizes the adduct creating the final product oxo^{8}dG.

Of the four nucleic acid bases in DNA, guanine has the lowest oxidation potential making it the most frequently oxidized DNA base (Crespo-Hernandez, Close et al. 2007). Based on this physical property, *in vivo* levels of oxo^{8}dG are considered a reliable biomarker for oxidative stress and DNA damage (Dizdaroglu, Jaruga et al. 2002). Increased oxo^{8}dG has been shown subsequent to both environmental (Qi, Reiter et al. 2000; Cardozo-Pelaez, Cox et al. 2005; Piao, Ma et al. 2005), and industrial exposures (Kamendulis, Jiang et al. 1999). Table 1 is a literature summary identifying increased levels of oxo^{8}dG subsequent to a variety of exposures to environmental and chemical conditions. There are two main points to be considered; (i) the breadth of literature investigating oxidative damage to DNA and (ii) elucidating the relationship between increased oxidative DNA damage and toxin-related pathologies. These two points identify a significant area in the literature that needs to be addressed in regards to the relevance of oxo^{8}dG formation. These two points also put forward the issue of whether increased levels of oxo^{8}dG merely serve as a marker of global oxidative stress, or whether increased levels of oxo^{8}dG are a pre-cursor for cellular toxicity.

Table 1. Literature summary outlining studies identifying increased levels of oxo^{8}dG as a result of different environmental and chemical exposures.

Species	Tissue and DNA Source	Exposure	8-OHdG Levels	Reference
Rat	Glial Cells (DITNC1)	Acrylonitrile	⇑⇑	Kamendulis et al 1999
Rat	Kidney	Potassium Bromate	⇑⇑	Cadenas et al 1999
Rat	Liver Mitochondria	Vitamin A Deficiency	⇑⇑	Barber et al 2000
Rat	Lung	Benzo-[a]- pyrene	⇑⇑	Stedeford et al 2001
Rat	Cortex Cerebellum	Arsenic trioxide	⇑⇑	Piao et al 2005
Rat	Cortex	Pre-natal, Lead	⇑⇑	Bolin et al 2006
Human	Mesothelial cells (MET5A)	Crocidolite asbestos	⇑⇑	Chen et al 1996
Human	Sperm	Cigarette smoke	⇑⇑	Fraga et al 1996
Human	Hepatoma Cells (HepG2)	Complex Mixture PM_{10} Particulate matter	⇑⇑	Gabelova et al 2007

" ⇑⇑ " Indicates a statistically significant Increase from control

Elevated levels of oxo^{8}dG have also been associated with the aging process, and a number of disease states including carcinogenesis and neurodegenerative disorders (Halliwell 1999). In the context of aging, the levels of oxo^{8}dG in heart and brain mitochondrial DNA have been demonstrated to inversely correlate with lifespan in mammalian species ranging from guinea pigs to horses (Barja and Herrero 2000). Furthermore, levels of oxo^{8}dG were increased with age in human and different rodent models, however these increases were not shown cumulatively throughout the entire organism. Table 2 summarizes studies measuring changes in oxo^{8}dG as a function of aging in human and various animal species. It is worth noting the species and tissue dependent variation in levels of oxo^{8}dG contained within these studies. However, the reported association of increased oxo^{8}dG and lifespan is under debate. It remains unclear whether increased levels of oxo^{8}dG are a result of diminished clearance, diminished repair, increased oxidative stress, or a combination of all.

Table 2. Literature summarizing changes in oxo^{8}dG as a function of aging in different species and model systems.

Species	Tissue and DNA Source	Control Age	Experimental Age	8-OHdG Levels	Reference
Mouse	Brainstem (Total DNA)	3 months	18 months	⇑⇑	Cardozo-Pelaez et al 1998
Mouse	Cerebellum, Caudate Putamen, Midbrain (Total DNA)	3 months	34 months	⇑⇑	Cardozo-Pelaez et al 1999
Human	Cerebral Corex (nuclear)	N/A	42 to 97 years	⇑⇑	Mecocci et al 1993
	Cerebellum (mitochondrial)			⇑⇑**	
Rat	Liver, Kidney, Intestine (Nuclear)	2 months	24 months	⇑⇑	Fraga et al 1990
	Urinary Output	2 months	12 & 24 months	⇓⇓	
Rat	Kidney, Brain, Spleen (Nuclear)	3 weeks	5 months	⇑⇑	Hirano et al 1996
Houseflies	Total DNA	5 Days	20 Days	⇑⇑	
	Mitochondrial DNA			⇑⇑**	Agarwal et al 1994

" ⇑⇑ " Indicates a statistically significant Increase from age-matched control
"⇑⇑**" Indicates a stastically significant increase compared to nuclear 8-OHdG levels
"N/A" Indicates not applicable

Studies show a relationship between increased levels of DNA damage and neurodegenerative diseases. Increased levels of oxidation have been suggested as a mechanism of injury to neuronal populations in these disorders. In relation to oxo^{8}dG, increased levels have been found in the brain regions affected in Alzheimer's disease (AD) (Lyras, Cairns et al. 1997; Gabbita, Lovell et al. 1998), and Parkinson's disease (PD) patients (Sanchez-Ramos 1994) when compared to age-matched controls. Increased levels of oxo^{8}dG have also been found in the urine, plasma, and cerebrospinal fluid of patients diagnosed with amyotrophic lateral sclerosis (ALS) (Bogdanov, Brown et al. 2000) suggesting that these diseases can be associated with global oxidative stress.

The existence of increased oxo^{8}dG in association with distinct tissues and cellular populations (PD, dopaminergic neurons; AD, glutamatergic neurons; ALS, motor neurons) reveals the existence of different regional capacities for removal and repair of oxo^{8}dG. This was demonstrated in studies assessing repair of oxo^{8}dG in brain tissue from patients diagnosed with PD or AD. Fukae et al identified increased levels of the mitochondrial isoform of the enzyme responsible for initiating repair (see below) of oxo^{8}dG in the substantia nigra isolated from PD brains (Fukae, Takanashi et al. 2005). Assessment of neuronal loss revealed significant reductions in dopaminergic neurons localized to the substantia nigra of sectioned midbrains. It was suggested that increased repair enzyme levels in the mitochondria account for the survival of remaining neurons in the substantia nigra. Full interpretation of the results is difficult however as no assessment of the nuclear isoform of the repair enzyme was done. However, it implicates that the discovery of regulatory mechanisms involved in removal of oxo^{8}dG are a

necessary area of investigation to understand neuronal fate in disease, or after toxicological challenges.

8-hydroxy-2'-deoxyguanosine DNA Glysoylase (Ogg1)

In the event that antioxidant systems (described above) fail to prevent oxo^{8}dG formation, mechanisms have evolved to compensate for oxidative damage to DNA by repairing damaged bases. Oxo^{8}dG is removed from DNA by an active mechanism called base excision repair (BER), a process that repairs single DNA base modifications. The initial step in repairing oxo^{8}dG is the recognition and incision of the oxidized guanine base, a process carried out by a specific N-glycosylase 8-hydroxy-2'-deoxyguanosine DNA glycosylase (Ogg1) (Boiteux and Radicella 2000). To date Ogg1 is considered the primary enzyme involved in initiating the repair of oxo^{8}dG and it is the rate-limiting enzyme in the oxo^{8}dG BER pathway (Klungland, Rosewell et al. 1999; de Souza-Pinto, Eide et al. 2001). Figure 2 outlines the main components involved in the BER pathway for oxo^{8}dG and the sequence in which they occur. Recognition of oxo^{8}dG paired with cytosine occurs first, followed by incision of the N-glycosidic bond leaving an apurinic (AP) site in the DNA strand. Activity by AP endonuclease (APE) creates a single strand break at the AP site by cleaving the phosphodiester bond. DNA polymerase inserts a guanine nucleotide in the empty site, with ligase activity re-establishing the phosphodiester bond. The final product of BER is the repaired DNA strand with an intact G:C base pair (Aspinwall, Rothwell et al. 1997; Hazra, Izumi et al. 1998) (Figure 2).

FIGURE 2

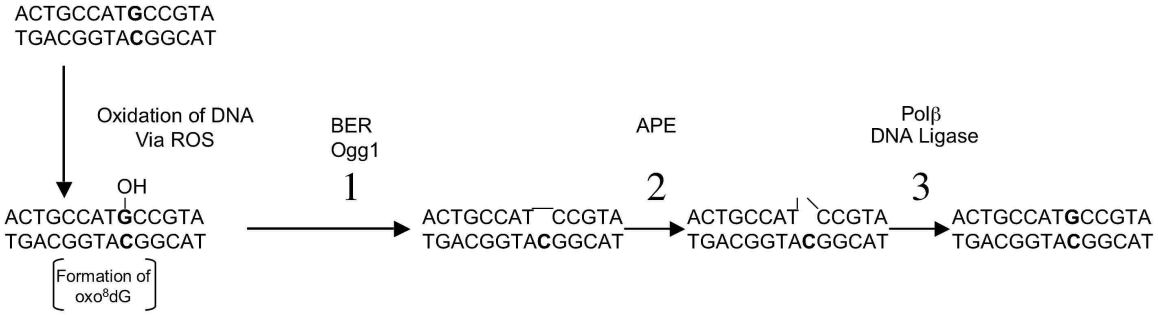

Adapted from (Wilson and Thompson 1997; Bohr 2002)

Figure 2

Base excision repair pathway for removal and replacement of oxo^{8}dG. Initial oxidation of guanine by ROS produces oxo^{8}dG across from cytosine. 1: Recognition of oxo^{8}dG and incision of the N-glycosidic bond by Ogg1 leaves an apurinic (AP) site in the DNA strand. 2: Activity by AP endonuclease creates a single strand break at the AP site. 3: DNA polymerase β (Polβ) inserts a guanine nucleotide in the empty site opposite cytosine. DNA ligase activity re-establishes the phosphodiester bonds creating an intact, repaired DNA strand.

Ogg1 is expressed ubiquitously, however in humans greater levels of expression have been demonstrated in the testes, kidney, and brain suggesting tissue specificity for the regulation of Ogg1 expression (Nishioka, Ohtsubo et al. 1999). In mice, low basal levels of Ogg1 mRNA were measured in all tissues sampled with the exception of the testes (Rosenquist, Zharkov et al. 1997). Levels of oxo^{8}dG have also been demonstrated as variable among different animal species and tissues examined (Hamilton, Guo et al. 2001). Hamilton et al showed that higher basal levels of oxo^{8}dG were present in mitochondrial DNA analyzed from different murine tissues (Hamilton, Guo et al. 2001) suggesting differential expression patterns for Ogg1 existing in different cellular compartments. Higher basal levels of oxo^{8}dG have been found in discrete brain regions of C57BL/6 mice; specifically cerebellum, cortex and pons medulla. It was also determined that increased oxo^{8}dG in these brain regions correlated with lower basal Ogg1 activity (Cardozo-Pelaez, Brooks et al. 2000).

These studies suggest the existence of regulatory facets for Ogg1 expression and or activity that are dependent on multiple factors; including species, tissue, and cell type. These findings reinforce the importance of determining the regulatory mechanisms and how they are associated with the differential expression of Ogg1 and its relation to oxo^{8}dG levels in specific cellular populations.

Regulatory Aspects of Ogg1

The hierarchical regulation of Ogg1 can be characterized in studies showing both post-transcriptional and post-translational modifications. Two main splice variants of mRNA have been demonstrated showing both nuclear (Ogg1-α), and mitochondrial (Ogg1-β) transcripts for the human isoform of Ogg1. The mitochondrial transcript is

produced by alternative splicing of exon 8 in place of exon 7 in the transcribed strand. Exon 7 is the region where the nuclear localization signal (NLS) is contained. In this process the NLS is removed from the transcribed strand of RNA producing the β-form and shifting the final destination of Ogg1 from the nucleus to the mitochondria. The two main splice variants can also be differentiated based on their final protein products with the α-form and β-forms being 345 and 424 amino acids in length respectively (Nishioka, Ohtsubo et al. 1999; Boiteux and Radicella 2000) (See Figure 3).

FIGURE 3

A.

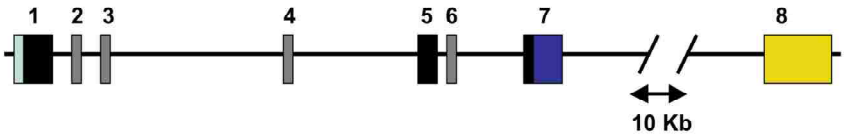

B.

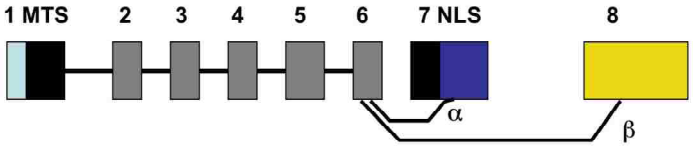

C.

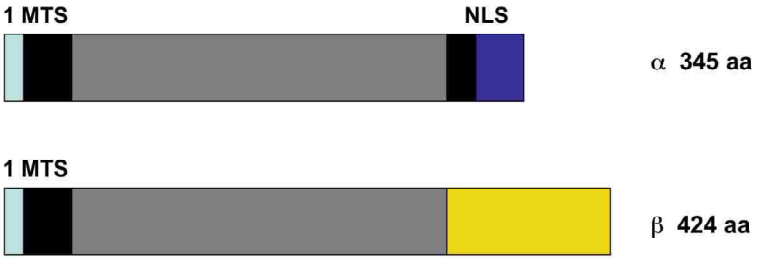

Adapted from (Boiteux and Radicella 2000)

Figure 3

(A) The genomic organization of the human Ogg1 gene showing exon-intron distribution of the gene. Mitochondrial targeting sequence is located in exon1, nuclear localization signal in exon 7. Exon 8 is located downstream (~ 10 Kb) from the main cluster of exons 1 through 7.

(B) Organization of the α-form and β-form splice variants of Ogg1. The α-form (nuclear) is produced by sequential joining of exons 1 to 7; the β-form (mitochondrial) is produced by excision of exon 7 with exon 8 splicing in its place thus effectively removing the NLS from the transcript.

(C) Linear representation of the α-form and β-forms of the human Ogg1 enzyme produced by alternative splicing events. The α-form (nuclear) is 345 amino acids in length. The β-form (mitochondrial) is 424 amino acids in length.

Besides the existence of alternative splice variants, post-translational regulation of Ogg1 has been shown to occur by a variety of mechanisms. Some of these regulatory events occur via amino acid modifications to the Ogg1 enzyme. Ogg1 has been reported to contain redox sensitive amino acids capable of modulating its activity. In particular, cysteine residues have been implicated in direct modulation of Ogg1 activity. A human lymphoblast culture line was used to demonstrate that hOgg1 activity was decreased as a consequence of oxidative stress from cadmium chloride exposure. It was also shown that recovery of hOgg1 activity could be accomplished by the addition of reducing agents to nuclear extracts and purified hOgg1 (Bravard, Vacher et al. 2006). This suggests that redox homeostasis is an essential component in maintaining basal Ogg1 activity. It also suggests that compounds participating in oxidative stress can have an indirect effect on Ogg1 activity if cellular levels of GSH are changed.

Phosphorylation of Ogg1 has also been shown to directly modulate enzymatic activity. Protein kinase C (PKC) was the first reported enzyme capable of *in vivo* phosphorylation of hOgg1. It was further shown, *in vitro*, that PKC was capable of phosphorylating Ogg1 in both purified and nuclear extracts (Dantzer, Luna et al. 2002). Phosphorylation of Ogg1 was also demonstrated in a yeast model system and it was suggested that both interaction and phosphorylation by Cdk4 protein kinase led to increases in Ogg1 activity. An additional protein kinase, c-abl, had no effect on incision activities but was also shown to phosphorylate Ogg1 (Hu, Imam et al. 2005) suggesting the existence of different protein kinase pathways involved in the regulation of Ogg1. The aforementioned studies suggest that there are many levels involved in Ogg1

regulation ranging from post-transcriptional, to direct modification of the functional Ogg1 enzyme. The studies also demonstrate that different regulatory aspects of Ogg1 should be considered collectively when characterizing different mechanisms of Ogg1 regulation, as it is clear that there are many variables involved.

Transcriptional Regulation of Ogg1

Despite the investigations into post-transcriptional and -translational regulatory mechanisms, little has been investigated regarding the pre-transcriptional pathways involved in modulating Ogg1 transcription. Numerous studies suggest that modulation of Ogg1 can occur at different levels in the hierarchy of gene expression. Table 3 summarizes these studies based on the different techniques used for assessment, and the corresponding changes in Ogg1 following treatment with different species and model systems. Measurement of Ogg1 activity is the most common determination with the measurement of Ogg1 mRNA levels being the second. While measurement of mRNA levels is a reliable assessment for changes in gene transcription, few of these studies address pre-transcriptional changes; specifically the function of distinct transcription factor pathways and their role in modulating Ogg1 (Table 3).

Table 3. Literature summary of changes in Ogg1 activity, expression and transcription subsequent to various exposure regiments.

Species	Tissue or Cell Type	Ogg1 Activity	Ogg1 mRNA	Ogg1 Protein	Ogg1 Promoter Activity	Exposure Type	Reference
Human	HeLa S3, GM00637 Fibroblast	⇓⇓	⇓⇓	⇓⇓	⇓⇓	$CdCl_2$	Youn et al 2006
Human	HCT116	⇑⇑	⇑⇑	⇑⇑	⇑⇑	Methyl methane sulfonate	Lee et al 2004
Human	A549 lung adenocarcinoma	⇓⇓	⇓⇓	⇓⇓	----	Sodium dichromate	Hodges et al 2002
Human	A549 lung adenocarcinoma	⇑⇑	⇑⇑	----	----	Crocidolite asbestos	Kim et al 2001
Mouse	Cerebellum, Cortex Pons medulla	⇑⇑	----	⇔	----	Diethyl maleate	Cardozo-Pelaez et al 2002
Mouse	Whole Brain	⇑⇑	⇔	⇑⇑	----	Ischemia Reperfusion	Lin et al 2000
Rat	Alveolar epithelial cells	⇓⇓	⇓⇓	⇓⇓	----	$CdCl_2$	Potts et al 2003
Rat	Frontal/Parietal Cortex	⇑⇑	----	----	----	Ischemia Reperfusion	Lan et al 2003
Rat	Lungs	⇓⇓	⇓⇓	----	----	Deisel Exhaust	Tsurudome et al 1999

" ⇑⇑ " Indicates a statistically significant Increase from control
" ⇓⇓ " Indicates a statistically significant decrease from control
" ⇔ " Indicates no statistical difference from control.
"----" Indicates not measured.

Previous characterization of the promoter for human Ogg1 (hOgg1) isolated from a human genomic library was performed in HeLa cells. The results suggest that hOgg1 is a housekeeping gene whose basal expression is constitutive and unchanged during the cell cycle. This conclusion is based largely on the absence of putative TATA or CAAT boxes (Dhenaut, Boiteux et al. 2000). A section of the promoter spanning 135 bp upstream of the transcription initiation site is essential for basal transcription of hOgg1 and contains putative binding sites for several transcription factors including Sp1 and p53 (Figure 4).

FIGURE 4

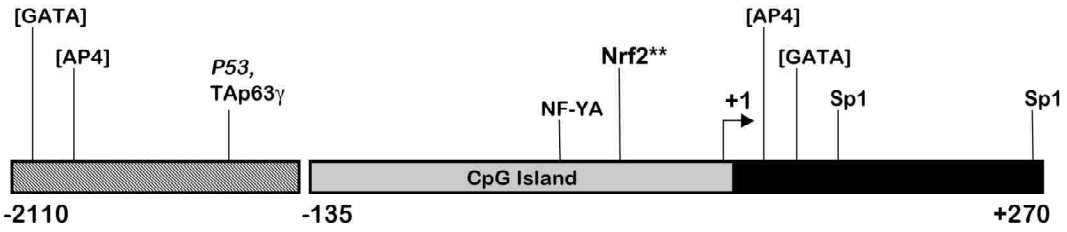

Adapted from (Dhenaut, Boiteux et al. 2000)

Figure 4

Map of a 2.1 Kb span of the human Ogg1 promoter. Putative or unverified transcription factor binding sites are enclosed in brackets. Binding sites for Sp1 (Youn, Kim et al. 2005), NF-YA (Lee, Kim et al. 2004) transcription factors have been previously confirmed and are located in a GC rich span of the promoter. A p53 and TAp63γ binding site has been identified between positions –785 to –750 (Chatterjee, Mambo et al. 2006; Upadhyay, Chatterjee et al. 2007). The putative binding site for Nrf2 (**) is located upstream of the transcription initiation site at position –47 to –44.

Few studies have linked transcriptional regulation of Ogg1 to specific transcription factor pathways. Of the existing reports, distinct transcription factors have been elucidated as interacting with the promoter for hOgg1, and having subsequent effects on transcriptional activity. The transcription factor NF-YA was reported to play a role as an inducible mechanism for hOgg1 upon exposure to the DNA alkylating agent methylmethane sulfonate. This was demonstrated by transcription factor binding to inverted CAATT motifs located at positions –97 and –71 of the hOgg1 promoter. This area of the promoter also contains a large CpG island suggesting that modulation of Ogg1 transcription can occur due to changes in promoter methylation (Lee, Kim et al. 2004). It was also demonstrated that Sp1 was important in the basal transcriptional of hOgg1 and this process could be negatively influenced by cadmium chloride via down regulation of gene transcription (Youn, Kim et al. 2005).

Recent evidence suggests the role of p53 in transcriptional regulation of hOgg1. Both p53 and Ta*p63*γ, a homologue of p53, have been shown to bind and modulate hOgg1 transcription (Chatterjee, Mambo et al. 2006; Upadhyay, Chatterjee et al. 2007). It has also been demonstrated that p53 can directly interact with hOgg1/ APE complexes, both being the first two enzymes involved in the oxo^{8}dG BER pathway. It was also suggested that interaction of p53 with hOgg1 and APE is facilitating an increase in both enzyme activities (Achanta and Huang 2004), however the mechanism by which such facilitation occurs remains uncharacterized.

These previous studies are the only ones linking defined transcription factor pathways to modulation of hOgg1, however work by Dhenaut & colleagues suggests the presence of a number of putative transcription factor binding sites in the hOgg1 promoter

(see Figure 4) (Dhenaut, Boiteux et al. 2000). Whether these putative transcriptional binding sites play a role in Ogg1 transcription, and under what conditions remains unresolved.

Many of the exposures outlined in Table 3 have a common aspect, specifically their association with oxidative stress and the induction of cellular stress response pathways. Under this notion, these studies can help to gain insight into the mechanism involved in the modulation of Ogg1 in the presence of compounds that effect levels of GSH (Cardozo-Pelaez, Stedeford et al. 2002; Merrill, Ni et al. 2002). Analysis of the hOgg1 promoter region reveals the existence of a putative Nrf2 binding site at positions –47 to – 44 (Dhenaut, Boiteux et al. 2000), however this site currently remains unverified in regards to its interaction with Nrf2 and cellular stress response. It does propose an interesting question; is Nrf2 capable of interacting with the hOgg1 promoter and is it involved in transcriptional regulation of Ogg1 expression?

Transcription Factor Nrf2

Nuclear-factor Erythroid factor 2 (NF-E2-related factor 2, Nrf2) is involved in regulating a well-characterized transcription factor pathway involved in the regulation of phase II xenobiotic metabolism and antioxidant genes including Nrf2 itself. A short list of these genes includes glutathione *S*-transferases (GST), NADP(H) quinone oxidoreductase (NQO1), GSH maintenence enzymes (GCL, GS, GR), hemeoxygenase I (HO-1), and system x_c transporter (Rushmore and Pickett 1990; Venugopal and Jaiswal 1996; Itoh, Chiba et al. 1997; Alam, Stewart et al. 1999; Chan and Kwong 2000; Sasaki, Sato et al. 2002; Lee, Calkins et al. 2003).

Nrf2 is considered the model redox/stress response pathway because its activation and translocation has been associated, in part, with changes in the cellular redox state. GSH is regarded as the first line of defense against cellular oxidative stress (Griffith 1999; Sies 1999) and changes in GSH have been regarded as a measure for shifts in cellular redox status. Work by others suggests that modulation of GSH via depleting agents acts as a regulator of cell response to oxidative stress by induction of Nrf-2 regulated genes (Prosperi, Ferbus et al. 1998; Dinkova-Kostova, Holtzclaw et al. 2002; Hansen, Watson et al. 2004). It is therefore plausible that changes in GSH could regulate the transcription of Ogg1 as previously suggested. A 6 hr *in vivo* exposure to diethyl maleate led to decreased levels of GSH and increased Ogg1 activity in specific brain regions (Cardozo-Pelaez, Stedeford et al. 2002). A similar exposure was performed in the human Hep G2 cell line. 6 hr exposure to etoximir resulted in significantly reduced levels of GSH, and significantly increased levels of hOgg1 mRNA (Merrill, Ni et al. 2002). It can then be suggested that increased hOgg1 transcription is occurring in an Nrf2 dependent manner as increased transcripts from a number of Nrf2-regulated genes (HO-1, GCLm, GR, MnSOD) were also demonstrated (Merrill, Ni et al. 2002).

Expanding the role for Nrf2 in stress response are studies showing its activation by components of signal transduction pathways; most notably map kinase pathways (Yu, Chen et al. 2000), phosphatidylinositol 3 kinase (PI3K) (Salinas, Diaz et al. 2003; Martin, Rojo et al. 2004), and protein kinase C (PKC) (Bloom and Jaiswal 2003; Hu, Imam et al. 2005).

Structurally Nrf2 is a basic leucine zipper (bZip) transcription factor that under normal conditions remains sequestered in the cytosol (Moi, Chan et al. 1994; Venugopal and

Jaiswal 1998). Sequestration of Nrf2 is facilitated by interaction with its inhibitory partner, kelch-like protein 1 (KEAP1) (Itoh, Wakabayashi et al. 1999; Dinkova-Kostova, Holtzclaw et al. 2002). Under basal conditions Nrf2-KEAP1 complexes are maintained in the cytosol tethered to the actin cytoskeleton where Nrf2 is continually targeted to the proteasome via an ubiquitin-dependent pathway (Nguyen, Sherratt et al. 2003). However, in the presence of ROS, xenobiotics or enzymatic activation, Nrf2 is released from KEAP1 and translocates to the nucleus where it interacts in partnership with small Maf binding proteins. The final function of active Nrf2 is to interact with its cognate binding sequence (reviewed in; (Itoh, Tong et al. 2004; Lee and Johnson 2004; Nguyen, Yang et al. 2004) a unique area in the promoter region of Nrf2 regulated genes called the antioxidant response element (ARE). Subsequent to the formation of Nrf2-Maf dimerization and transcription complex binding, genes containing ARE binding sequences in their promoter are transcribed (Figure 5).

FIGURE 5

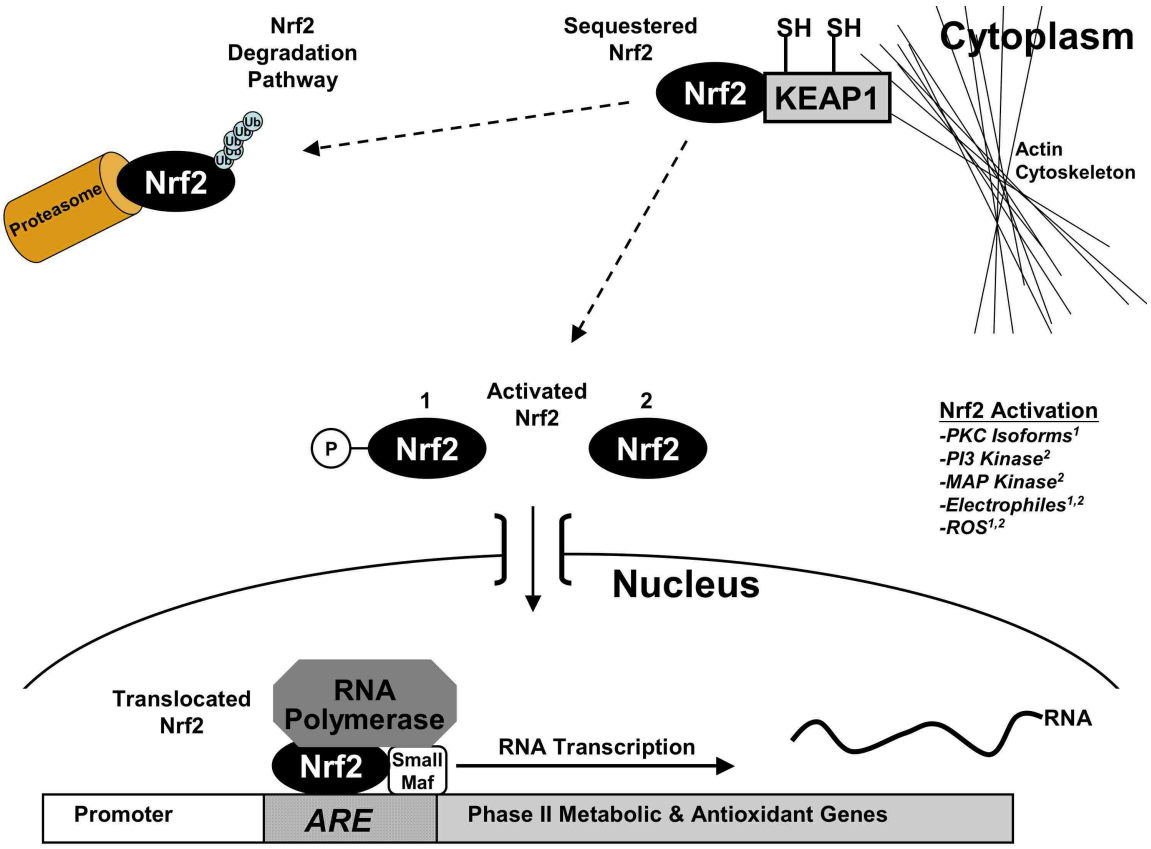
Nrf2
Degradation
Pathway
Sequestered
Nrf2
SH SH
Cytoplasm
Nrf2
KEAP1
Actin
Cytoskeleton
Proteasome
Nrf2
Ub
1
Activated
Nrf2
2
P
Nrf2
Nrf2
Nrf2 Activation
-PKC Isoforms[1]
-PI3 Kinase[2]
-MAP Kinase[2]
-Electrophiles[1,2]
-ROS[1,2]
Nucleus
Translocated
Nrf2
RNA
Polymerase
Nrf2
Small
Maf
RNA Transcription
RNA
Promoter
ARE
Phase II Metabolic & Antioxidant Genes

Figure 5

The pathways of activation for transcription factor Nrf2 in mammalian cells. Sequestered Nrf2 represents the inactive form of Nrf2 and its ubiquitin-dependent degradation via the proteasome. Activity by PKC (as of yet distinct isoforms unidentified) leads to phosphorylation and subsequent activation of Nrf2[1]. The presence of ROS (GSH modulation), has also been shown to activate Nrf2 via modification of thiol groups on KEAP1[2]. Electrophilic compounds (tBHQ) has been shown to activate Nrf2 by both of the aforementioned mechanisms[1,2]. Activated Nrf2 translocates in to the nucleus interacting with small Maf proteins and binds to the ARE. RNA transcription complexes are formed leading to transcription of Nrf2-regulated genes.

The core ARE sequence was identified by Rushmore and colleagues as being analogous to AP-1 binding sites, however, the ARE differed in its core binding sequence (see below) (Rushmore and Pickett 1990). Dhenaut and colleagues analysis of the hOgg1 promoter (Dhenaut, Boiteux et al. 2000) identified an additional core ARE sequence that has since been characterized as interacting with Nrf2 in an equivalent manner (Ongwijitwat and Wong-Riley 2004). However, whether the proposed Nrf2 binding sequence located in the hOgg1 promoter (Dhenaut, Boiteux et al. 2000) is involved in the regulation of Ogg1 gene transcription remains unverified.

Antioxidant Response Element Core Binding Sequence

5′ – GTGACnnnGC – 3′ (Rushmore and Pickett 1990)

5′ – TTCC – 3′ (Dhenaut, Boiteux et al. 2000; Ongwijitwat and Wong-Riley 2004)

The redox sensitivity of Nrf2 activation has been identified by two unique characteristics of the KEAP1-Nrf2 dimeric complex. The first is a string of amino acids located in the Neh2 domain of Nrf2. The motif is composed of glu-thr-gly-glu (ETGE) and is characterized as the docking region for KEAP1 (Itoh, Wakabayashi et al. 1999; McMahon, Thomas et al. 2004). The second, and redox sensitive characteristic, is the presence of distinct cysteine residue located in KEAP1. Specifically, cysteines 257, 273, 288 and 297 have been identified as the most reactive residues (Dinkova-Kostova, Holtzclaw et al. 2002) in a cysteine rich region of KEAP1. Figure 6 demonstrates the structural and redox-sensitive features of both Nrf2 and KEAP1.

FIGURE 6

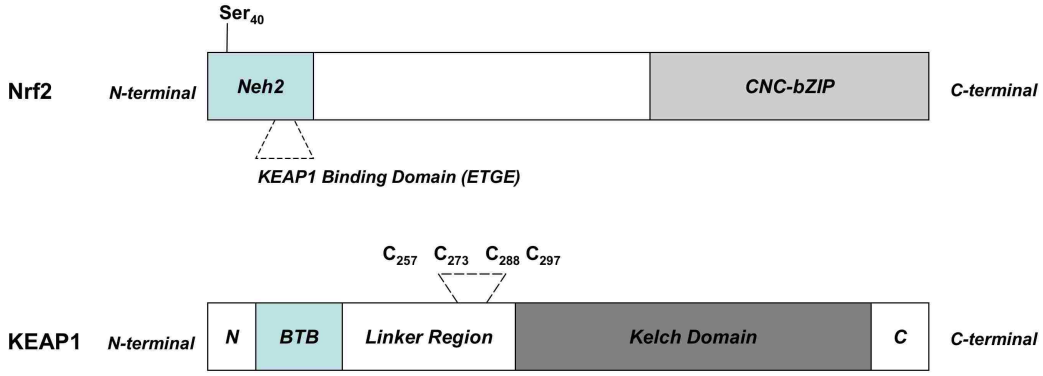

Adapted from (Itoh, Wakabayashi et al. 1999; Dinkova-Kostova, Holtzclaw et al. 2002)

Figure 6

Protein map and structural organization of Nrf2 and KEAP1. Highlighted features include the KEAP1 binding domain consisting of an ETGE motif located in the Neh2 domain of Nrf2. The linker region of KEAP1 is composed of multiple cysteine residues with four highly reactive residues present in close proximity to one another. The linker region has been identified as the redox-sensitive portion of KEAP1 capable of undergoing cysteine oxidation.

Recent evidence suggests an integral role for C273, C288 in Zn^{2+} coordination. This was characterized by the displacement of zinc from KEAP1-Nrf2 complexes in the presence of Nrf2 inducing compounds. Zinc displacement resulted in subsequent cysteine modifications, and conformational changes in KEAP1 that led to the release of Nrf2 thereby initiating the first component of Nrf2 activation (Dinkova-Kostova, Holtzclaw et al. 2005).

To date no link has been established between Nrf2 and Ogg1 regulation despite published data suggesting response trends for Ogg1 that are similar to Nrf2 regulated genes (Table 3). Previous work has demonstrated an inducible response by Ogg1 that follows decreased levels of GSH (Cardozo-Pelaez, Stedeford et al. 2002; Merrill, Ni et al. 2002) however these studies have not identified any mechanism responsible for this induction. Despite the lack of evidence for Ogg1 regulation via Nrf2, it is worth noting that in mice deficient for Nrf-2 expression (*-/- null phenotype*), basal levels of oxo^8dG are higher than levels in wild-type controls (Li 2004); the activity for Ogg1 however was not assessed in this study. Increased levels of oxo^8dG in the Nrf-2 -/- mice were also demonstrated after exposure to diesel exhaust particles and cigarette smoke (Aoki, Sato et al. 2001; Rangasamy, Cho et al. 2004). It is difficult to establish the cause of increased oxo^8dG levels in these studies, as a lack of Nrf2 constitutes the decreased expression of many antioxidant genes. However, the increased levels of oxo^8dG present in Nrf2 null mice suggest Ogg1 as a potential Nrf2-regulated gene for investigation.

CHAPTER TWO

Transcriptional Regulation of 8-hydroxy-2'-deoxyguanosine DNA Glycosylase by the Cellular Redox State and Transcription Factor Nrf2

Abstract

8-hydroxy-2'-deoxyguanosine DNA glycosylase is the rate-limiting enzyme involved in the removal of 8-hydroxy-2'-deoxyguanosine via the base excision repair pathway. Transcriptional regulation of human Ogg1 is sensitive to redox changes via modulation of intracellular GSH in HEK 293T cells. In response to changes in GSH, changes in hOgg1 transcriptional activity occur similar to genes regulated by the transcription factor Nrf2. It was determined that a four base pair run (TTCC) located at positions – 47 to – 44 in the hOgg1 promoter is essential for basal transcription of the Ogg1 gene as determined by site-directed deletion. In addition, the putative Nrf2 site is capable of interacting with nuclear protein extracts from HEK 293T cells as determined by electrophoretic mobility shift assays (EMSA). Further investigation suggests the involvement of the transcription factor Nrf2 as determined by parallel, and competition EMSA using consensus Nrf2 and Sp1 oligonucleotides. Additional evidence for Nrf2 binding to this region of the hOgg1 promoter was demonstrated by increased binding subsequent to exposure by *tert*-butylhydroquinone, a known Nrf2 inducing agent. We conclude that the transcription factor Nrf2 is an important factor in the inducible regulation of Ogg1 and that these changes are ultimately dependent on the redox status of the cell, mainly via intracellular levels of GSH.

Introduction

Oxidative damage to DNA occurs from a variety of sources including environmental causes such as ionizing radiation as well as genotoxic compounds like heavy metals and peroxides (Kehrer 2000). It can also occur during normal cellular processes such as ATP synthesis where reactive oxygen species are produced as a byproduct of electron transfer (Giulivi, Boveris et al. 1995). One specific form of DNA damage is the lesion 8-hydroxy-2'-deoxyguanosine (oxo^{8}dG) that occurs via oxidation of the DNA base guanine. Oxo^{8}dG is one of the most commonly formed DNA lesions and is considered a cellular biomarker for both oxidative stress and DNA damage (Dizdaroglu, Jaruga et al. 2002). Cellular systems are in place to regulate levels of genomic oxo^{8}dG by repairing the damaged base. The repair process is accomplished by an enzymatic pathway called base excision repair (BER). The initial step in BER involves the recognition and incision of oxo^{8}dG, a process carried out by a specific N-glycosylase Ogg1 (Boiteux and Radicella 2000). Ogg1 is the main enzyme involved in initiating the repair of oxo^{8}dG and is the rate-limiting enzyme in the BER pathway (Klungland, Rosewell et al. 1999; de Souza-Pinto, Eide et al. 2001). Ogg1 is expressed ubiquitously, however greater levels of expression have been detected in the testes, kidney, and brain of humans indicating a tissue specific organization for the regulation of Ogg1 expression (Nishioka, Ohtsubo et al. 1999). These results suggest the existence of regulatory mechanisms for Ogg1 expression and/or activity that are specific to tissue and cell type.

Different aspects of Ogg1 regulation have been demonstrated in studies showing both post-transcriptional and post-translational modifications. Evidence for these

modifications included the existence of nuclear and mitochondrial targeted transcript splice variants (Nishioka, Ohtsubo et al. 1999) and amino acid modifications via both oxidation and phosphorylation. (Dantzer, Luna et al. 2002; Hu, Imam et al. 2005; Bhakat, Mokkapati et al. 2006; Bravard, Vacher et al. 2006). These studies demonstrate that modulation of Ogg1 can occur at different levels in the hierarchy of gene expression.

Despite the discovery of the aforementioned post-transcriptional and post-translational regulatory mechanisms, little has been investigated regarding the pre-transcriptional pathways involved in regulating Ogg1 transcription. The promoter for hOgg1 has been sequenced and hOgg1 was characterized as a housekeeping gene whose expression is constitutive and unchanged during the cell cycle (Dhenaut, Boiteux et al. 2000; Lee, Kim et al. 2004). Evidence for the transcriptional regulation of hOgg1 was demonstrated via the transcription factor Sp1, an integral component in the basal transcription of Ogg1 (Youn, Kim et al. 2005). Of the studies investigating changes in Ogg1, many identify a unique aspect; the association with oxidative stress and the induction of cellular stress response pathways. Transcription factor Nrf2 regulates a well-characterized stress response pathway involved in the induction of phase II xenobiotic metabolism, and antioxidant genes (Itoh, Chiba et al. 1997). Nrf2 is further characterized as a molecular redox switch because its activation and translocation are intimately associated with levels of intracellular GSH (Dinkova-Kostova, Holtzclaw et al. 2002; Hansen, Watson et al. 2004). Dhenaut and colleagues reported the existence of a potential/putative Nrf2 binding site in the hOgg1 promoter (Dhenaut, Boiteux et al. 2000). Published data implies response trends for Ogg1 that are similar to Nrf2 regulated

genes making Nrf2 a candidate for investigation as a transcriptional regulator of Ogg1 (Cardozo-Pelaez, Stedeford et al. 2002; Merrill, Ni et al. 2002).

The goal of these experiments was to test the hypothesis that the DNA repair enzyme Ogg1 is transcriptionally regulated by the transcription factor Nrf2, and that transcriptional changes in Ogg1 are mediated by the intracellular antioxidant GSH. To test the hypothesis the following objectives were designed:

1) Characterize the transcriptional activity of the putative Nrf2 binding site located at positions –47 to –44 of the human Ogg1 promoter.
2) Characterize nuclear protein interaction at the putative Nrf2 binding site located at positions –47 to –44 of the human Ogg1 promoter.
3) Characterize the changes in hOgg1 transcriptional activity subsequent to exposure to Nrf2 inducing compounds and modulation of cellular GSH.

To accomplish this, reporter gene expression vectors under the regulation of the hOgg1 promoter were constructed. Site-directed deletion of the putative Nrf2 binding site (–47 to –44) in the hOgg1 promoter was used to assess the transcriptional relevance of this region. Changes in promoter activity were measured by changes in GFP reporter gene expression. Assessment of nuclear protein interaction with the Nrf2 site was determined by electrophoretic mobility shift assays. Nuclear extracts were utilized from both untreated and tBHQ (an Nrf2 inducer) treated HEK 293T cells. Redox response capacity of Ogg1 transcription was determined using a more sensitive reporter gene system involving luciferase expression vector regulated by the hOgg1 promoter. Changes in luciferase reporter gene activity were measured. These assays were

performed using Nrf2 inducing compounds t-butyl hydroquinone, diethyl maleate, and a membrane permeable GSH analog, glutathione monoethyl ester. As a surrogate measure of stress response and redox status, GSH was measured from cell cultures exposed to the latter conditions; Nrf2 induction and GSH modulation.

Materials & Methods

Cell Culture and Transient Transfections

HEK 293T human embryonic kidney cells (ATCC, #CRL-11268) were grown in 1X Dulbecco's Modification of Eagle's Medium with 4.5 g/L glucose and L-glutamine, 10% fetal bovine serum, 1 mM sodium pyruvate, 1X non-essential amino acids, 1000 international units penicillin, 1 mg/mL streptomycin, 50 μg/mL gentamicin sulfate. All media reagents were purchased from CellGro® technologies (Mediatec Inc., Herndon, VA) and incubated at 37°C in a humidified 5% CO_2 atmosphere. Transfections were performed using PolyFect® lipid transfection reagent (QIAGEN, Valencia, CA). Cell densities for FACS measurement of GFP was performed at a starting density of 3.0 x 10^5 cells/well in 6-well tissue costar tissue culture plates (Corning Life Sciences, Lowell, MA) and grown in normal growth media for 24 hr. Two μg total plasmid DNA/well was used with 20 μL PolyFect® reagent for GFP transfections. Cell density for luciferase assays was performed at a starting density of 1.5 x 10^5 cells/ well in 24-well tissue costar tissue culture plates (Corning Life Sciences, Lowell, MA) and grown in normal growth media for 24 hr. 0.5 μg of target vector was co-transfected with 10 ng of reference vector and 5 μL of PolyFect® reagent. For over-expression of Nrf2, luciferase expression vectors were co-transfected with 0.5 μg of pEF-Nrf2, or an empty control vector (pEF-

Basic) to ensure specificity. Twenty four hr post-transfection HEK 293T cells were treated with normal growth media or media containing 25 μM tert-butylhydroquinone (tBHQ) (Alfa Aesar, Ward Hill, MA) 25 μM diethyl maleate (DEM) (Sigma, St Louis, MO), or 1 & 2 mM glutathione monoethyl ester (GSH-mee) (EMD Bioscience, San Diego, CA).

Construction of the Expression Vector pAM/hOgg1-hrGFP-WPRE-BGH-polyA

All plasmids were constructed using basic molecular biology protocols. A GFP reporter gene expression vector (pAM/hOgg1-*hr*GFP-WPRE-BGH-polyA) was produced by ligation of a 2.1 Kb fragment of the human Ogg1 promoter into the linearized promoterless pAM/-hrGFP-WPRE-BGH-PolyA expression vector. The hOgg1 promoter fragment was generated by polymerase chain reaction using primers with unique restriction sites Asp718 and BamHI (see Appendix A, section 3). PCR reactions were composed of the following reagents and set up in sterile 0.25 mL reaction tubes (Axygen Scientific, Union City, CA): 5 μL of 10X PCR buffer (Invitrogen Life Technologies, Carlsbad, CA), 1.5 μL of 50 mM $MgCl_2$ (Invitrogen Life Technologies, Carlsbad, CA), 2.5 μL of 2.5 mM dNTP's (Roche Applied Science, Indianapolis, IN), 2.5 μL of 5 μM forward and reverse primers (Integrated DNA Technologies Inc., Coralville, IA), 0.25 μL *Taq* polymerase (Invitrogen Life Technologies, Carlsbad, CA), 50 ng template DNA isolated from SHSY-5Y neuroblastoma cells, with a final volume of 50 μL using sterile nuclease free H_2O. Reactions were run using a DNA Engine thermal cycler (MJ Research, Waltham, MA) as follows: 94° C for 3 min, **94° C for 45 sec, 65° C for 30 sec, 72° C for 90 sec, **amplification steps repeated 33X, 72° C 10 min. Blunt ended PCR products were ligated into the pCR®-Blunt II-TOPO (Invitrogen Life Technologies,

Carlsbad, CA) sequencing vector. TOPO reactions were set up under the following conditions: 4 μL fresh hOgg1 promoter PCR reaction, 1 μL TOPO salt solution (Invitrogen Life Technologies, Carlsbad, CA), 1 μL pCR®-Blunt II-TOPO sequencing vector. Reactions were mixed gently and incubated at 25° C for 5 min. Following incubation TOPO reactions were transformed into DH5α chemically competent *Escherichia coli* (Invitrogen Life Technologies, Carlsbad, CA) via heat shock protocols setup as follows: 50 μL of competent cells were transferred to a sterile 1.5 mL eppendorf tube on wet ice, 6 μL of the TOPO reaction was gently added, mixed and incubated on ice for 30 min. Reactions were heat shocked at 42° C for 20 sec and placed on ice for 2 min. 450 μL of S.O.C. recovery media (Invitrogen Life Technologies, Carlsbad, CA) was added to transformation reactions and incubated at 37° C, shaker speed 225 rpm for 60 min. Transformation reactions were grown overnight at 37° C on LB agar plates containing (100 μg/mL) ampicillin to select transformed colonies via antibiotic resistance. Single colonies were selected and grown in liquid LB broth containing ampicillin (100 μg/mL). TOPO vectors were extracted and purified using Mini-prep plasmid DNA purification kits (QIAGEN, Valencia, CA). The purified TOPO vector containing the 2.1 Kb hOgg1 promoter fragment underwent restriction digest analysis using Asp718 and BamHI restriction enzymes (Roche Applied Science, Indianapolis, IN) to verify the presence of the 2.1 Kb fragment in the TOPO vector. Promoter sequencing was performed by Murdock Sequencing Facility, University of Montana. Following verification by restriction digest analysis and sequencing, the 2.1 Kb fragment was resolved and separated on a 0.8% agarose gel containing 1.5 μg/mL ethidium bromide to visualize the separated fragments via ultra-violet light. The fragment was cut from the

agarose gel and purified using the QIAquick gel purification system (QIAGEN, Valencia, CA) with final purified promoter fragments suspended in sterile nuclease free H_2O. Promoter fragments were ligated into a linearized promoterless pAM/-*hr*GFP-WPRE-BGH-polyA expression vector. The linearized vector was generated by restriction enzyme digest of the pAM/CAG-*hr*GFP-WPRE-BGH-polyA expression vector using Asp718 and BamHI restriction enzymes. Separation and purification of the linearized pAM/promoterless vector was performed as described above with the final linearized vector suspended in sterile nuclease free H_2O. The linearized vector underwent further processing by reacting the vector with shrimp alkaline phosphatase (SAP) (Roche Applied Science, Indianapolis, IN) under the following conditions in sterile 0.25 mL reaction tubes (Axygen Scientific, Union City, CA): 50 ng of linearized vector, 1X SAP buffer, 1 U SAP enzyme, final volume brought to 10 μL using sterile nuclease free H_2O. Reactions were run using a DNA Engine thermal cycler (MJ Research, Waltham, MA) under the following conditions: 37° C for 10 min, 65° C for 15 min to heat inactivate the SAP enzyme. Ligation reactions were set up as a 3:1 molar ratio using the following calculation:

$$\text{ng of insert to use} = \frac{\text{ng of vector} \times \text{size of insert (Kb)}}{\text{size of insert (Kb)}} \times \text{molar ratio } \frac{3}{1}$$

Based on the molar ratio calculation, ligation reactions were set up as follows in sterile 0.25 mL reaction tubes (Axygen Scientific, Union City, CA): 60 ng insert (hOgg1 promoter fragment), 1X T4 ligation buffer, 1 U T4 DNA ligase (Promega, Madison, WI), final volume brought to 10 μL using sterile nuclease free H_2O. Ligation reactions were incubated overnight at 4° C. Ligation reactions were transformed, amplified and purified as described above. Verification of the newly constructed pAM/hOgg1-*hr*GFP-WPRE-

BGH-polyA expression vector was performed by restriction digest analysis as described above.

Construction of the Deletion Vector pAM/hOgg1(Δ -47 – 44)

The Nrf2 deletion plasmid was generated from the pAM/hOgg1-*hr*GFP-WPRE-BGH-polyA expression vector (described above) using Stratagene Quick-Change mutagenesis system (Stratagene, Cedar Creek, TX) and site-specific mutagenesis primers (see Appendix A, section 4) to generate a new GFP reporter construct. A four nucleotide run upstream of the transcription initiation site spanning from position – 47 to – 44 was deleted from the human Ogg1 promoter and was designated as pAM/hOgg1(Δ -47 - 44). Mutagenesis reactions were set up using a control reaction and an experimental reaction. The control reaction is based on the mutagenesis of a non-functional β-galactosidase gene into a functional one capable of utilizing X-GAL and producing a β-gal$^+$, blue colony phenotype therefore indicating successful mutation of parental plasmid DNA. Control reactions were set up according to manufacturer's instructions as follows in sterile 0.25 mL reaction tubes (Axygen Scientific, Union City, CA): 1X reaction buffer, 10 ng pWhitescript® 4.5 Kb control plasmid 125 ng control primer # 1, 125 ng control primer # 2, 1 μL dNTP's, volume brought to 50 μL with sterile nuclease free H_2O, and 2.5 U *Pfu Turbo* polymerase. Experimental reactions were set as follows in separate sterile 0.25 mL reaction tubes (Axygen Scientific, Union City, CA): 1X reaction buffer, 25 ng pAM/hOgg1-*hr*-GFP-WPRE-BGH-polyA expression vector, 125 ng forward deletion primer, 125 ng reverse deletion primer, 1 μL dNTP's, volume brought to 50 μL with sterile nuclease free H_2O and 2.5 U *Pfu Turbo* polymerase. Reactions were run using a DNA Engine thermal cycler (MJ Research, Waltham, MA) under the following

conditions: [Control rxn, 95° C for 30 sec, **95° C for 30 sec, 55° C for 60 sec, 68° C for 5 min, **repeat amplification cycle 12X]; [Experimental rxn, 95° C for 30 sec, **95° C for 30 sec, 55° C for 60 sec, 68° C for 5 min, **repeat amplification cycle 16X]. Reactions were placed on ice for 2 min following thermal cycling to cool reactions to 37° C. 10 U of *Dpn I* restriction enzyme was added to each reaction and gently mixed and incubated at 37° C for 60 min to digest parental plasmids. Reactions were placed on ice and transformed into XL-1 Blue supercompetent cells (Stratagene, Cedar Creek, TX). Heat shock transformation of XL-1 Blue cells was performed under the following conditions: 50 μL XL-1 Blue cells were transferred to a pre-chilled 14 mL Falcon (BD Biosciences) polypropylene tube on wet ice. 1 μL of *Dpn I* digested reaction was added and gently mixed. Transformations were incubated on ice for 30 min and heat shocked at 42° C for 45 sec. Transformations were placed on ice for 2 min prior to the addition of 0.5 mL of NYZ^{+} recovery broth pre-heated to 42° C. Transformations were incubated at 37° C, shaker speed of 225 rpm for 1 hr. Following incubation, both control and experimental transformations were plated at volumes of 250 μL on LB ampicillin (100 μg/mL) plates also containing 20 mM IPTG and 80 μg/mL X-GAL. Mutation efficiency was calculated based on the percentage of blue colonies present on the control reaction plate. Single colonies grown on the experimental plates were selected and grown in liquid LB ampicillin broth (100 μg/mL). The pAM/hOgg1(Δ -47 - 44) vectors were extracted and purified using Mini-prep plasmid DNA purification kits (QIAGEN, Valencia, CA). The purified vector underwent restriction digest analysis using Asp718 and BamHI restriction enzymes (Roche Applied Science, Indianapolis, IN) to verify the

presence of the 2.1 Kb fragment. Deletion constructs were sequenced by Murdock Sequencing Facility, University of Montana.

Construction of the Expression Vector pGL3/hOgg1-Luc+

A vector expressing the firefly luciferase enzyme, designated as pGL3/hOgg1-Luc+, was constructed by ligation of the same 2.1 Kb fragment from the hOgg1 promoter (described above) into the pGL3-Basic expression vector (Promega, Madison, WI) using *Asp*718 and *Bgl*II restriction sites.

Mammalian Nrf2 Expression Vectors

Mammalian Nrf2 expression vectors, pEF-Basic and pEF-Nrf2, were kindly provided by Dr. Jeffrey Johnson (University of Wisconsin School of Pharmacy, Madison, Wisconsin).

FACS Analysis of GFP Expression

HEK293T cells were transfected using PolyFECT reagent (QIAGEN, Valencia, CA) as described above. Four different transfection groups were set up using the following vectors and one group receiving no plasmid DNA: pAM/CAG-*hr*GFP-WPRE-BGH-polyA, pAM/hOgg1-*hr*GFP-WPRE-BGH-polyA, pAM/hOgg1(Δ -47 - 44). Cells were harvested in culture media and centrifuged at 1500 rpm for 5 min at 4° C. Cells were washed 1X in cold sterile PBS and centrifuged again at 1500 rpm for 5 min at 4° C. Final cell suspensions were diluted to 5 x 10^5 cells/mL and in cold, sterile PBS and measurement of GFP was performed using a FACS Aria Flow cytometer (BD Biosciences, San Jose, CA). Excitation was set at λ = 488nm with an Argon gas laser, emission was measured at λ = 510 nm using a 530/30 filter set. Total fluorescence was

calculated from 10,000 cells per group with final results expressed as the median population fluorescence.

PCR Verification of GFP Plasmid Transfections

Cultures of HEK 293T cells transfected with GFP expression vectors as described above were processed for genomic isolation of DNA using a Wizard® Genomic DNA Purification Kit (Promega, Madison, WI). Extraction procedures were performed by transferring cell suspensions to 1.5 mL sterile eppendorf tubes and centrifuging at 13,000 rpm, 25° C for ~ 10 sec. Supernatants were removed and cells were suspended in residual PBS followed by addition of 600 μL of Nuclei Lysis Solution. 3 μL of 4 mg/mL RNAse A suspended in10 mM Tris-HCl pH = 7.4, 1 mM EDTA pH = 8.0 (TE) was added to each sample and mixed by inversion 6X. Samples were incubated in a 37° C water bath for 30 min and cooled to 25° C for 5 min. 200 μL of Protein Precipitation Solution was added to each sample and vortexed for 20 sec. Samples were incubated on ice for 5 min and centrifuged at 13,000 rpm, 25° C for 4 min. Supernatants were carefully removed and transferred to a new sterile 1.5 mL eppendorf tube. 600 μL of 25 C 2-propanol added to each sample and gently mixed by inversion until white thread like strands of DNA appeared. Samples were centrifuged at 13,000 rpm, 25° C for 1 min with the supernatant carefully removed so as not to disturb the DNA pellet. 600 μL 70% ethanol was added as a wash step and samples were centrifuged at 13,000 rpm 25° C for 1 min. Ethanol was carefully removed and sample tubes dried on bench paper for 10 – 15 min or until tubes were absent of ethanol. 100 μL of TE buffer was added to each sample, mixed well, and rehydrated overnight at 4 C. Purified DNA was utilized for PCR of the *hr*GFP gene as verification of positively transfected cell cultures. PCR reactions

were set up as described above using 25 ng total DNA and run using a DNA Engine thermal cycler (MJ Research, Waltham, MA).

Synthetic Oligonucleotide Radio Labeling

Synthetic oligonucleotide probes containing transcription factor binding sites were radio-labeled with γ-[^{32}ATP] prior to annealing to a complementary strand (Integrated DNA Technologies Inc., Coralville, IA). Reactions were set up under the following conditions: 39 μL ddH_2O, 5 μL 10X T4 kinase buffer, 2 μL (20 pmoles) of sense strand synthetic oligonucleotide, 3 μL of γ-[^{32}ATP] (7,000 mCi / mmole) (MP Biomedicals, Solon, OH), 1 μL of T4 polynucleotide kinase (Roche Applied Science, Indianapolis, IN) to a 500 μL eppendorf tube. The reaction mixture was mixed well and incubated at 37° C for 30 min. Subsequent to incubation, the reaction mixture was added to a pre-spun G25 sephadex column and allowed to sit for 2 min. The column was spun at 5000 rpm for 3 min. 5 μL of labeling buffer was added composed of the following reagents: 10 mM Tris-HCl, 1 mM EDTA pH = 7.9, 33 mM NaCl, pH = 8.0. Following addition of labeling buffer, 2 μL (20 pmoles) of the synthetic complement oligonucleotide (Integrated DNA Technologies Inc., Coralville, IA) was added. The mixture was heated to 95° C in a water bath and allowed to cool to 25° C overnight. The radio labeled double stranded probes were stored at –20° C until utilized. Unlabeled (cold) double stranded oligonucleotide probes were prepared under the following conditions at a final concentration of 20 pmoles/μL: 30 μL of labeling buffer, 10 μL (1000 pmoles) sense strand oligonucleotide, 10 μL (1000 pmoles) of anti sense strand oligonucleotide. Annealing reactions were heated to 95° C in a water bath and allowed to cool to 25° C overnight.

Nuclear Protein Extraction

Nuclear proteins from cultured HEK 293T cells were extracted according to the protocol published by Basha et al. (Basha, Wei et al. 2005) with modifications. Cell cultures were extracted using sterile PBS containing 1.3% protease inhibitor cocktail (Roche Applied Science, Indianapolis, IN), transferred to a 15 mL conical vial, and centrifuged at 125 x g for 6 min. Samples were washed using 1 mL sterile PBS with protease inhibitors, transferred to a sterile 1.5 mL eppendorf tube and centrifuged at 125 x g for 5 min. The wash step was repeated and the PBS supernatant removed following centrifugation. Sample pellets were suspended in 250 μL of buffer A containing the following reagents: 10 mM HEPES buffer pH = 7.9, 1.5 mM $MgCl_2$, 0.5 mM DTT, 0.5 mM EDTA, and 0.2 mM phenylmethanesulfonyl fluoride (PMSF). Samples were mixed well and homogenized using a VirSonic Ultrasonic Cell Disruptor 100© (VirTis, Gardiner, NY) using five consecutive 2 sec bursts on ice. Following homogenization, samples were centrifuged at 6000 rpm for 2 min at 4° C with the supernatant carefully removed. 150 μL of buffer A was added and samples were sonicated and centrifuged. The supernatant was removed and samples were suspended in 100 μL of buffer C composed of the following reagents: 20 mM HEPES buffer pH = 7.9, 1.5 mM $MgCl_2$, 0.5 mM DTT, 0.5 mM EDTA, 420 mM NaCl, 20% glycerol, 0.2 mM PMSF, 2 ng/mL aprotinin, 0.5 ng/mL leupeptin, 6 μL of 6% Triton X-100. Samples were vortexed and sonicated for 2 sec on ice. Final suspensions were centrifuged at 14000 rpm for 10 min at 4° C, snap frozen in liquid N_2 and stored at – 80° C until utilized for gel mobility shift assays. Total protein values were obtained using the bicinchoninic acid (BCA) protein determination assay (Pierce, Rockford, IL).

Electrophoretic Mobility Shift Assay EMSA

Changes in transcription factor binding were performed using the gel electrophoretic mobility shift assay (EMSA). Nuclear extracts were collected from HEK293T cells as described above. Oligonucleotides containing sequences corresponding to transcription factor binding sites from the human Ogg1 promoter were obtained from a commercial source (Integrated DNA Technologies Inc., Coralville, IA): Consensus Nrf2 binding site, putative hOgg1 Nrf2 binding site, Sp1 Oligo Set 1 (detailed oligonucleotide sequences can be referenced in Appendix A, Section 2). Oligonucleotides were 5' end labeled using [γ-^{32}P] ATP and binding reactions were set up as follows: 0 to 30 μg of nuclear extract normalized to equal volumes of 20 μL, 0.4 pmoles of labeled probe, 10 μL of binding buffer containing the following reagents: 20% glycerol, 5 mM $MgCl_2$, 2.5 mM EDTA, 2.5 mM DTT, 250 mM NaCl, 50 mM Tris-Hcl pH = 7.5, 0.2 μg/μL poly dI-dC. Binding reactions were incubated at 25° C for 30 min and separated on a 6% native polyacrylamide gel composed of the following reagents: 3.42 mL 40% acrylamide/ bis-acrylamide, 2 mL of 10X TBE buffer, 17.16 ddH_2O, 210 μL 10% ammonium persulfate, 21 μL N,N,N',N'-Tetramethylethylenediamine (BioRad). Gel reagents were mixed and cast into glass gel plates at a volume of 22.5 mL and allowed to polymerize. Samples were loaded and run in 0.5X TBE buffer for 2 hr at 200 V to resolve protein-DNA complexes. Following complex separation, the gel was removed using a 7 x 9 inch piece of blot paper (Bio-Rad Laboratories, Hercules, CA), encased in cellophane plastic wrap and placed into an imaging cassette holder (Bio-Rad Laboratories, Hercules, CA). An imaging plate (Fuji Film Life Science, Stamford, CT) was exposed to gels for approximately 30 to 60 min. Imaging plates were read using a

FLA-3000 Series Fuji Film Fluorescent Image Analyzer (Fuji Film Life Science, Stamford, CT) and ImageGauge© version 4.22 analysis software (Fuji Photo Film Co., LTD, Stamford, CT).

Fluorescent Measurement of Cellular GSH

Assessment of intracellular GSH was measured fluorescently as described previously (Cox 2007)(Appendix B). Media containing Hoechst 33342 (Molecular Probes, Carlsbad, CA, USA) was added to a final concentration of 0.5 μg/mL Hoechst 33342/well and incubated for 30 min at 37° C. Plates were drained of media and a 40 μM solution of dibromobimane suspended in sterile pre-warmed phosphate buffered saline was gently added to a final volume of 200 μL/well and incubated at 37° C for 30 min. Fluorescent measurement was performed using a SPECTRAmax© Gemini XS fluorescent plate reader (Molecular Devices, Sunnyvale, CA).

Dual Luciferase Reporter Gene Assays

HEK293T cells were co-transfected as described above with luciferase expression plasmids (pGL3-hOgg1-Luc+, pRL-TK-*renilla*-Luc+), or control plasmid (pGL3-Basic). Following timed exposures, lysates were collected and measured for *firefly* and *renilla* luciferase activities using the Dual Luciferase Assay (DLR) system (Promega, Madison, WI). Individual wells were lysed using 100 μL 1X PLB® lysis buffer and rocked for 30 min. Lysates were collected and stored at – 80° C until utilized. DLR assays were set up as follows with all reagents equilibrated to room temperature: 100 μL of LARII® firefly luciferase substrate was added to 20 μL lysate for measurement of firefly luciferase activity under regulation of the hOgg1 promoter fragment (pGL3-hOGG1). 100 μL of substrate STOP & GLO® reagent was added to assess the reference vector activity (pRL-

TK-*renilla*-Luc+). Endpoint luminescence was measured for both reactions using a SpectraMAX® Gemini XS Micro-plate reader (Molecular Devices, Sunnyvale, CA) with the following settings: *firefly* luciferase emission λ = all wavelengths, *renilla* luciferase emission λ = 488 nm, PMT setting = Auto, measurement frequency = 10 reads/well. Values were normalized by the ratio of *firefly* luciferase activity to *renilla* luciferase activity and expressed as percent change from day and time-matched control. Experimental data was combined from independent experiments collected from independent days.

Statistical Analysis

One-way ANOVA analysis was used with the students Neuman-Keuls post-hoc test to evaluate differences between control and experimental groups for changes in GSH and luciferase activity. Statistical tests were performed using GraphPad® Prism statistical software (Sorrento, CA) with a $p < 0.05$ considered statistically significant.

Results

To evaluate the putative Nrf2 binding site capacity for modulating hOgg1 promoter function, a 2.1 Kb fragment of the hOgg1 promoter fragment was cloned into a GFP expression vector (pAM/hOgg1-promoter). Using site-directed mutagenesis, a four base pair run at position -47 to -44 (TTCC), proposed to be a binding site for Nrf2, was deleted from that region of the hOgg1 promoter. Twenty-four hr post-transfection, GFP expression in the non-specific pAM/CAG control vector and in the pAM/hOgg1-promoter GFP expression vector was strong, indicating that the cells were functionally expressing GFP (Figure 7A, top & middle). However, deletion of four base pairs from the hOgg1 promoter resulted in a visual attenuation of GFP expression compared to both the pAM/CAG and pAM/hOgg1-promoter expression vectors (Figure 7A, bottom). The reduction in GFP expression was visually equivalent to the no plasmid control cultures (data not shown) indicating that fluorescence was specific to cultures receiving functional expression vectors.

FIGURE 7A

pAM/CAG-promoter

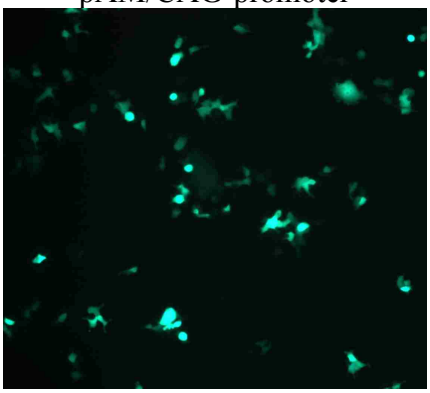

pAM/hOgg1-promoter

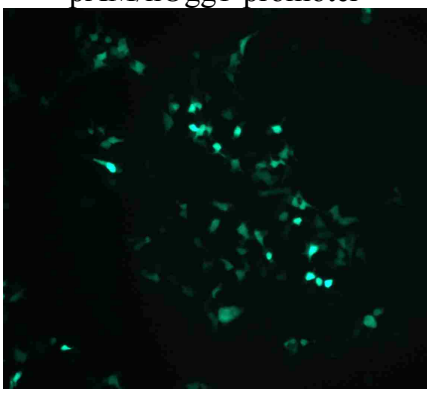

pAM/hOgg1-(Δ-47-44)

Figure 7A

Microscopic analysis of GFP expression in HEK293T cells under the regulation of different promoters. (A) Non-specific CAG promoter [pAM/CAG-promoter], hOgg1 promoter [pAM/hOgg1-promoter], hOgg1 promoter with the putative Nrf2 binding site deleted by site-directed mutagenesis, pAM/hOgg1-(Δ-47-44). (n = 6 per transfection group).

The experiment was independently repeated and assessed by flow cytometry revealing similar results. Deletion of the putative Nrf2 binding site decreased fluorescence to levels near the no plasmid control (Figure 7B) consistent with the results seen in Figure 7A. The results indicate that this area of the hOgg1 promoter is necessary for basal transcription as indicated by the loss of GFP expression in the absence of the putative Nrf2 binding site; region –47 to –44 of the hOgg1 promoter.

FIGURE 7B

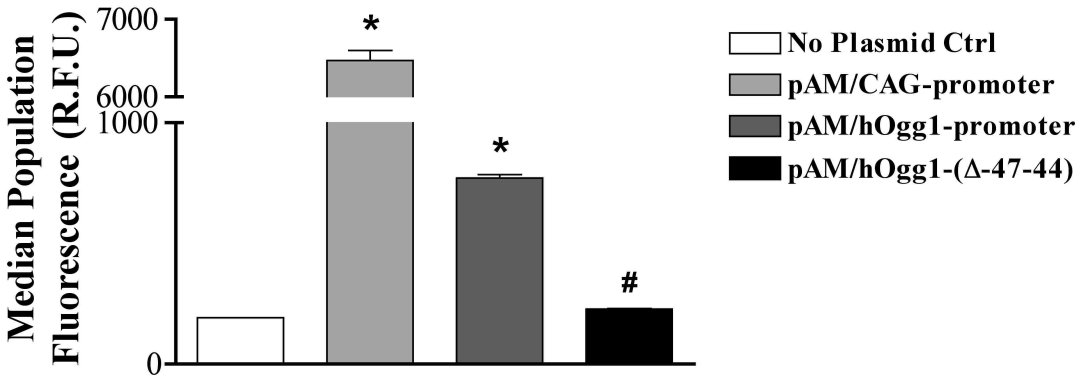
Median Population Fluorescence (R.F.U.)
7000
6000
1000
0
*
*
#
No Plasmid Ctrl
pAM/CAG-promoter
pAM/hOgg1-promoter
pAM/hOgg1-(Δ-47-44)

Figure 7B

Flow cytometric analysis of GFP expression from the promoters outlined in Figure 7A. Data is represented as mean ± S.E.M. (n = 6 to 9) * Denotes significant difference from no plasmid control fluorescence. # Denotes significant difference in fluorescence from experimental vectors pAM/CAG-promoter & pAM/hOgg1-promoter. $P < 0.05$.

To verify transfection efficiencies, PCR was performed on DNA extracts from HEK 293T cells transfected with the different GFP expression vectors. This was performed to verify successful transfection via the presence or absence of the *hr*GFP reporter gene. Figure 7C summarizes the results revealing the absence of DNA amplification in the no plasmid control cultures (lane 2). PCR amplification from the pAM/hOgg1 vector was positive in lanes 3 and 4 that contained stock plasmid DNA and extracted pAM/hOgg1 vector DNA respectively. Lanes 5 and 6 also had positive PCR amplification from the pAM/hOgg1-(Δ-47-44) stock and extracted cellular DNA validating the existence of the *hr*GFP gene in the transfected cultures containing the deletion construct.

FIGURE 7C

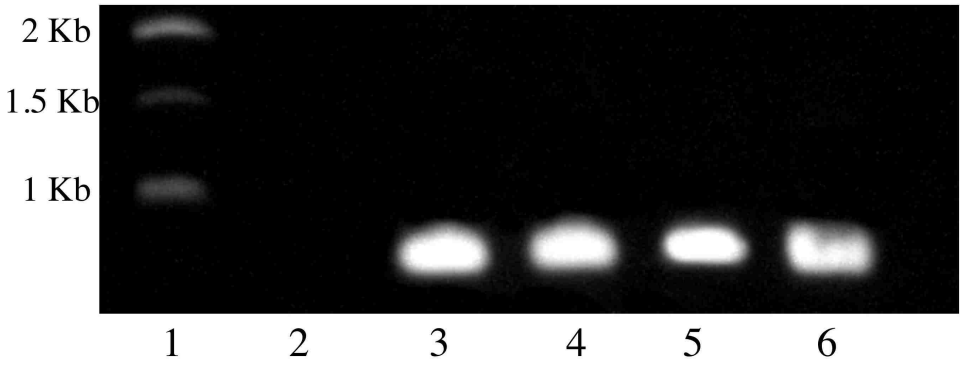

Figure 7C

PCR verification of the presence of the *hr*GFP gene from transfected HEK293T cultures (n = 2 per transfection group). PCR reactions from 25 ng DNA of transfected cultures: Lane 1 DNA size ladder, Lane 2 no plasmid control, Lane 3 stock pAM/hOgg1 vector DNA, Lane 4 DNA extracted from pAM/hOgg1 transfected cultures, Lane 5 stock pAM/hOgg1-(Δ-47-44) vector, Lane 6 DNA extracted from pAM/hOgg1-(Δ-47-44) transfected cultures.

Gel mobility shift assays have been successfully used to identify protein interaction with specific sequences of DNA. To evaluate protein interaction with the reported putative Nrf2 site in the hOgg1 promoter, nuclear extracts from untreated and tBHQ treated HEK 293T cells were incubated with γ-^{32}P labeled, double stranded oligonucleotides containing a 25 base pair span of the hOgg1 promoter (H-Nrf2) containing the sequence that could serve as a Nrf2 binding site. As shown in figure 8A, untreated nuclear extracts incubated with the labeled hOgg1 probe produced a shifted band whose density increased with increasing amounts of total protein (Left Panel). This band intensity decreased with co-incubation of an equivalent amount of unlabeled (cold) hOgg1 probe indicating specificity for protein interaction with that sequence of the hOgg1 promoter (Left Panel). Figure 8A also demonstrates that incubation with the consensus Nrf2 probe yields a band that shifts to an equivalent distance as the hOgg1-Nrf2 shifts, and yields an increase in density with increasing amounts of total protein (Right Panel).

Nrf2 has been shown to activate and translocate to the nucleus upon addition of inducing compounds including *tert*-butylhydroquinone (tBHQ). This leads to an increase in the nuclear levels of Nrf2 (Lee, Moehlenkamp et al. 2001; Hansen, Watson et al. 2004). Nuclear extracts from HEK 293T cells exposed to 25 μM tBHQ for 6 hr resulted in increased binding that remained constant at 10 and 20 μg total protein when compared to untreated control bands (Figures 8A Middle Panel). This is further summarized in Figure 8C by the representative bar plot. The intensity of the band produced with 20 μg of protein from the tBHQ treated cells had an equivalent density as the band produced at 30 μg protein from untreated cells (Figure 8C). The increase in binding seen with tBHQ

exposure is expected considering tBHQ increases nuclear levels of Nrf2 via activation and translocation of the transcription factor subsequent to tBHQ exposure (Lee, Moehlenkamp et al. 2001). It also demonstrates that binding to the putative Nrf2 site of the hOgg1 promoter is also increased by tBHQ treatment as evidenced in Figure 8A (Gel), and Figure 8C (Bar Plot).

FIGURE 8

A

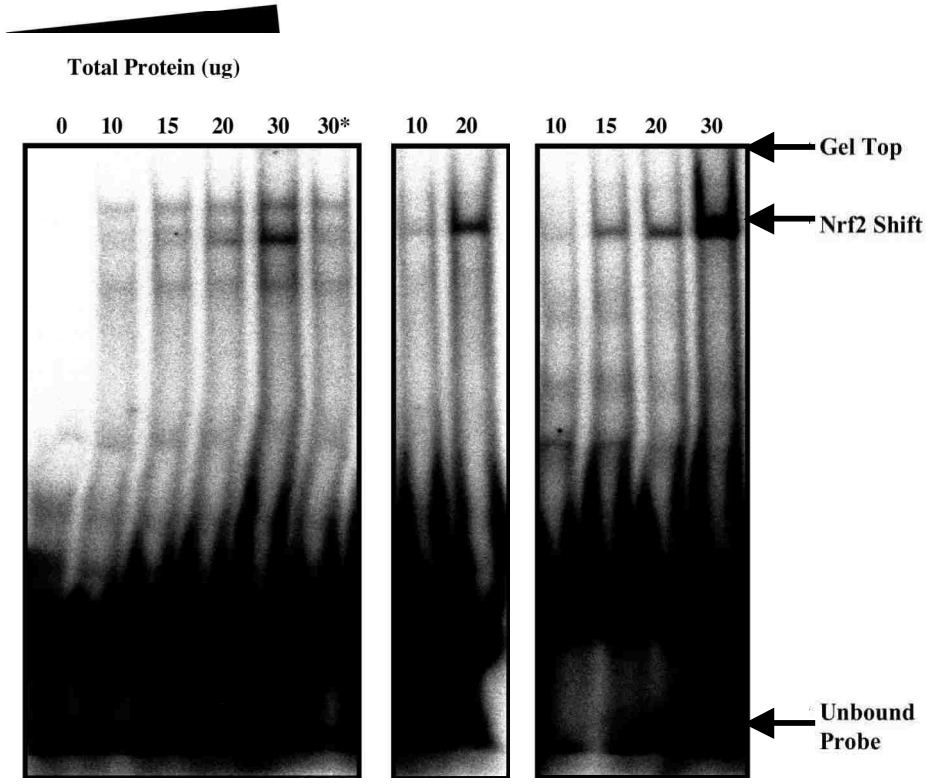
Total Protein (ug)
0 10 15 20 30 30* 10 20 10 15 20 30
Gel Top
Nrf2 Shift
Unbound Probe
Panel: Left Middle Right

FIGURE 8

B

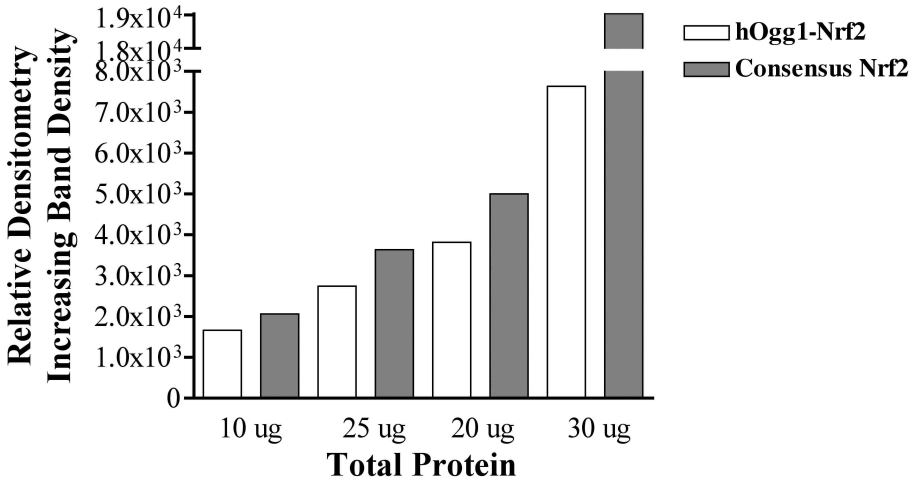
Relative Densitometry
Increasing Band Density
1.9x10⁴
1.8x10⁴
8.0x10³
7.0x10³
6.0x10³
5.0x10³
4.0x10³
3.0x10³
2.0x10³
1.0x10³
0
10 ug
25 ug
20 ug
30 ug
Total Protein
hOgg1-Nrf2
Consensus Nrf2

C

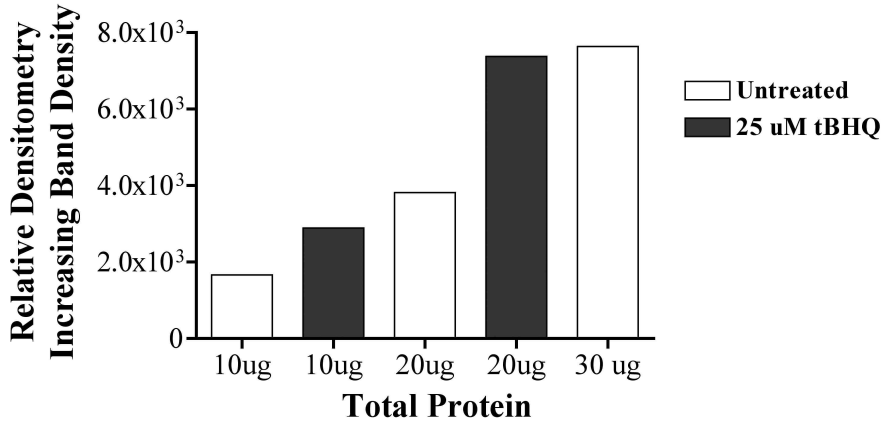
Relative Densitometry
Increasing Band Density
8.0x10³
6.0x10³
4.0x10³
2.0x10³
0
10ug
10ug
20ug
20ug
30 ug
Total Protein
Untreated
25 uM tBHQ

Figure 8

EMSA binding analysis of the putative Nrf2 binding site in the hOgg1 promoter. EMSA was performed using γ-^{32}P labeled, double stranded oligonucleotide probes containing the putative Nrf2 binding site from the hOgg1 promoter. Arrows point to Nrf2 shifted bands and unbound probe.

(A) Binding reactions using nuclear extract from untreated HEK293T cells over a protein range of 0 to 30 μg total protein incubated with labeled hOgg1-Nrf2 or consensus Nrf2 probe (Left & Right Panels). Addition of 2X unlabeled (cold) hOgg1-Nrf2 probe to 30 μg of total protein (indicated by 30*) outcompetes the labeled (hot) hOgg1 probe for binding (Left Panel). Binding reactions using nuclear extracts from HEK293T cells treated for 6 hr with the Nrf2 inducing compound tBHQ (25 μM) (Middle Panel).

(B) Representative plot of relative band densities from EMSA reactions in Figure 8A with increasing amounts of total protein from untreated HEK 293T cells (representing Figure 8A Left & Right Panels).

(C) Representative plot of relative band densities from EMSA reactions in Figure 8A using nuclear extracts from untreated HEK293T cells, and cells treated for 6 hr with 25 μM of the Nrf2 inducing compound tBHQ (representing Figure 8A Left & Middle Panels).

In order to determine the binding specificity of the putative Nrf2 recognition sequence with nuclear protein, cross-competition EMSA analysis was done against the consensus sequence for Nrf2. As seen in Figure 9A the consensus Nrf2 probe (C-Nrf2) shifts to an equivalent migration distance as the hOgg1 probe (H-Nrf2) similar to the data in Figure 8. Cross competition experiments were also performed to determine binding specificity for both consensus Nrf2 and hOgg1-shifted bands. Co-incubation of labeled consensus Nrf2 probe with unlabeled hOgg1 probe outcompetes protein interaction with the consensus Nrf2 probe. Similarly co-incubation of the hOgg1 probe with unlabeled consensus Nrf2 probe outcompetes binding with the hOgg1 fragment suggesting the protein binding to the hOgg1 promoter can bind to a consensus Nrf2 sequence with an equivalent specificity. It is worth noting that although there are two other bands present in the hOgg1-Nrf2 binding reactions, those bands are not outcompeted by the presence of unlabeled consensus Nrf2 probe (Figure 9A).

FIGURE 9A

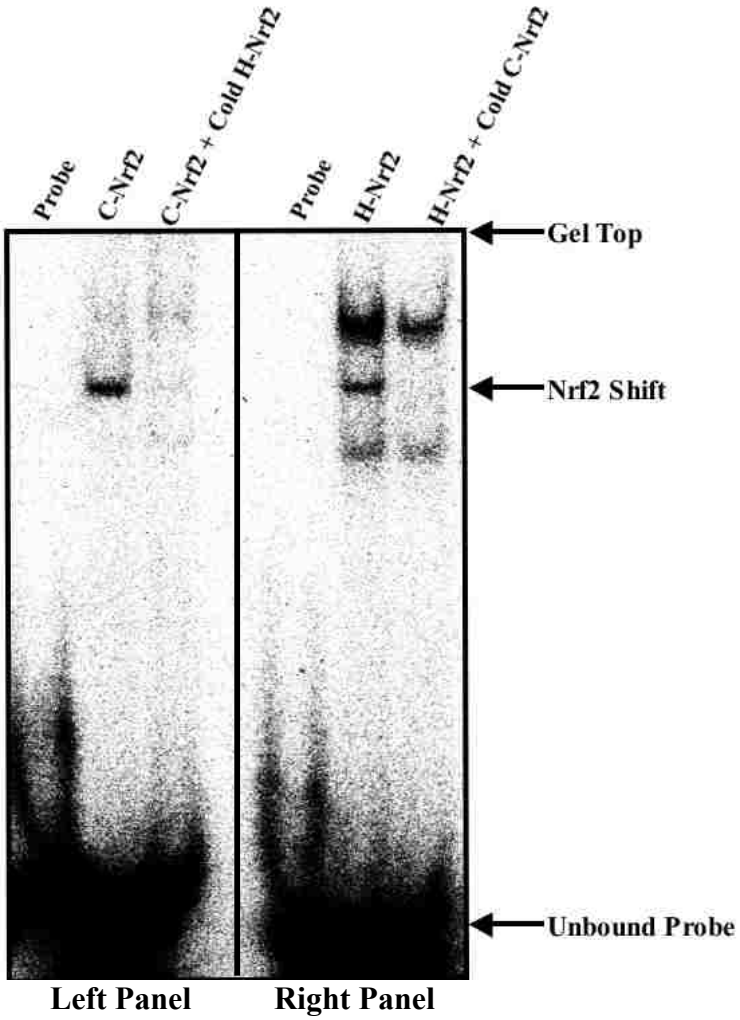
Probe
C-Nrf2
C-Nrf2 + Cold H-Nrf2
Probe
H-Nrf2
H-Nrf2 + Cold C-Nrf2
Gel Top
Nrf2 Shift
Unbound Probe
Left Panel
Right Panel

Figure 9A

Competitive binding analysis of the putative Nrf2 site in the hOgg1 promoter. Competition EMSA were performed using 30 μg nuclear extracts from untreated HEK293T cells, and γ-^{32}P labeled probes containing the consensus (C-Nrf2) and putative hOgg1 Nrf2 binding site (H-Nrf2). Arrows point to the Nrf2 shifted band and unbound probe. Left Panel: Labeled consensus Nrf2 was co-incubated with 100X unlabeled hOgg1-Nrf2 probe (indicated by C-Nrf2 + Cold H-Nrf2). Right Panel: Labeled hOgg1-Nrf2 was co-incubated with 100X unlabeled C-Nrf2 probe (indicated by H-Nrf2 + Cold C-Nrf2).

To assess the specificity for binding on the consensus Nrf2 probe, competition EMSA was performed using a radiolabeled probe containing a binding sequence for Sp1 transcription factor (Figure 9B). Co-incubation of unlabeled (cold) consensus Nrf2 probe with labeled probe containing an Sp1 binding sequence derived from the hOgg1 promoter shows that the unlabeled consensus Nrf2 probe has no effect on Sp1 binding (Figure 9B). Furthermore co-incubation of an unlabeled different Sp1 probe disrupts interaction with the hOgg1 Sp1 probe. These findings reaffirm that binding is similar between the consensus Nrf2 and hOgg1 fragments, and also shows that the consensus Nrf2 binding sequence does not interfere with binding at the Sp1 transcription factor binding sequence.

FIGURE 9B

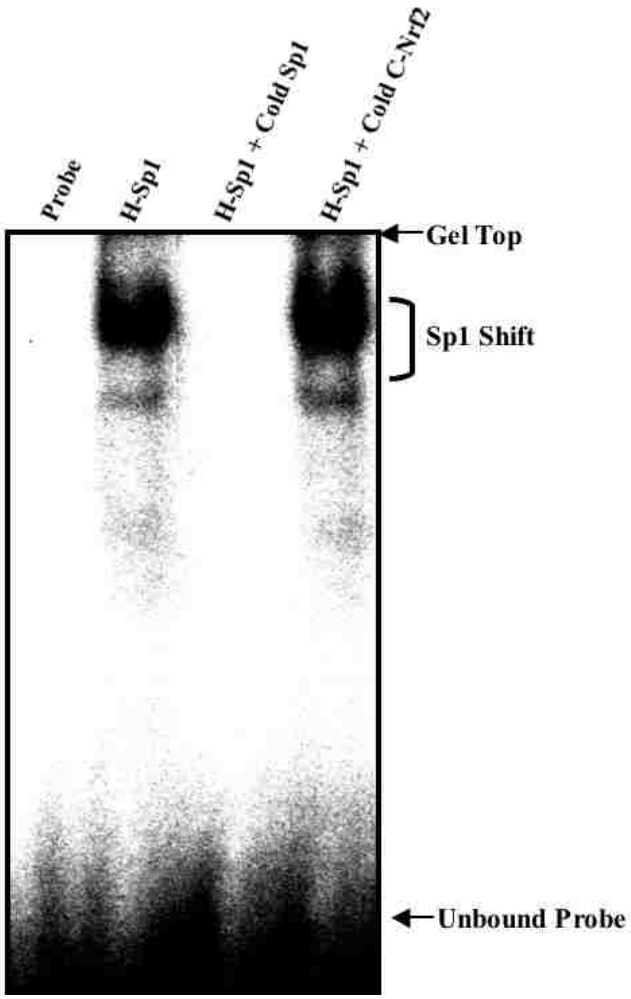
Probe
H-Sp1
H-Sp1 + Cold Sp1
H-Sp1 + Cold C-Nrf2
Gel Top
Sp1 Shift
Unbound Probe

Figure 9B

Competitive protein binding analysis of the putative Nrf2 site in the hOgg1 promoter. Competition EMSA were performed using γ-^{32}P labeled, double stranded oligonucleotide probes containing an Sp1 binding site from the hOgg1 promoter and the consensus Nrf2 (C-Nrf2) binding site. The Sp1 shifted bands are indicated by the bracket and unbound probe by the arrow. Additional competition EMSA showing displacement of Sp1 binding by unlabeled Sp1 probe (H-Sp1 + Cold Sp1) but not unlabeled consensus Nrf2 probe (H-Sp1 + Cold C-Nrf2).

It has been established that changes in the redox state of the cell lead to changes in the transcription of genes regulated by the transcription factor Nrf2. To test the role of Nrf2 in the transcriptional regulation of hOgg1 in relation to levels of GSH, the 2.1 Kb fragment of the hOgg1 promoter was cloned into a firefly luciferase expression vector and transcriptional changes were assessed using known Nrf2 inducing compounds; tBHQ and DEM (Lee, Moehlenkamp et al. 2001). As a surrogate measure of antioxidant response, levels of GSH were also measured in parallel with each dual luciferase reporter (DLR) assay (Figures 10 through 13). Figure 10 summarizes the changes in GSH and hOgg1 transcriptional activity associated with treatment of 25 μM tBHQ for 24 hr. As shown in Figure 10A tBHQ increases GSH after a 24 hr exposure indicative of an Nrf2 mediated change. The activity of hOgg1 transcription (luciferase activity) yielded similar results with an increase in luciferase activity at 24 hr compared to untreated controls (Figure 10B). Serving as transfection control, the promoterless, pGL-Basic vector cultures yielded values less than 5% of luciferase activity in both untreated and tBHQ treated cultures.

FIGURE 10

A

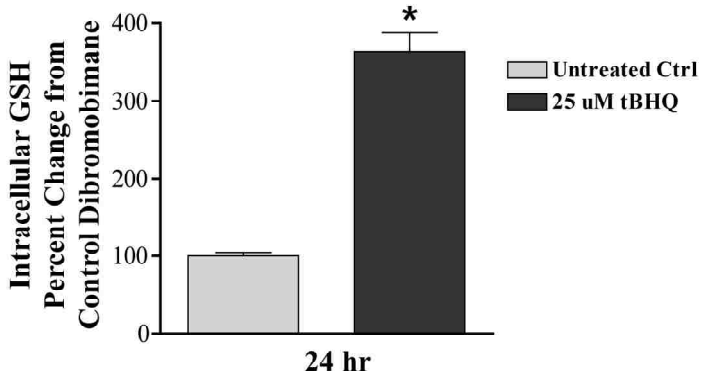
Intracellular GSH
Percent Change from
Control Dibromobimane
400
300
200
100
0
*
Untreated Ctrl
25 uM tBHQ
24 hr

B

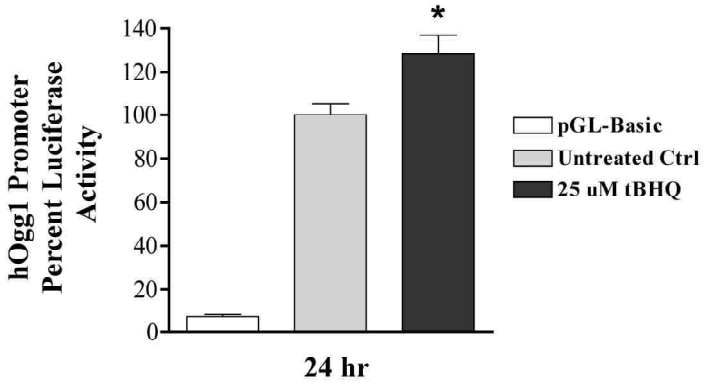
hOgg1 Promoter
Percent Luciferase
Activity
140
120
100
80
60
40
20
0
*
pGL-Basic
Untreated Ctrl
25 uM tBHQ
24 hr

Figure 10

Analysis of GSH levels and modulation of the hOgg1 promoter in HEK293T cells treated for 24 hr with 25 μM tBHQ. (A) Levels of GSH are reported as percent of untreated control values assessed by changes in dibromobimane fluorescence. Data is represented as mean ± S.E.M. (n = 30). ***** Denotes significant difference from control GSH values. $P < 0.05$.

(B) Transcriptional modulation of the hOgg1 promoter by tBHQ assessed by measurement of dual luciferase enzymes. Final values were calculated by normalization to *Renilla* luciferase activity and expressed as percent of untreated control. Data is represented as mean ± S.E.M. (n = 5 - 10). ***** Denotes significant difference from day and time-matched control luciferase activity, $P < 0.05$.

To further investigate modulation of Ogg1, a different, known Nrf2 inducing compound, DEM (Lee, Moehlenkamp et al. 2001; Kaur, Kalia et al. 2006), was used to determine changes in GSH and hOgg1 transcription activity in HEK 293T cells. Figure 11A demonstrates that at 18 hr, a dose of 25 μM DEM caused no change in GSH when compared to untreated controls while at 24 hr there was a significant increase in GSH (Figure 11A). The transcriptional activity of hOgg1 yielded similar results to the levels of GSH with no change in luciferase activities occurring at 18 hr, and a significant increase at 24 hr of DEM exposure relative to the untreated control and 18 hr treatment groups (Figure 11B). Serving as transfection control, the promoterless pGL-Basic vector yielded values less than 5% of luciferase activities in both untreated and DEM treated cultures (Figure 11B). This pattern of induction of hOgg1 promoter activity by exposure to Nrf2 inducing compounds is similar to previous work looking at other Nrf2 regulated genes; including the induction of NQO1 by tBHQ (Lee, Moehlenkamp et al. 2001), and the induction of GCL, and MnSOD by DEM (Kaur, Kalia et al. 2006). These findings suggest that modulation of hOgg1 transcription is sensitive to intracellular levels of GSH and the transcription factor Nrf2 as indicated by increased promoter activity subsequent to Nrf2 induction.

FIGURE 11

A

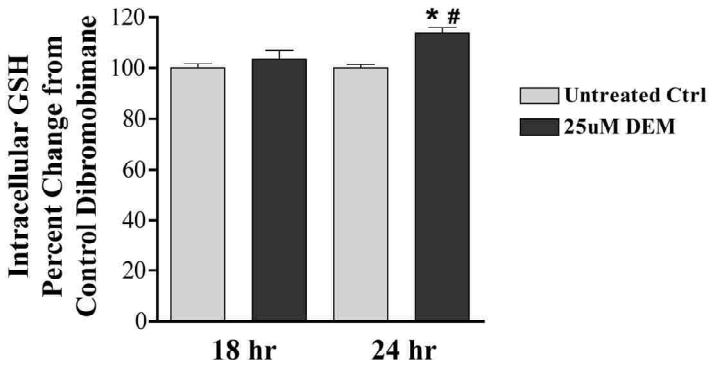
Intracellular GSH
Percent Change from
Control Dibromobimane
120
100
80
60
40
20
0
* #
18 hr
24 hr
Untreated Ctrl
25uM DEM

B

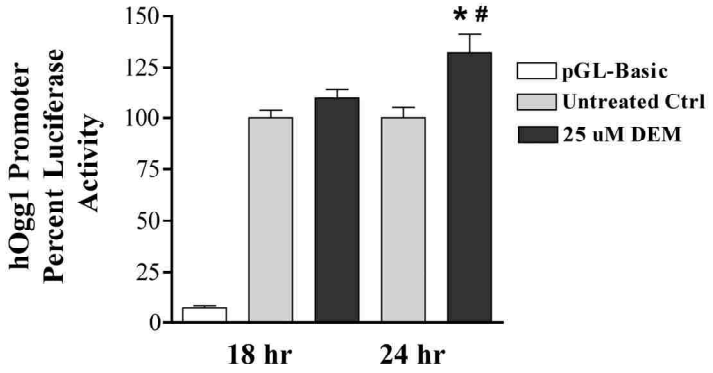
hOgg1 Promoter
Percent Luciferase
Activity
150
125
100
75
50
25
0
* #
18 hr
24 hr
pGL-Basic
Untreated Ctrl
25 uM DEM

Figure 11

Analysis of GSH levels and modulation of the hOgg1 promoter in HEK293T cells treated for 18 and 24 hr with 25 μM DEM. (A) Levels of GSH are reported as percent of untreated control values assessed by changes in dibromobimane fluorescence. Data is represented as mean ± S.E.M. (n = 6). ***** Denotes significant difference from control GSH values. # Denotes significant difference from 18 hr exposure group. $P < 0.05$. (B) Transcriptional modulation of the hOgg1 promoter by DEM assessed by measurement of dual luciferase enzymes. Final values were calculated by normalization to *Renilla* luciferase activity and expressed as percent of untreated control values. Data is represented as mean ± S.E.M. (n = 5 - 16). ***** Denotes significant difference from control luciferase activity. # Denotes significant difference from 18 hr exposure group. $P < 0.05$.

Both tBHQ and DEM are known inducers of Nrf2, however mechanistically it is reported that their mode of induction differs (Lee, Moehlenkamp et al. 2001). Activation of Nrf2 by DEM is a process more dependent on cellular oxidative stress initially facilitated by a reduction in GSH; a reduction that recovers via activation of Nrf2, and expression of genes involved in synthesis and homeostasis of cellular GSH. The redox-mediated modulation of hOgg1 transcriptional activity was tested by administration of the GSH derivative glutathione monoethyl ester (GSH-mee); ultimately shifting the cellular environment to a more reductive state. As shown in Figure 12A, levels of GSH were increased as early as 1 hr post-administration of 1 and 2 mM GSH-mee. At the 1 mM dose, levels of GSH remained increased until 18 hr where they returned close to control levels and remained at that level at 24 hr. The 2 mM dose was still elevated at 18 hrs and did not return to control levels until 24 hr (Figure 12A). Figure 12 B and C represent the 18 and 24 hr time points shown in Figure 12A expressed as percent of control GSH. Considering the early time points (Figure 12A), the levels of GSH were increased significantly for a substantial period of time (> 12 hr), creating a shift in the cellular redox environment to a more reductive state.

Promoter activity was subsequently assessed at the 18 and 24 hr time points to determine what effects 1 and 2 mM GSH-mee have on modulation of hOgg1 transcriptional activity. Figure 12C shows that at 18 hr, both 1 and 2 mM GSH-mee modulate hOgg1 transcriptional activity in a negative manner by decreasing transcriptional activity. The reduction in hOgg1promoter activity recovers by 24 hr suggesting that modulation of the hOgg1 promoter by GSH is a temporal event. It also suggests an Nrf2 dependent mechanism as others have shown that administration of

reducing agents can attenuate the induction of Nrf2 (Lee, Moehlenkamp et al. 2001; Kim, Hu et al. 2003) keeping it bound and sequestered in the cytosol by its inhibitory protein KEAP1 (Dinkova-Kostova, Holtzclaw et al. 2002).

FIGURE 12

A

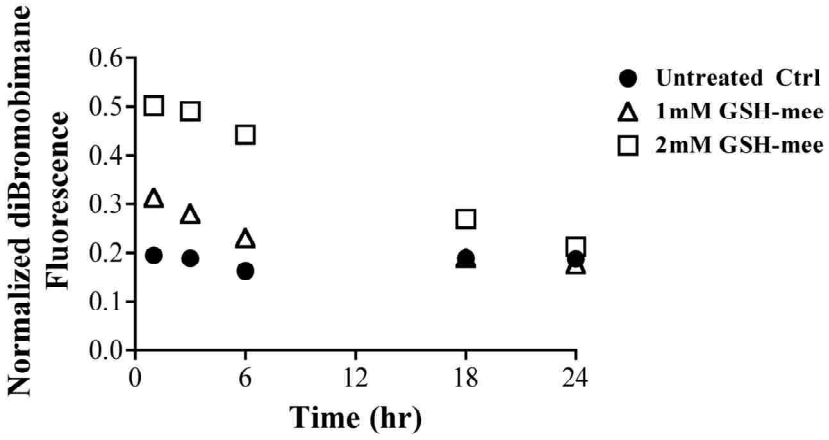
Normalized diBromobimane Fluorescence
0.6
0.5
0.4
0.3
0.2
0.1
0.0
0
6
12
18
24
Time (hr)
Untreated Ctrl
1mM GSH-mee
2mM GSH-mee

B

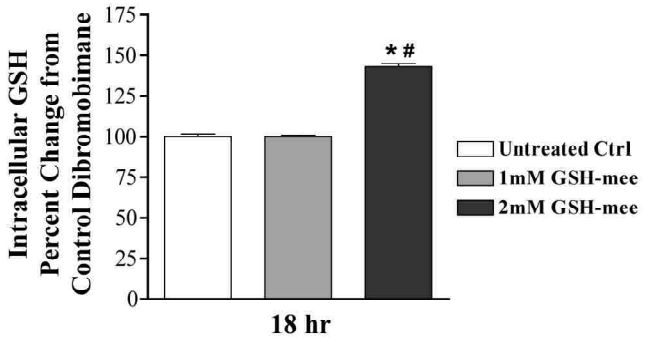
Intracellular GSH Percent Change from Control Dibromobimane
175
150
125
100
75
50
25
0
* #
18 hr
Untreated Ctrl
1mM GSH-mee
2mM GSH-mee

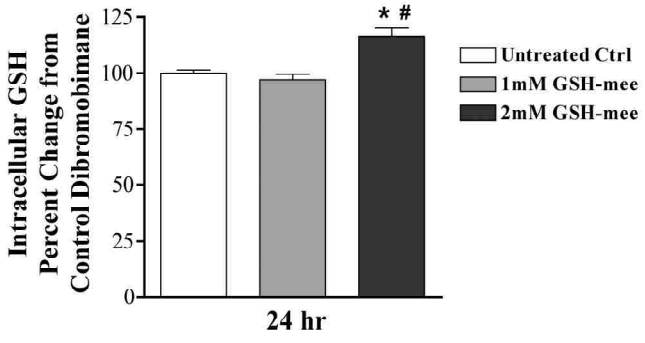
Intracellular GSH Percent Change from Control Dibromobimane
125
100
75
50
25
0
* #
24 hr
Untreated Ctrl
1mM GSH-mee
2mM GSH-mee

Figure 12

Analysis of GSH levels in HEK293T cells treated for 0 to 24 hr with 1 and 2 mM GSH-mee assessed by changes in dibromobimane fluorescence.

(A). Levels of GSH are reported as the level of dibromobimane fluorescence normalized to Hoechst 33342 fluorescence. Data is represented as mean ± S.E.M. (n = 5 - 6). ***** Denotes significant difference from control GSH values. # Denotes significant difference from 18 hr exposure group. $P < 0.05$.

(B) Analysis of GSH levels in HEK293T cells treated for 18 and 24 hr with 1 and 2 mM GSH-mee assessed by changes in dibromobimane fluorescence. Levels of GSH are reported as percent of untreated control values assessed by changes in dibromobimane fluorescence. Data is represented as mean ± S.E.M. (n = 5 - 6). ***** Denotes significant difference from control GSH values. # Denotes significant difference from 18 hr exposure group. $P < 0.05$.

FIGURE 12

C

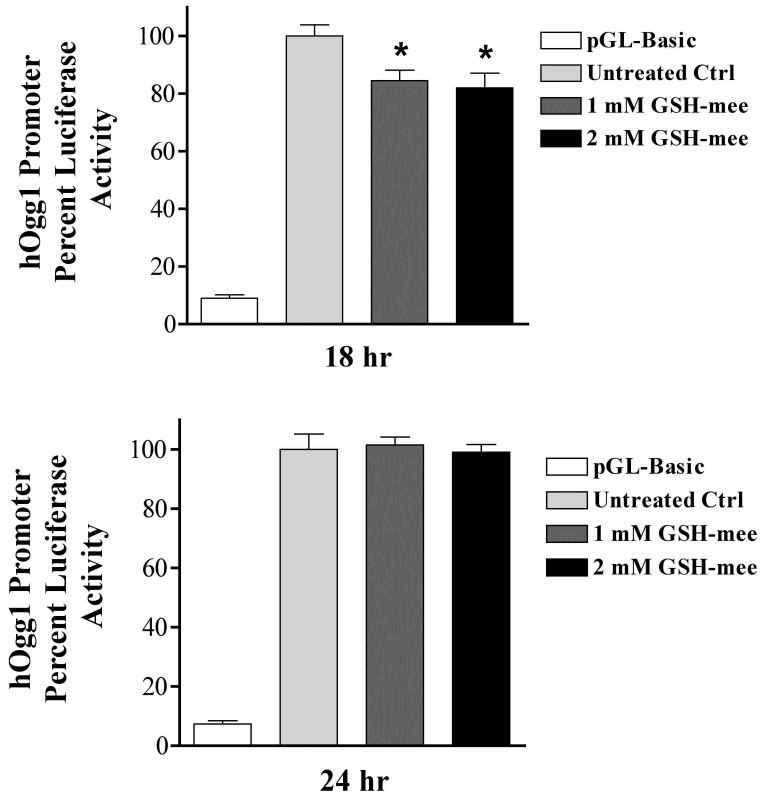
hOgg1 Promoter Percent Luciferase Activity
100
80
60
40
20
0
*
*
pGL-Basic
Untreated Ctrl
1 mM GSH-mee
2 mM GSH-mee
18 hr
hOgg1 Promoter Percent Luciferase Activity
100
80
60
40
20
0
pGL-Basic
Untreated Ctrl
1 mM GSH-mee
2 mM GSH-mee
24 hr

Figure 12

(C) Transcriptional modulation of the hOgg1 promoter by 1 and 2 mM GSH-mee assessed by measurement of dual luciferase enzymes. Final values were calculated by normalization to *Renilla* luciferase activity and expressed as percent of untreated control values. Data is represented as mean ± S.E.M. (n = 5 - 16) ***** Denotes significant difference from day and time matched control luciferase activity. $P < 0.05$.

These results support the notion that hOgg1 transcriptional regulation can occur similar to Nrf2 regulated genes by the presence of tBHQ and DEM (Figures 10 and 11B). They also show that an increased level of cellular GSH attenuates hOgg1 transcriptional activity (Figure 12C). To directly test the influence of Nrf2 in GSH mediated regulation of hOgg1 transcriptional activity, the addition of a mammalian Nrf2 expression vector was done in tandem with the DLR vectors. Figure 13 demonstrates that in the presence of empty control vector (pEF-Basic) and 1 mM GSH-mee for 18 hr, hOgg1-regulated luciferase activity is decreased when compared to untreated controls; results similar to those in Figure 12C. However, the addition of an additional vector expressing Nrf2 (pEF-Nrf2) showed no change from control in the presence of 1 mM GSH-mee for 18 hr. This suggests that over expression of Nrf2 was sufficient to recover the down modulation of hOgg1 transcriptional activity by 1 mM GSH-mee (Figures 12C and 13) supporting the argument for the existence of an Nrf2 regulatory site in the hOgg1 promoter.

FIGURE 13

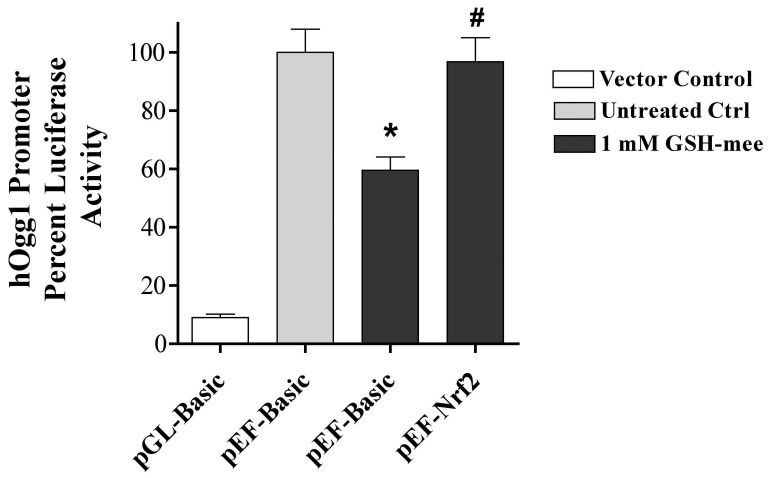
hOgg1 Promoter
Percent Luciferase
Activity
100
80
60
40
20
0
*
#
pGL-Basic
pEF-Basic
pEF-Basic
pEF-Nrf2
Vector Control
Untreated Ctrl
1 mM GSH-mee

Figure 13

Analysis of Nrf2 overexpression on modulation of hOgg1 promoter activity. HEK293T cells co-transfected with control vector (pEF-Basic) or an Nrf2 expression vector (pEF-Nrf2) were treated with 1 mM GSH-mee for 18 hr. Transcriptional modulation of the hOgg1 promoter was assessed by measurement of dual luciferase enzymes. Final values were calculated by normalization to *Renilla* luciferase activity and expressed as percent of untreated time and vector matched control. Data is represented as mean ± S.E.M. (n = 8 - 10). ***** Denotes significant difference from day and time-matched control luciferase activity. # Denotes significant difference from the control vector (pEF-Basic) GSH-mee exposed group. $P < 0.05$.

Conclusions

A four base pair run (TTCC) located at positions – 47 to – 44 in the hOgg1 promoter is essential for basal transcription of hOgg1-regulated GFP expression as determined by site-directed deletion and subsequent loss of GFP reporter gene expression. This region of the hOgg1 promoter is also capable of interacting with nuclear proteins from HEK293T cells as determined by electrophoretic gel mobility shift assays. In addition parallel-binding experiments using consensus Nrf2 oligonucleotides produced an equally shifted band as the hOgg1-Nrf2 experimental oligonucleotide. Further investigation into binding specificity suggests the involvement of the transcription factor Nrf2 as determined by competition experiments using consensus Nrf2, and Sp1 oligonucleotides. The transcriptional regulation of hOgg1 is sensitive to cell redox status as established by changes in both hOgg1-regulated luciferase activities and intracellular GSH in HEK293T cells exposed to the GSH modulating compounds tBHQ, DEM (increased transcription) and GSH-mee (decreased transcription). In addition, both increases and decreases in hOgg1 transcriptional activity were mediated temporally demonstrating changes characteristic of an acute stress response. Nrf2 over expression was able to counteract decreased hOgg1 transcriptional activity produced by GSH-mee again suggesting a role for Nrf2. In conclusion the transcription factor Nrf2 is important in the inducible regulation of Ogg1 and these changes are dependent on the redox status of the cell via modulation of intracellular GSH.

CHAPTER THREE

Effects of Sodium Arsenite on 8-hydroxy-2'-deoxyguanosine DNA Glycosylase Transcription and Activity

ABSTRACT

Arsenic (As) is a naturally occurring element found widely distributed in the environment. Arsenic is also considered an environmental toxin and has been associated with a myriad of adverse health effects. This statement is firmly supported by the high prevalence of health issues in areas of the world with high levels of arsenic in their drinking water. Exposure to arsenic has also been associated with oxidative stress and damage to DNA; specifically oxo^{8}dG. This study identified dramatic increases in the cellular antioxidant GSH, and varied changes in SOD activities subsequent to arsenite exposure in actively dividing and NGF treated PC12 cells. Assessment of Ogg1 activity and Ogg1 mRNA levels demonstrated a significant decrease for both subsequent to arsenite exposure. Further testing revealed no direct effect by arsenite on Ogg1 activity. Levels of oxo^{8}dG did not significantly change subsequent to arsenite exposure however increased trends were evident. Characterization of Sp1 binding revealed that treatment with sodium arsenite could decrease Sp1 binding at two unique Sp1 sites in the human Ogg1 promoter. We conclude that sodium arsenite can disrupt both the transcription and activity of Ogg1 in PC12 cells. This occurred despite the induction of cellular stress response via increases in GSH and Mn SOD activity.

INTRODUCTION

Arsenic and the Environment

Arsenic (As) is a naturally occurring element found widely distributed in both organic and inorganic forms. Inorganic arsenic is found environmentally in two main oxidation states; pentavalent arsenate As (V) and trivalent arsenite As (III) forms. The majority of environmental exposures to arsenic occur through drinking water, however to a lesser extent exposure can also occur via dietary consumption. An FDA study reported the average adult has a daily intake of 53 μg, 20% being in the inorganic forms (Brown and Ross 2002).

Occupational exposure to arsenic also occurs mainly via inhalation from smelting processes, and power plant combustion of fossil fuels. Arsenic contamination of soils and groundwater can also occur as a consequence of other anthropogenic activities such as mineral extraction, waste processing, and pesticides (Bates, Smith et al. 1992).

Despite the numerous anthropogenic sources, most arsenic related health effects occur from exposure to natural sources, mainly through drinking water. Epidemiological studies identify unique locations associated with arsenic related health effects. For example, in countries such as India, Bangladesh, and Taiwan arsenic levels in drinking water are found in high concentrations. In some of these countries drinking water levels can range from 10 to as high as 1000 part per billion (ppb) depending on the geographical region (Rahman, Tondel et al. 1999; Berg, Tran et al. 2001; Nordstrom 2002; Pi, Yamauchi et al. 2002). In some rural areas of the United States, levels of arsenic in drinking water can reach between 50 to 100 ppb (Lewis, Southwick et al. 1999); concentrations well above the maximum contaminant level of 10 ppb set by the EPA in 2001. The prevalence of high drinking water levels of arsenic in distinct geographical

regions reveals a dire need for determining the significance of arsenic-related health effects.

Epidemiologic Evidence of Arsenic-related Health Effects

Numerous adverse health effects have been associated with arsenic exposure in both dose and time-dependent relationships. Epidemiologic studies have examined areas of the world identified with high levels of arsenic in drinking water to assess this relationship. Studies looking at dose-response relationships have demonstrated increased mortality rate ratios in populations as a function of increasing water arsenic levels. This was demonstrated in the Taiwanese general population in relation to various organ cancers (Bates, Smith et al. 1992). Increased mortality rates associated with various cardiovascular diseases were demonstrated in a study identifying U.S. based populations exposed to more moderate levels of arsenic in drinking water (~5 to 100 ppb) (Engel and Smith 1994). A study in Bangladesh suggested a dose-response relationship between arsenic exposure levels and hypertension based on populations exposed to well water arsenic ranging in concentrations of ~10 to 1000 ppb (Rahman, Tondel et al. 1999).

In addition to dose-response studies, exposure duration of arsenic has been investigated as a factor of arsenic-mediated health effects. Chronic arsenic exposure was assessed in three villages located in southwestern Taiwan. The study concluded that residents were at greater risk for ischemic heart disease when exposed to arsenic for longer periods of time (Huang, Tseng et al. 2007).

Cumulatively, the epidemiologic evidence suggests a stronger incidence of adverse health effects in populations exposed to significant levels of arsenic in their

drinking water. These studies also reinforce the concept that both level and duration of arsenic exposure are relevant factors in the corresponding health effects.

Arsenic Uptake and Metabolism

Many of the mechanisms regarding uptake and distribution of inorganic arsenic are still uncertain, however some distinct cellular components have been identified in the aforementioned processes. The inorganic forms are the main arsenic species facilitating human exposure. Both As (V) and As (III) are capable of uptake and distribution in mammalian cells. As (V) has been shown to enter cells via cellular phosphate carrier systems. As (III) was initially thought to enter cells by passive diffusion. However, recent evidence implicates an active transport mechanism responsible for arsenite uptake in mammalian cells (Liu, Shen et al. 2002; Aposhian, Zakharyan et al. 2004).

The metabolism for arsenic is a multi-step, multi-enzyme process. Figure 14 outlines the most current metabolic pathways for arsenic metabolism. Arsenate is reduced to the more toxic inorganic form arsenite, by the enzymatic activity of arsenate reductase (Figure 14, Reaction 1) by utilization of sulfhydryl groups on lipoic acid as one source of electrons. Further conversion can occur via arsenite methyltransferase by the addition of methyl groups to produce different organic forms of arsenate (MMA V, and DMA V) containing either one or two methyl groups (Reactions 2 & 4). The methyl donor for these reactions has been identified as *S*-adenosylmethionine. Methylated arsenic species can undergo further reduction via the enzymatic activity of MMAV and DMAV reductase producing methylated arsenite compounds (MMA III, and DMA III). The antioxidant GSH can serve as an electron donor in these reactions and is rate limiting in the production of MMA III (Reactions 3 & 5).

FIGURE 14

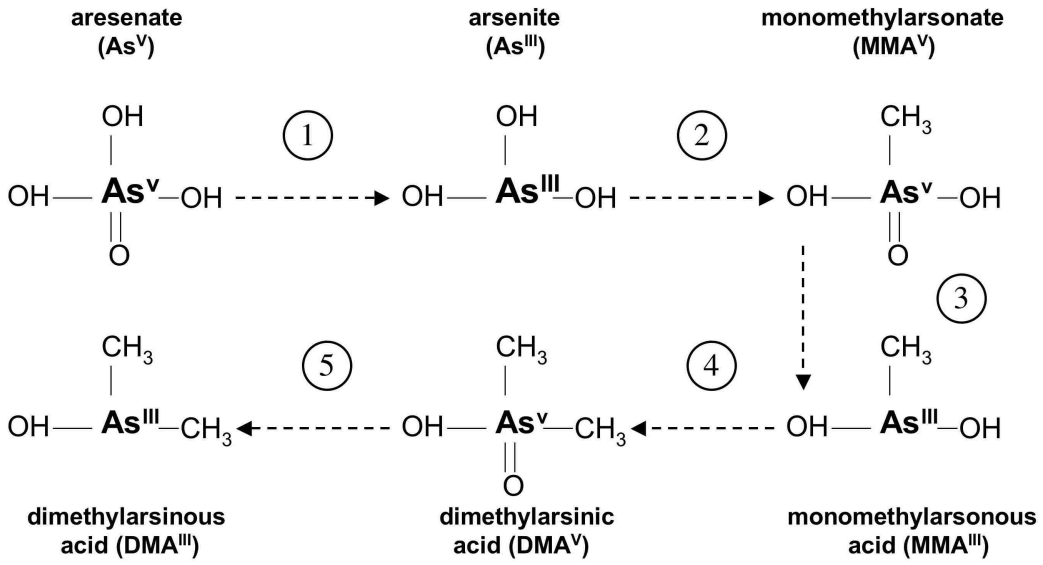

Adapted from (Wallace 1998; Aposhian, Zakharyan et al. 2004)

FIGURE 14

Metabolic pathways identifying the reduction and methylation that inorganic arsenic compounds undergo in mammalian systems. Reactions 1, 3, and 5 identify arsenic reduction reactions reliant on sulfhydryl groups as the electron source. Reactions 2 and 4 identify reactions facilitating the addition of methyl groups reliant on *S*-adenosylmethionine. Metabolic transformation is performed via enzymatic activities.

All six different metabolites have been identified in humans. The presence of such a diverse number of arsenic metabolites is a large confounder when studying arsenic toxicity because each form has been shown to be toxic to mammalian cells (Aposhian, Zakharyan et al. 2004). The non-methylated forms of arsenic (As V, and As III) are considered more cytotoxic while the methylated forms considered more genotoxic (MMA DMA V, and MMA DMA III), (Wanibuchi, Salim et al. 2004).

Arsenic and Oxidative Damage to DNA

Epidemiological studies and evidence from animal exposures indicate that exposure to inorganic arsenic increases the risk of cancer in different organs including the lungs, kidneys and skin (Bates, Smith et al. 1992; Germolec, Spalding et al. 1998; Wanibuchi, Salim et al. 2004; Mo, Xia et al. 2006). Despite the high association between arsenic exposure and cancer risk a clear cellular mechanism for arsenic induced carcinogenesis has not been identified. One mechanism proposed for arsenic-mediated toxicity and its role in carcinogenesis is the overproduction of free radicals. ROS-mediated cellular damage from arsenic has been demonstrated in studies of arsenic exposure in both acute and chronic conditions. Acute exposures at low micro-molar levels of As(III) have been shown to increase different ROS including superoxide anion, hydrogen peroxide, peroxynitrite, and hydroxyl radical (Barchowsky, Klei et al. 1999; Barchowsky, Roussel et al. 1999; Liu and Jan 2000; Bunderson, Brooks et al. 2004). Increased superoxide anion production was attributed largely to increased activity of NADPH oxidase of which superoxide is a product of enzymatic activity (Smith, Klei et al. 2001). As discussed in Chapter 1, superoxide can be converted to hydrogen peroxide via SOD activity. Superoxide can also react with nitric oxide and form peroxynitrite, a

free radical compound capable of nitrating tyrosine residues of proteins (Beckman and Koppenol 1996). Hydrogen peroxide, also shown to be elevated after arsenic exposure, can participate as a substrate in the Fenton reaction producing hydroxyl radical. This demonstrates multiple ways that an overproduction of superoxide can lead to the formation of more harmful free radicals. Increased oxidative stress has been demonstrated in a study looking at the effects of chronic arsenic exposure in humans. The results showed correlations between increased lipid peroxidation and the levels of arsenic in serum and whole blood. It was also shown that chronic exposure resulted in decreased levels of the antioxidant GSH measured in whole blood (Pi, Yamauchi et al. 2002). Additional support for free radical mediated toxicity has been gathered from studies demonstrating that the administration of antioxidants compounds such as ascorbic acid, α-tocopherol, and *N*-acetylcysteine can reduce arsenic toxicity in both acute and chronic models of exposure (Flora 1999; Ramanathan, Balakumar et al. 2002).

The interaction of arsenic-induced ROS with DNA has been reported to generate DNA protein cross-links and oxidative lesions including oxo^{8}dG (Yamanaka, Takabayashi et al. 2001; Bau, Wang et al. 2002; Pu, Jan et al. 2007). Oxo^{8}dG has also been reported as pro-mutagenic due to the tendency to pair with adenine over cytosine during DNA replication, a process that can facilitate GC to TA transversions (Figure 15) (Shibutani, Takeshita et al. 1991; Cheng, Jungst et al. 2002; Klungland and Bjelland 2007).

FIGURE 15

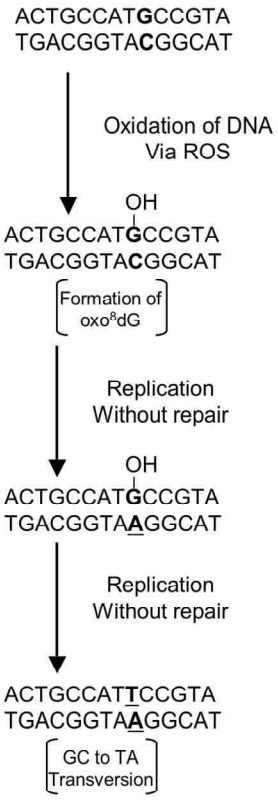
ACTGCCATGCCGTA
TGACGGTACGGCAT
Oxidation of DNA
Via ROS
OH
ACTGCCATGCCGTA
TGACGGTACGGCAT
Formation of
oxo8dG
Replication
Without repair
OH
ACTGCCATGCCGTA
TGACGGTAAGGCAT
Replication
Without repair
ACTGCCATTCCGTA
TGACGGTAAGGCAT
GC to TA
Transversion

FIGURE 15

Molecular pathway for GC to TA transversions. Initial oxidation of guanine forms oxo^{8}dG paired with cytosine. In the absence of oxo^{8}dG removal, DNA polymerase pairs adenine with oxo^{8}dG during replication. An additional round of replication incorporates thymine with adenine completing the transversion.

It is worth noting that increased GC to TA transversions can precede cellular transformation, and this type of genetic mutation has been identified in the p53 tumor suppressor gene of human cancers (Hollstein, Sidransky et al. 1991; Yu, Berlin et al. 2002).

Whether arsenic exposure mediates cancer by this mechanism is unresolved, however increased levels of oxo^{8}dG have been demonstrated subsequent to arsenic exposure. A study examining skin samples from patients diagnosed with arsenic-related Bowen's carcinoma showed increased levels of oxo^{8}dG suggesting arsenic as the causative agent (Matsui, Nishigori et al. 1999). Increased damage was also seen in mice exposed to arsenic by demonstrating increased levels of oxo^{8}dG in target organs associated with arsenic induced carcinogenesis; lungs, liver, kidney, bladder and skin (Yamanaka, Takabayashi et al. 2001). Additional evidence has been collected from genetic models deficient in repair of oxo^{8}dG. In Ogg1 null mice chronically exposed to arsenic in drinking water, examination of the liver revealed elevated levels of oxo^{8}dG in conjunction with increased tumor development in the liver, lungs and lymph nodes when compared to both wild type and heterozygous littermates (Wanibuchi, Salim et al. 2004). These reports present a strong association between exposure to arsenic and increased levels of oxo^{8}dG. In addition these reports present evidence that increased DNA damage is a process associated with the carcinogenic process. However, by not defining a clear role for oxo8dG in the carcinogenic process, only presents the data in a descriptive fashion. The most compelling evidence for the role of oxo^{8}dG in carcinogenesis is from studies utilizing the Ogg1 null model that suggests a decreased capacity to repair oxo^{8}dG may facilitate carcinogenic processes.

Cells have evolved mechanisms to compensate for oxidative damage to DNA by repairing damaged nucleotides. Oxo^{8}dG is removed from DNA by the BER pathway carried out by the specific DNA-glycosylase Ogg1 (Boiteux and Radicella 2000). Ogg1 is constitutively expressed (Dhenaut, Boiteux et al. 2000) and it is the main enzyme involved in initiating the repair of oxo^{8}dG (Klungland, Rosewell et al. 1999; Minowa, Arai et al. 2000; de Souza-Pinto, Eide et al. 2001). Studies have shown a modulation of Ogg1 in response to oxidative stress from various sources (Table 1). In rats exposed to diesel exhaust particles, both Ogg1 activity and mRNA were decreased in lung tissue post-exposure (Tsurudome, Hirano et al. 1999). Studies using cadmium chloride, another carcinogenic metal, have shown effects on Ogg1 transcription and activity. *In vitro* experiments using purified enzyme extracts of murine Ogg1 showed decreased enzyme activity in the presence of cadmium (Zharkov and Rosenquist 2002). It was also demonstrated in rat lung that cadmium chloride decreased the levels of Ogg1 mRNA (Potts, Watkin et al. 2003). Exposure of cadmium has also shown to negatively effect human Ogg1 activity and transcription suggesting the existence of a conserved mechanism among different species for down regulation of Ogg1 (Youn, Kim et al. 2005). Arsenic however, has not been described as having any distinct effect on Ogg1 activity, however changes in Ogg1 mRNA levels from whole blood has been linked to an increased risk of skin hyperkeratosis in males chronically exposed to well water arsenic (Mo, Xia et al. 2006).

Whether changes in oxo^{8}dG subsequent to arsenic exposure are related to changes in DNA repair capacity remains uncharacterized, however studies have shown an inverse relationship between Ogg1 activity and levels of oxo^{8}dG (Cardozo-Pelaez, Brooks et al.

2000; Cardozo-Pelaez, Stedeford et al. 2002) suggesting that increased levels oxo^{8}dG can be a result of attenuated DNA Ogg1 capacity. Based on the similarities between cadmium and arsenic (oxidative stress, oxo^{8}dG, carcinogenesis), and the data showing down regulation of Ogg1 transcription by cadmium, the effect that arsenic exposure has on transcriptional regulation of Ogg1 is a likely venue of investigation.

The goal of these experiments was to test the hypothesis that increased levels of oxo^{8}dG induced by an acute exposure to sodium arsenite are a result of changes in antioxidant and Ogg1 response capacity. To test the hypothesis the following objectives were designed:

1) Characterize the dose-response to sodium arsenite via measurement of cell viability in PC12 cells.

2) Characterize changes in antioxidant systems via measurement of intracellular GSH and Cu/Zn, Mn SOD activities in PC12 cells subsequent to sodium arsenite exposure.

3) Characterize changes in Ogg1 transcription and activity, and levels of oxo^{8}dG in PC12 cells subsequent to sodium arsenite exposure.

An additional goal of these experiments was to elucidate differential effects in antioxidant and DNA repair capacity between non-NGF, and NGF treated PC12 cells. This is addressed given the fact of organ and cell specific effects subsequent to arsenic exposure.

Materials and Methods

Chemicals and Reagents

All chemicals and reagents were obtained from Sigma Aldrich, (St Louis, MO) unless otherwise indicated.

Preparation of arsenite-treated samples

PC12 rat pheochromocytoma cells obtained from American Type Culture Collection (ATCC # CRL-1721) were grown in 1X RPMI 1640 media containing 5% fetal bovine serum, 10% horse serum, 2 mM L-glutamine, 1mM sodium pyruvate, 25 U/mL penicillin G / streptomycin; all media reagents were obtained from CellGRO Technologies (MediaTech, Herndon, VA). Cells were plated on 100 mm costar tissue culture dishes coated (Corning Life Sciences, Lowell, MA) with 0.05 mg/mL collagen from calfskin and incubated at 37° C in a humidified 5% CO_2 atmosphere. Cells were grown in normal growth media until approximately 80 - 90% confluent. Normal growth media was removed at this point and plates divided into two groups either receiving normal growth media, or growth media supplemented with NGF at a final concentration of 50 ng/mL. The NGF treated group was allowed to incubate until a differentiated phenotype was observed as assessed by conversion from round to polygonal morphology, and process extension. Media was replaced under the following conditions: Control groups received normal or NGF supplemented growth media, exposure groups received normal or NGF supplemented growth media containing sodium arsenite at a final concentration of 10 μM. Cultures were harvested and processed at 24 hr post sodium arsenite exposure.

Cell samples were harvested and washed 2X with 5 mL sterile PBS, with a

subsequent 1 mL wash in 10 mM EDTA, pH 7.0. Cells were sonicated in 300 μL of 10 mM EDTA, pH 7.0 using a VirTis VirSonic Ultrasonic Cell Disruptor 100© (VirTis, Gardiner, NY). Following centrifugation at 14,000 rpm, 4° C for 15 min, supernatants were divided for GSH and SOD activity analysis. Aliquots for GSH were analyzed the same day while aliquots for SOD, and remaining cell pellets were stored at - 80° C until subsequent analysis and extractions were performed. Protein concentration in each cytosolic extract was determined using a Bio-Rad Protein Assay Kit (Bio-Rad Laboratories, Hercules, CA).

Cell Viability Assays

Cell viabilities were determined using an LDH Cytotoxicity Detection kit according to manufacturer's protocols (Roche Applied Science, Indianapolis, IN). The assay measures the activity of lactate dehydrogenase released from the cytosol of damaged cells into the media. Briefly, PC12 cells were seated at a density of 3×10^4 cells / well in collagen-coated 96-well costar plates (Corning Life Sciences, Lowell, MA) using normal or 50 ng/mL NGF supplemented growth media at a final volume of 300 μL. Cells were grown overnight and washed 2X the following day with fresh media. Following wash protocols a subsequent replacement of 300 μL of regular, or NGF supplemented growth media was performed. Actively dividing and NGF treated PC12 cells were then exposed to either untreated or 10 μM sodium arsenite treated media with one cell group exposed to 2 % Triton-X as a positive control. 24 hr later, 100 μL of media was removed from each well and placed into a new 96-well plate. 100 μL of a reaction mixture containing manufacturer catalyst, Diaphorase/NAD+, iodotetrazolium chloride, and sodium lactate was prepared fresh and added to each well and incubated at

15 - 25° C for 30 min in the absence of light. Absorbance was measured at λ 490 – 492 nm with a reference wavelength of λ 600 nm using a SpectraMax© 340 96-well plate reader (Molecular Devices, Sunnyvale, CA) and quantified using SOFTmax® PRO software (Molecular Devices, Sunnyvale, CA). Percent of cell viability relative to control was calculated using the following formula with values defined as such:

Equation 1 Value = (measured O.D. – average blank O.D.)

Equation 2 $$\% \text{ Cytotoxicity} = \frac{(\text{experimental value} - \text{untreated ctrl value})}{(\text{Triton ctrl value} - \text{untreated ctrl value})} \times 100$$

Quantification of Total Reduced GSH

Protein was precipitated from cytosolic extracts (see above) using 6.5 % sulfosalicylic acid (SSA) centrifuged at 10,000 rpm, 4° C for 10 min. Levels of total reduced GSH were determined in each sample as previously described (Cardozo-Pelaez, Brooks et al. 2000). 95 μL of cytosolic supernatant and 30 μL of 10 mM EDTA were added in duplicate to individual wells in costar 96-well microplates (Corning Life Sciences, Lowell, MA). A reaction mixture containing 5,5'-dithio-bis-2-nitrobenzoic acid (DTNB) suspended in 0.5 M Na_2HPO_4 buffer at a final concentration of 10 mM was added at a volume of 200 μL per well bringing the final volume per well to 325 μL. Reactions were then incubated for 15 min at room temperature. Optical densities were determined at λ = 412 nm using a SpectraMax© 340 96-well plate reader (Molecular Devices, Sunnyvale, CA). The content of GSH in the samples was quantified using SOFTmax® PRO software (Molecular Devices, Sunnyvale, CA) by comparison to a standard curve constructed with known amounts of total GSH suspended in 10 mM EDTA at final volume of 325 μL. The standard curve for GSH ranged from 0 to 100

nmoles in concentration. Final values were expressed as nanomoles GSH per milligram of protein per sample using the Bio-Rad protein assay (Bio-Rad Laboratories, Hercules, CA).

Measurement of Total, Copper/Zinc, and Manganese SOD Activities

SOD activity was measured as previously described with slight modifications (Cardozo-Pelaez, Song et al. 1998). This assay is based on the formation of a chromogenic complex via reaction of an artificially generated superoxide anion ($O_2\bullet^-$) with hydroxylamine as an intermediate electron carrier. A subsequent reaction is carried out reacting the hydroxylamine intermediate with α-napthylamine, producing a chromogenic nitrite compound that is measurable at λ = 593 nm. In the presence of SOD activity there is an inhibition of the production of the chromogenic compound. Supernatant from PC12 cell homogenates were incubated for 20 min in a 25° C water bath with reaction mixture 1 composed of the following reagents: 150 μL of 65 mM KH_2PO_4 buffer, 15 μL of xanthine stock solution (1.5 mM suspended in 0.025 N NaOH), and 15 μL hydroxylamine chloride stock solution (1 mM in KH_2PO_4 buffer). The reaction was initiated by the addition of 75 μL of xanthine oxidase stock solution (0.2 mg protein/mL suspended in ice cold H_2O). An aliquot of 100 μL of reaction mixture 1 was added to 100 μL of reaction mixture 2 composed of the following reagents: sulfanilic acid stock solution (19mM suspended in 75 % H_2O, 25 % glacial acetic acid) and 100 μL of α-napthylamine stock solution (7 mM suspended 75 % H_2O, 25 % glacial acetic acid) in a costar 96-well microplate (Corning Life Sciences, Lowell, MA) and incubated for 20 min at room temperature. Optical densities were determined at λ = 539 nm using a SpectraMax© 340 micro-plate reader (Molecular Devices). The activity of total SOD

was determined using SOFTmax PRO® (Molecular Devices, Sunnyvale, CA) software by comparing samples to a standard curve of percent inhibition of nitrite formation relative to SOD activity, constructed using known amounts of purified bovine liver SOD. Mn SOD activity was differentiated from Cu/Zn SOD activity with the addition of potassium cyanide stock solution (5 mM suspended KH_2PO_4 buffer) in reaction mixture 1. The difference between total and KCN-inhibited SOD activities was defined as Mn SOD activity. Data was expressed as units of SOD activity per milligram of protein per sample using the Bio-Rad protein assay (Bio-Rad Laboratories, Hercules, CA).

Synthetic Oligonucleotide Radio Labeling

A 24 bp synthetic oligonucleotide probe containing the following nucleotide sequence, 5′ - GAA CTA GTG XAT CCC CCG GGC TGC - 3′ (X=oxo^{8}dG), was labeled with γ-[^{32}ATP] prior to annealing to its complementary strand (Trevigen, Gaithersburg, MD). Reactions were set up under the following conditions: 39 μL ddH_2O, 5 μL 10X T4 kinase buffer, 2 μL (20 pmoles) of synthetic oligonucleotide containing the oxo^{8}dG lesion, 3 μL of γ-[^{32}ATP] (7,000 mCi / mmole) (MP Biomedicals, Solon, OH), 1 μL of T4 polynucleotide kinase (Roche Applied Science, Indianapolis, IN) to a 500 μL eppendorf tube. The reaction mixture was mixed well and then incubated at 37° C for 30 min. Subsequent to incubation, the reaction mixture was added to a pre-spun G25 sephadex column and allowed to sit for 2 min. The column was spun at 5000 rpm for 3 min. 5 μL of labeling buffer was added followed by 2 μL (20 pmoles) of the synthetic complement oligonucleotide (Trevigen). The mixture was heated to 95° C in a water bath and allowed to slowly cool to room temperature overnight. The labeled double stranded probe was stored at –20° C until utilized. Prior to use, the labeled probe was

diluted 1:200 (5 μL into 1000 μL) using nuclease free sterile H_2O.

Determination of Ogg1 Activity

Nuclear protein extracts were prepared from leftover nuclear pellets by homogenization at 4° C in 250 μL of glycosylase extraction buffer containing the following reagents: 20 mM Trizma-base pH = 8.0, 1 mM EDTA, 0.5 mM spermine, 0.5 mM spermidine, 1 mM DTT , 50% Glycerol , and 1.3 % Protease Inhibitor Cocktail (Roche Applied Science, Indianapolis, IN). Following the addition of 25 μL of 2.5 M KCl, the homogenate was rocked for 30 min at 4° C. Samples were centrifuged at 14,000 rpm for 30 min. Supernatants were removed and stored along with the remaining pellet at – 80° C until utilized. Total protein was determined in each sample using the Bio-Rad protein assay (Bio-Rad Laboratories, Hercules, CA).

Ogg1 activity was determined by incubation of glycosylase extracts with the radio labeled probe. The reaction was initiated by incubating 30 μg of total protein in glycosylase extracts and the double stranded, labeled probe in 15 and 5 μL each of the following reaction buffers respectively: [Cold Nicking Buffer; 20 μL of 0.5 M HEPES buffer, pH = 7.9, 40 μL of 0.1 M EDTA, 40 μL of 5 mM DTT, 40 μL 100X bovine serum albumin (New England Biolabs, Ipswich, MA), 255 μL of ddH_2O]; [Hot Nicking Buffer; 20 μL of 0.5 M HEPES buffer, pH = 7.9, 40 μL of 0.1 M EDTA, 40 μL of 5 mM DTT, 40 μL 100X bovine serum albumin, 250 μL of ddH_2O, 5 μL of the 1:200 diluted labeled probe]. Reaction mixtures were incubated for 2 hr at 37° C in a heating block and placed on ice. 20 μL of loading buffer containing 90 % formamide, 10 mM NaOH and 1X blue-orange dye (Promega, Madison, WI) was added to each sample. After 3 min of heating at 95° C, samples were placed back on ice, briefly centrifuged and loaded into a

20 % acrylamide denaturing gel composed of the following reagents: 22.5 mL of 40 % acrylamide/ bis-acrylamide 7M urea, 200 μL of 10 % ammonium persulfate, 20 μL N,N,N',N'-Tetramethylethylenediamine (Bio-Rad Laboratories, Hercules, CA), mixed well and cast into gel plates at a volume of 22.5 mL. Following gel polymerization at room temperature, samples were loaded and run using 1X TBE running buffer for 2 hr at 400 mV. Following fragment separation the gel was removed and encased in cellophane plastic wrap in an imaging cassette holder (Bio-Rad Laboratories, Hercules, CA). An imaging plate (Fuji Film Life Science, Stamford, CT) was exposed to the gels for approximately 16 to 20 hr. Gels were imaged and quantified using a FLA-3000 Series Fuji Film Fluorescent Image Analyzer (Fuji Film Life Science, Stamford, CT) and ImageGauge© version 4.22 analysis software (Fuji Photo Film Co., LTD, Stamford, CT). The capacity of the extract to incise oxo^{8}dG was expressed as a percentage of the ratio of cleaved synthetic probe to the total probe used using the following formula, (DU = densitometric units):

$$\% \text{ Activity} = \frac{\text{DU cut fragment}}{\text{DU cut and uncut fragments}} \times 100$$

Determination of oxidative damage to DNA (oxo^{8}dG)

To quantify oxo^{8}dG levels in each sample, the pellet left over from the glycosylase extraction was utilized to isolate genomic DNA. Purified DNA was prepared for HPLC analysis by resolving it into deoxynucleoside components. Nuclear pellets were rinsed 1X in 1 mL of DEB buffer containing the following reagents: 0.1 M Tris-HCl, 0.1 M NaCl, and 20 mM EDTA. Pellets were centrifuged at 5000 rpm for 5 min at 4° C and separated from the DEB wash buffer. 300 μL of a DNAse free RNAse was added to each nuclear pellet mixed well and incubated in a 37° C water bath for 1 hr with

frequent mixing during the 1 hr duration. The RNAse solution was composed of the following reagents: 33 U of RNAse T_1, 200 μg RNAse A (Roche Applied Science, Indianapolis, IN) suspended in DEB buffer. An additional 300 μL of proteinase-detergent solution was added to each sample and incubated in a 37° C water bath for an additional 1 hr with frequent mixing during the 1 hr duration. The solution consisted of the following: 300 μg Proteinase K, and 1 % sodium dodecyl sulfate suspended in DEB buffer. The protein fraction was separated from genomic DNA using three consecutive organic extractions.

Organic extraction #1 was performed by adding 750 μL of phenol, mixed well and centrifuged at 5000 rpm for 5 min at 4° C allowing the reaction mixture to separate into two different phases; an organic (bottom) and aqueous (top) phase.

Organic extraction #2 was performed by removal and transfer of the aqueous phase (top layer) of organic extraction 1 to a Light Phase Lock® gel separation tube (Brinkmann Instruments Inc., Westbury, NY). 250 μL of a 25:24:1 ratio of phenol:chloroform:isoamyl alcohol mixture was added to each sample, mixed and centrifuged at 5000 rpm for 15 min at 25° C.

Organic extraction #3 was performed by removal and transfer of the aqueous layer of organic extraction 2 to a Light Phase Lock® gel separation tube. 250 μL of a 24:1 ratio of chloroform:isoamyl alcohol mixture was added to each sample, mixed well and centrifuged at 10000 rpm for 15 min at 25° C.

The DNA was precipitated by the addition of 30 μL 3 M sodium acetate pH = 5.0 and 1 mL of ice cold 100 % ethanol, inverted gently multiple times and incubated overnight at – 20° C. Following overnight incubation, samples were centrifuged at 3200

rpm for 30 min at 4° C. Following centrifugation the 100 % ethanol was carefully removed from the precipitated DNA pellet and 1 mL of 70 % ethanol was added, mixed well and then centrifuged at 4000 rpm for 25 min at 4° C. Following the second centrifugation, the 70 % ethanol was carefully removed so at to not disturb the precipitated DNA pellet. Samples were inverted on bench paper for approximately 10 to 15 min to allow removal of any residual ethanol. Precipitated genomic DNA was then hydrolyzed to resolve DNA bases into their deoxynucleoside components. This was first accomplished by adding 100 μL of 20 mM sodium acetate pH = 5.0 to each sample. DNA pellets were mixed well and incubated for 3 min at 95° C in a heating block in order to denature the DNA. Samples were removed to ice and 10 μL (1 U/μL) of Nuclease P1 (suspended in 20 mM sodium acetate pH = 5.0) was added to each sample for 45 to 60 sec subsequent to transfer to ice. Samples were mixed well and incubated for 30 min in a 37° C water bath with frequent mixing occurring during the 30 min duration. 20 μL of 1 M Tris-Hcl pH = 8.0 was added to each sample and mixed well. 5 μL (2 U/μL) of Alkaline Phosphatase (suspended in 1 M Tris-HCl pH = 8.0) was added to each sample, mixed well and incubated for 1 hr in a 37° C water bath with frequent mixing occurring during the 1 hr duration. 20 μL of 3 M sodium acetate was added to each sample and mixed well. Samples were spun down briefly to collect residual liquids together and transferred to an Ultrafree-MC© (30 Kda) filtration tube (Millipore Corp., Bedford, MA) and centrifuged at 4500 rpm for 25 min at 25° C. Subsequent to centrifugation, samples were lyophilized using a speed vac for approximately 2 hr or until samples were dry, and stored at – 20° C until analyzed by HPLC.

Analysis of the levels of oxo^{8}dG, expressed as the ratio of oxo^{8}dG / 2-deoxyguanosine (2-dG) was performed as follows. Oxo^{8}dG and 2-dG were resolved by HPLC with a reverse phase YMCbasic column (4.6 mm x 150 mm; particle size 3 μm) (YMC Inc., Wilmington, NC) and quantified using a CoulArray electrochemical detection system (ESA Inc., Chelmsford, MA). An isocratic mobile phase consisting of 100 mM sodium acetate, pH 5.2, 4 % methanol (HPLC Grade) was prepared in sterile H_2O passed through C18 Sep-Pak cartridges (Waters Corp., Milford, MA) and then utilized to elute DNA nucleosides from the column. Prior to use the mobile phase was filtered using a 0.2 μm nylon filter and degassed by sonication. Potentials for the four coulometric analytical cells of the CoulArray system, placed in series, were as follows: 50, 125, 175, 200, 250, 380, 500, 700, 785, 850, 890, 900 mV. Calibration curves were generated from standards of 2-dG ranging from 100 ng to 2 μg (0.350–7.01 nmol) and oxo^{8}dG (Cayman Chemical Company, Ann Arbor, MI) ranging from 5 to 100 pg (17.6–353 fmol). The calibration curve for oxo^{8}dG was created based on the peak area of the oxo^{8}dG standard, eluting at 9.0 min, in the 250 mV channel. The calibration curve for 2-dG was created based on the sum of peak areas of the 2-dG standard, eluting at 7.8 min, in the 850, 890, and 900 mV channels. The electrochemical cells were allowed to equilibrate and wake up standards (three times the highest concentration of calibration standards) were injected before calibration standards as suggested by ESA in order to obtain highest sensitivity. The ratio of oxo^{8}dG and 2-dG was calculated by comparing the peak area and sum of peak areas, respectively, from a 10 μL injection of reconstituted enzymatic hydrolysate of the DNA sample with the calibration curves for oxo^{8}dG and 2-dG respectively. Levels of oxo^{8}dG in the samples were expressed relative to the content

of 2-dG (e.g. the molar ratio of oxo^{8}dG to 2-dG [fmol of oxo^{8}dG / nmol of 2-dG]). Data were recorded, analyzed, and stored using CoulArray for Windows data analysis software (ESA Inc., Chelmsford, MA).

RNA Isolation

Total RNA from PC12 cells was isolated using TRIzol reagent (Invitrogen Life Technologies, Carlsbad, CA) as described by the manufacturer. Cell cultures were harvested and washed 1X in sterile PBS. Subsequent to washing the cells were immediately processed for RNA isolation by adding 2 mL of TRIzol reagent and sonicating the samples for 6 sec on ice using a VirSonic Ultrasonic Cell Disruptor 100© (VirTis, Gardiner, NY). In between samples, the sonicator tip was washed with the following reagents to ensure no RNA cross contamination could occur between samples. The wash protocol was as follows: wash vessel 1 – 0.1 % DEPC (v/v) sterile H_2O; wash vessel 2 – 1 % SDS (w/v); wash vessel 3 – 70 % ethanol; wash vessel 4 – 0.1 % DEPC sterile H_2O. For each stage of the wash cycle the tip was submerged and activated for 3 sec. Following sonication the samples were incubated for 5 min at room temperature to completely dissociate nucleoprotein complexes. Organic separations were then performed by two successive chloroform extractions performed as follows: 400 μL of chloroform was added to each sample, shaken vigorously by hand for 15 sec, and placed on ice for 10 min. Following incubation on ice, samples were centrifuged at 12000 x g for 30 min at 4° C. The aqueous layer was removed into a fresh sterile tube. Following the two successive chloroform extractions 1 mL of sterile, 100 % 2-propanol was added to each sample, mixed well, incubated for 30 min at room temperature, shaken vigorously for 15 sec, and incubated on ice for 10 min. Samples were centrifuged at 12000 x g for

10 min at 4° C to pellet the RNA down to the bottom of the tube, at this time the supernatant was carefully removed from the RNA. The RNA was washed with 2 mL of sterile 75 % ethanol with vigorous pipetting of the RNA pellet. Samples were centrifuged at 7500 x g for 5 min at 4° C, supernatant removed, and samples inverted on bench paper and allowed to air dry for 10 – 15 min or until no ethanol was observed. RNA pellets were dissolved in 50 μL of sterile 0.1 % DEPC H_2O and incubated for 10 min at 60° C. Samples were analyzed spectrophotometrically to determine the concentration of each sample (ng/μL), and the $A_{260/280}$ to determine sample purity. RNA was stored at –80° C until utilized for quantitative RT-PCR.

Quantitative Real Time PCR Analysis

Real-time RT-PCR was performed using the ABI PRISM® 7700 Sequence Detection System (Applied Biosystems, Foster City, CA). Rat Ogg1 and hypoxanthine guanine phosphoribosyl transferase (HPRT) sequences were obtained from NCBI using Genbank accession numbers NM_030870 & XM_343829 respectively. PCR primers and dual-labeled probes specific for rat and Ogg1 and HPRT (Integrated DNA Technologies Inc., Coralville, IA) were designed using Primer Express® Version 1.5 (Applied Biosystems, Foster City, CA). Detailed sequences for primers & probes used for RT-PCR can be referenced from Appendix A, Section I.

HPRT served as an endogenous control to account for any off target effects and for normalization of Ogg1 transcript levels. All samples were diluted and DNase-treated prior to reverse transcription. Reactions for DNAse treatment were set up in sterile 0.25 mL PCR vials (Axygen Scientific, Union City, CA) as follows: 1 μL of 10X reaction buffer, 1 μL (1 U) of RNAse free DNAse (Promega, Madison, WI), 50 ng sample RNA,

bring reaction mixture to a final volume of 8 μL with DEPC treated sterile H_2O. Each sample was assayed in triplicate plus one no amplification control containing no reverse transcriptase. The RT reactions were set up in 96-well optical plates (Applied Biosystems, Foster City, CA) with the reaction buffer composed of the following reagents at a final volume of 10 μL: 1x reverse transcriptase buffer, 500 μM dNTP's (Roche Applied Science, Indianapolis, IN), 400 nM assay-specific reverse primer (Integrated DNA Technologies Inc., Coralville, IA), 10 U reverse transcriptase (Stratagene, Cedar Creek, TX), and 4 μL DNase-treated sample RNA (25 ng). Cycling conditions for the RT reaction were performed using a DNA Engine gradient thermal cycler (MJ Research, Waltham, MA) as follows: 25° C for 10 min, 48° C for 30 min, and 95° C for 5 min, 8° C. PCR reactions were carried out using the above generated cDNA template. 50 μL of PCR master mix solution was then added to each sample. The PCR master mix solution was composed of the following reagents: 1X PCR buffer (Invitrogen Life Technologies), 5 mM $MgCl_2$ (Invitrogen Life Technologies, Carlsbad, CA), 200 μM dNTP's (Roche Applied Science, Indianapolis, IN), 1X ROX dye (Invitrogen Life Technologies, Carlsbad, CA), 400 nM assay-specific forward primer, 400 nM assay-specific reverse primer, 100 nM assay-specific dual-labeled probe (Integrated DNA Technologies Inc., Coralville, IA), and 1.25 U Taq polymerase (Invitrogen Life Technologies, Carlsbad, CA). Thermal cycling conditions for the ABI PRISM® 7700 Sequence Detector were as follows: 95° C for 60 sec, 40 cycles of 95° C for 12 sec, and 60° C for 30 sec. Analysis of raw data was performed using the SDS version 1.9 analysis software (Applied Biosystems, Foster City, CA) to obtain a C_t value for each sample. C_t

values represent the cycle number that produced a significant change from baseline fluorescence (ROX dye).

Final values were obtained by direct comparison. This was accomplished by multi step calculation of the raw data (C_t Values) obtained from each sample. The change in fluorescence between Ogg1 and HPRT was calculated first by the difference in the respective threshold cycles (ΔC_{t1}; Equation 1). ΔC_{t1} values will be normalized to a value deemed the calibrator (Equation 2). The calibrator's value was assigned by calculating the mean ΔC_{t1} from control samples.

Equation 1 $\Delta C_{t1} = C_tOgg1 - C_tHPRT$

Equation 2 $\Delta\Delta C_t = \Delta C_{t1}$ (individual sample) - ΔC_{t1} (Average of control)

Final values are presented as a percentage of untreated control values. The comparative C_t method was validated by comparison of PCR efficiencies between the target and reference genes. HPRT was chosen as the reference gene over the more commonly used18s ribosomal RNA based on experimentally collected data. The PCR efficiencies of Ogg1 and HPRT have been determined to be approximately equal by previous experimentation.

Nuclear Protein Extraction

Nuclear proteins from cultured PC12 cells were extracted according to the protocol published by Basha et al. (Basha, Wei et al. 2005) with modifications. Cell cultures were removed using sterile PBS containing 1.3 % protease inhibitor cocktail (Roche Applied Science, Indianapolis, IN), transferred to a 15 mL conical vial, and centrifuged at 125 x g for 6 min. Samples were washed again using 1 mL sterile PBS with protease inhibitors, transferred to a sterile 1.5 mL eppendorf tube and centrifuged

again at 125 x g for 5 min. The wash step was repeated and the PBS supernatant removed following centrifugation. Sample pellets were suspended in 250 μL of buffer A containing the following reagents: 10 mM HEPES buffer pH = 7.9, 1.5 mM $MgCl_2$, 0.5 mM DTT, 0.5 mM EDTA, and 0.2 mM phenylmethanesulfonyl fluoride (PMSF). Samples were mixed well and homogenization was performed using a VirSonic Ultrasonic Cell Disruptor 100© (VirTis, Gardiner, NY) using five consecutive 2 sec bursts on ice. Following homogenization, samples were centrifuged at 6000 rpm for 2 min at 4° C with the supernatant carefully removed. 150 μL of buffer A was added and samples were sonicated and centrifuged. The supernatant was removed and samples were suspended in 100 μL of buffer C composed of the following reagents: 20 mM HEPES buffer pH = 7.9, 1.5 mM $MgCl_2$, 0.5 mM DTT, 0.5 mM EDTA, 420 mM NaCl, 20% glycerol, 0.2 mM PMSF, 2 ng/mL aprotinin, 0.5 ng/mL leupeptin, 6 μL of 6 % Triton X-100. Samples were vortexed, sonicated for 2 sec on ice. Final suspensions were centrifuged at 14000 rpm for 10 min at 4° C, snap frozen in liquid N_2 and stored at – 80° C until utilized for gel mobility shift assays. Total protein values were obtained using the bicinchoninic acid (BCA) protein determination assay (Pierce, Rockford, IL).

Gel Mobility Shift Assay

Changes in Sp1 transcription factor binding were determined using the electrophoretic mobility shift assay (EMSA). Nuclear extracts were collected from PC12 cells as described above. Oligonucleotides containing sequences corresponding to Sp1 binding sites in the human Ogg1 promoter (GENBank accession number AF_521807) were obtained from a commercial source (Integrated DNA Technologies Inc., Coralville, IA) containing the following sequences [Sp1-1, 5'-GCA AGG AGG GGG CGG GAC CTA

CAC-3'; Anti-sense GTG TAG GTC CCG CCC CCT CCT TGC], [Sp1-2, Sense, TCC TTG TCT GGG CGG GGT CTT TGG; Anti-sense, CCA AAG ACC CCG CCC AGA CAA GGA]. Oligonucleotides were 5' end radio labeled using [γ-^{32}P] ATP as described above. Binding reactions were set up as follows: 30 μg of nuclear extract normalized to equal volumes of 20 μL, 0.4 pmoles of labeled probe, 10 μL of binding buffer containing the following reagents: 20 % glycerol, 5 mM $MgCl_2$, 2.5 mM EDTA, 2.5 mM DTT, 250 mM NaCl, 50 mM Tris-Hcl pH = 7.5, 0.2 ug/μL poly dI-dC. Binding reactions were incubated at room temperature for 30 min and separated on a 6 % native polyacrylamide gel composed of the following reagents: 3.42 mL 40 % acrylamide/ bis-acrylamide, 2 mL of 10X TBE buffer, 17.16 mL ddH_2O, 210 μL 10 % ammonium persulfate, 21 μL N,N,N',N'-Tetramethylethylenediamine (Bio-Rad Laboratories, Hercules, CA). Gel reagents were mixed well and cast into glass gel plates at a volume of 22.5 mL and allowed to polymerize at room temperature. Samples were loaded and run in 0.5X TBE buffer for 2 hr at 200 V in order to resolve bound protein-DNA complexes. Following complex separation the gel was removed using a 7 x 9 inch piece of blot paper (Bio-Rad Laboratories, Hercules, CA) and encased in cellophane plastic wrap into an imaging cassette holder (Bio-Rad Laboratories, Hercules, CA). An imaging plate (Fuji Film Life Science, Stamford, CT) was then exposed to the gels for approximately 30 to 60 min. Imaging plates were read using a FLA-3000 Series Fuji Film Fluorescent Image Analyzer (Fuji Film Life Science, Stamford, CT) and ImageGauge© version 4.22 analysis software (Fuji Photo Film Co., LTD, Stamford, CT).

Data analysis and statistics

Differences in viability curves in PC12 cells were assessed using non-linear

regression analysis and comparison of fit for the two dose-response curves. Difference from control viability was calculated using one-way analysis of variance (1-way ANOVA) with Dunnet's post hoc analysis. Two-way analysis of variance (2-way ANOVA) was used to determine an interaction between cell status and treatment for antioxidants, Ogg1 activity, and oxo^{8}dG with a Bonferroni posttest to determine group differences. A students t-test was used to evaluate differences in Ogg1 mRNA between control and arsenite treated cells in actively dividing PC12 cells. Statistical tests were performed using GraphPad® Prism statistical software (Sorrento, CA) with a $p < 0.05$ considered statistically significant.

Results

Cultures of actively dividing and NGF treated PC12 cells were exposed to sodium arsenite for 24 hr. Viability plots were determined by LDH leakage into the culture media (Figure 16). Goodness of fit analysis determined a statistical difference between the two plots indicating that NGF treated PC12 cells are more susceptible to increasing concentrations of sodium arsenite. One-way ANOVA analysis with Dunnet's post-hoc analysis determined no significant difference in cell viability from control until a dose of 40 μM sodium arsenite. This was equivalent in both actively dividing and NGF treated PC12 cells (Figure 16). Based on the viability plots, NGF treated PC12 cells are more susceptible to increasing concentrations of sodium arsenite than their actively dividing counterparts.

FIGURE 16

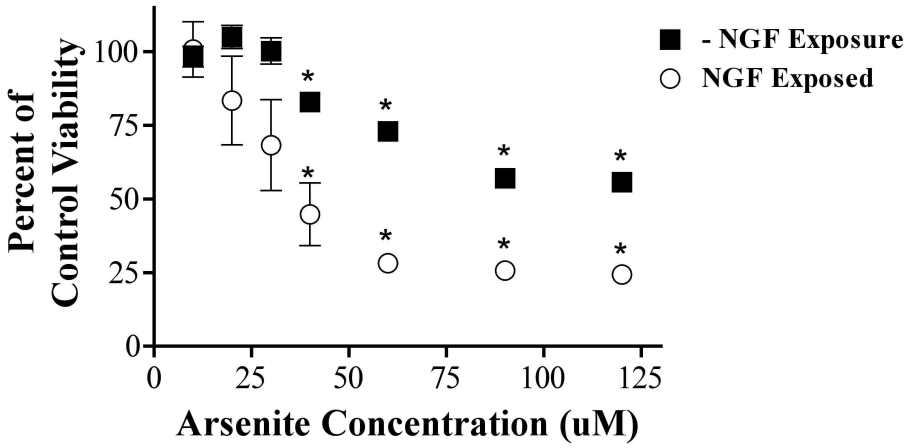
Percent of Control Viability
100
75
50
25
0
0
25
50
75
100
125
Arsenite Concentration (uM)
- NGF Exposure
NGF Exposed
*

Figure 16

The effect of increasing doses of sodium arsenite on the viability of actively dividing and NGF treated PC12 cells exposed for 24 hr as determined by release of lactate dehydrogenase. Values expressed as percent of untreated control cells for actively dividing, open squares (■) and NGF treated populations, open circles (❍). Data is expressed as mean ± S.E.M. (n = 6). * Denotes a significant difference from group matched control, $P < 0.05$.

A concentration of 10 μM sodium arsenite was chosen for further studies based on the viability experiments (Figure 16) and additional in vitro studies exposing cell and tissue cultures to non-lethal doses of inorganic arsenite (Parrish, Zheng et al. 1999; Hu, Jin et al. 2002). 10μM is a dose that is potent enough to facilitate cellular responses without inducing cell death therefore allowing us to determine any biochemical changes preceding cellular demise.

An acute exposure to sodium arsenite elicited an increase in intracellular GSH levels in both actively dividing and NGF treated PC12 cells. Biochemical analysis in actively dividing PC12 cells revealed a 5-fold increase in GSH while the NGF treated PC12 cells had approximately a 2-fold increase (Figure 17). Analysis by two-way ANOVA identified a significant interaction effect between arsenite and cell status ($F=23.74$; $df=1,36$; $p < 0.05$), as well as individual effects by arsenite ($F=292.90$; $df=1,36$; $p < 0.05$) and cell status; defined as actively dividing or NGF treated ($F=25.74$; $df=1,36$; $p < 0.05$). It is interesting to note that although there is a difference in basal levels of GSH between actively dividing and NGF treated PC12 cells, exposure to arsenite led to a plateau in GSH suggesting that the ability of PC12 cells to respond to toxic insult is independent of their cellular status. The response could also be characterized by a greater increase in GSH in actively dividing PC12 cells. Under this guise the actively dividing PC12 cells demonstrate a better response capacity to arsenite treatment. These disparities in levels of GSH could be further explained by examination of components of the GSH synthetic pathway as well as rates of cellular GSH excretion between non-NGF, and NGF treated cells.

FIGURE 17

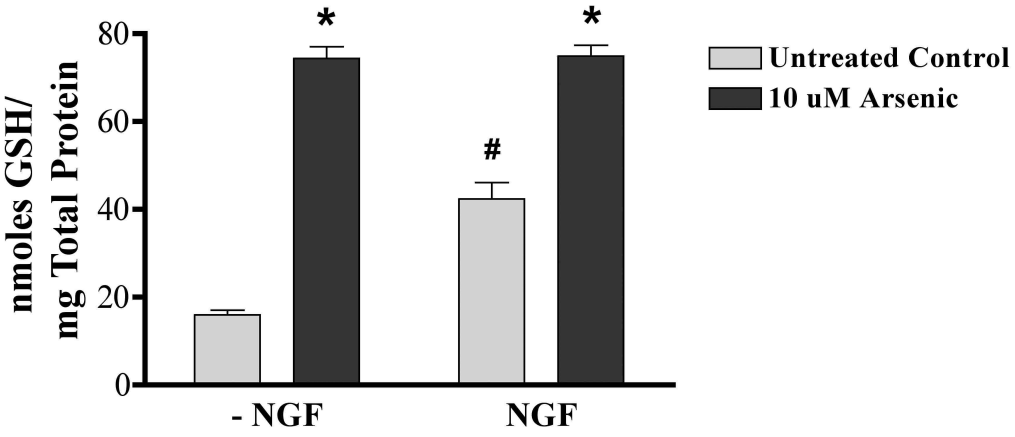
nmoles GSH/
mg Total Protein
80
60
40
20
0
*
*
#
- NGF
NGF
Untreated Control
10 uM Arsenic

Figure 17

Levels of GSH were determined in actively dividing and NGF treated PC12 cells exposed to 10 μM sodium arsenite for 24 hr. Columns represent mean ± SEM. (n= 10). * Indicates a statistical significant difference from control $P < 0.05$. # Indicates a statistical significant difference from untreated actively dividing PC12 cells $P < 0.05$.

Cells maintain additional antioxidant systems to handle a variety of free radical species produced during oxidative stress. SOD isoforms are responsible for the enzymatic dismutation of superoxide into H_2O_2 and are important mediators of oxidative stress. Table 4 summarizes the effects of both NGF treatment, and sodium arsenite exposure on SOD activities in actively dividing and NGF treated PC12 cells. Analysis by two-way ANOVA for Cu/Zn SOD revealed no significant interaction or arsenite effect, however, there was a significant effect for cell status ($F=27.49$; $df=1,34$; $p < 0.05$) indicating that Cu/Zn SOD activity is significantly reduced as a consequence of NGF exposure. Two-way ANOVA for Mn SOD activity revealed a significant interaction effect ($F=5.13$; $df=1,35$; $p < 0.05$), and a significant effect by arsenite on Mn SOD levels in actively dividing PC12 cells ($F=4.62$; $df=1,35$; $p < 0.05$).

TABLE 4. Copper/Zinc and Manganese SOD levels in actively dividing and NGF treated PC12 cells exposed for 24 hr to 10 μM sodium arsenite.

	Actively Dividing		NGF Treated	
	Mn SOD	**Cu/Zn SOD**	**Mn SOD**	**Cu/Zn SOD**
Control	11.97 ± 0.34	30.32 ± 1.30	15.38 ± 1.43	11.87 ± 0.63[#]
Arsenite	22.27 ± 4.47*	24.22 ± 4.17	15.61 ± 0.96	13.17 ± 0.68

Arsenic has been reported to have effects on both the transcription (Andrew, Karagas et al. 2003) and activity of DNA repair enzymes (Tran, Prakash et al. 2002; Hartwig, Blessing et al. 2003) however; studies have not demonstrated an effect of arsenic on rat Ogg1 activity or expression. Treatment with sodium arsenite for 24 hr decreased the enzymatic activity of Ogg1 in both actively dividing and NGF treated PC 12 cells (Figure 18A). A 3-fold decrease in excision activity was evident in the actively dividing cells, which also had a larger increase in GSH (Figure 17). Two-way ANOVA analysis indicates a significant interaction between arsenite treatment and cell status on Ogg1 excision activity ($F=79.66$; $df=1,22$; $p < 0.05$). There was also an effect by arsenite ($F=179.30$; $df=1,22$; $p < 0.05$) and cell status alone ($F=79.31$; $df=1,22$; $p < 0.05$). Ogg1 activity remained attenuated even in the presence of increased total protein used in reactions. Nuclear extracts from actively dividing PC12 cells were used ranging from 0 to 40 μg total protein. Decreased Ogg1 activity remained constant in the arsenite exposed PC12 cells compared to control (Figure 18C).

FIGURE 18

A.

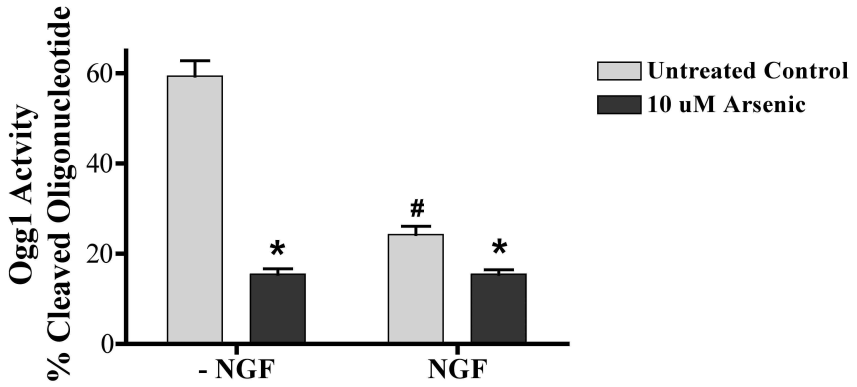
Ogg1 Actvity
% Cleaved Oligonucleotide
60
40
20
0
*
#
*
- NGF
NGF
Untreated Control
10 uM Arsenic

B.

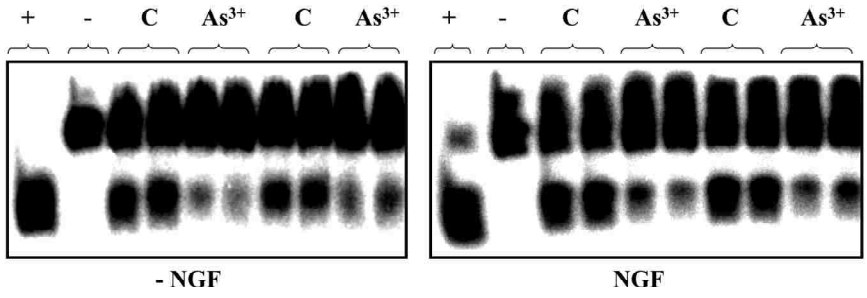
+
-
C
As3+
C
As3+
+
-
C
As3+
C
As3+
- NGF
NGF

FIGURE 18

C.

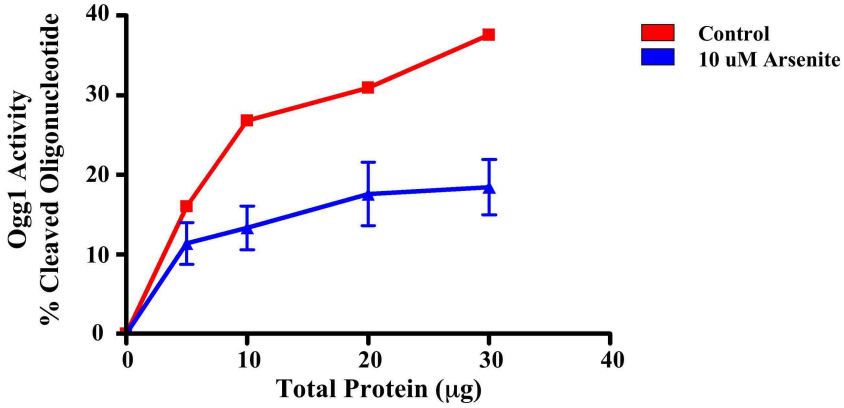
Ogg1 Activity
% Cleaved Oligonucleotide
40
30
20
10
0
0
10
20
30
40
Total Protein (μg)
Control
10 uM Arsenite

Figure 18

Ogg1 activity in actively dividing and NGF treated PC12 cells 24 hr after exposure to 10 μM sodium arsenite (A). Columns represent mean ± SEM. (n = 5 - 9). * Indicates a statistical significant difference from control $p < 0.05$. # Indicates a statistical significant difference from actively dividing PC12 control cells $p < 0.05$.

(B) Typical gel image used for the analysis of extracts to cleave oxo^{8}dG; each sample ran in duplicate. Formamidopyrimidine-DNA glycosylase (3 U) activity was used as a positive control; C = control, A = 10μM arsenite treatment.

(C) Ogg1 activity plot in nuclear extracts from actively dividing PC12 cells exposed to 10 μM sodium arsenite for 24 hr. Activity expressed relative to increasing total protein levels in reaction mixture. Data points represent mean ± SEM. (n = 4).

Important to note is that the enzymatic activity of Ogg1 is lower basally by > 50 % in the NGF treated control cells compared to the actively dividing control group (Figure 18A). The NGF treated PC12 cell control group also had an increased level of GSH approximately 2X higher than actively dividing control PC12 cells (Figure 17). This trend for a reduction in Ogg1 activity in the presence of increased GSH, either by NGF or arsenite treatment was analyzed by Pearson test for correlation in both the actively dividing and NGF treated PC12 cells (Figure 19). Both actively dividing and NGF treated PC12 cells demonstrated an inverse relationship between the levels of GSH and Ogg1 activity in both untreated and arsenite treated samples; (actively dividing Pearson r = -0.9473, $r^2 = 0.8973$, $p < 0.05$; NGF treated Pearson r = -0.9400; $r^2 = 0.8835$, $p < 0.05$). These results suggest an association between Ogg1 activity and the cellular redox state as defined by levels of GSH.

FIGURE 19

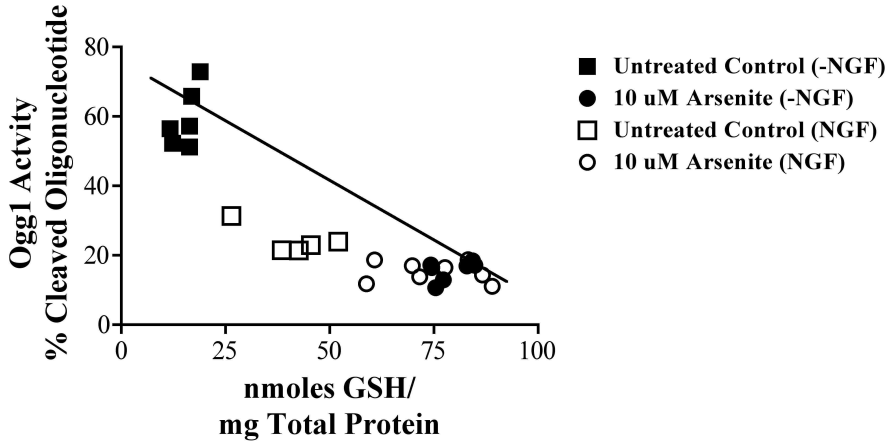
Ogg1 Actvity
% Cleaved Oligonucleotide
80
60
40
20
0
0
25
50
75
100
nmoles GSH/
mg Total Protein
Untreated Control (-NGF)
10 uM Arsenite (-NGF)
Untreated Control (NGF)
10 uM Arsenite (NGF)

Figure 19

Pearson plot of Ogg1 activity versus levels of GSH as a function of either NGF, or arsenite treatment in actively dividing and NGF treated PC12 cells. (■) Represents actively dividing PC12 cells receiving no sodium arsenite treatment. (●) Represents actively dividing PC12 cells exposed to 10 μM sodium arsenite for 24 hr. (□) represents NGF treated PC12 cells receiving no sodium arsenite exposure. (○) represents NGF treated PC12 cells exposed to 10 μM sodium arsenite for 24 hr.

Although *in vitro* biochemistry cannot completely mimic biological conditions, previous work has shown no direct effects on DNA repair enzymes, other than Ogg1, via arsenite exposure. This was demonstrated in separate studies characterizing the effects of arsenite on DNA ligase (Hu, Su et al. 1998) and Fpg; the bacterial homologue of Ogg1 (Asmuss, Mullenders et al. 2000). Because a reduction in Ogg1 activity was seen subsequent to arsenite exposure in both actively dividing and NGF treated PC12 cells, any direct effect of arsenite on enzymatic function was determined by pre-treating glycosylase protein extracts with sodium arsenite prior to incubation with the oxo^{8}dG substrate. Glycosylase extracts obtained from actively dividing PC12 cells were collected and 20μg total protein was pre-incubated for 30 min, 37^{o}C with increasing concentrations (0, 10, 50, and 100μM) of sodium arsenite. Following pre-incubation the assay was completed as described in materials and methods and activity was measured as a function of incubation time of enzyme with substrate. Figure 20 summarizes the direct effects of sodium arsenite on Ogg1 activity. There was no change in enzyme activity even at concentrations of arsenite equivalent, or greater to, arsenite levels that resulted in a significant loss in cell viability (Figure 16 and 20). Additional glycosylase extracts obtained from murine cerebellum were used in the same fashion as the PC12 cells. There was no inhibitory effect of arsenite (0 – 25 μM, data not shown) on mouse Ogg1 activity as well. This suggests that arsenite does not have a direct effect on enzyme activity under these *ex vivo* experimental conditions and that the decreases previously seen (Figure 18) are due to *in vivo* changes via changes to other cellular systems.

FIGURE 20

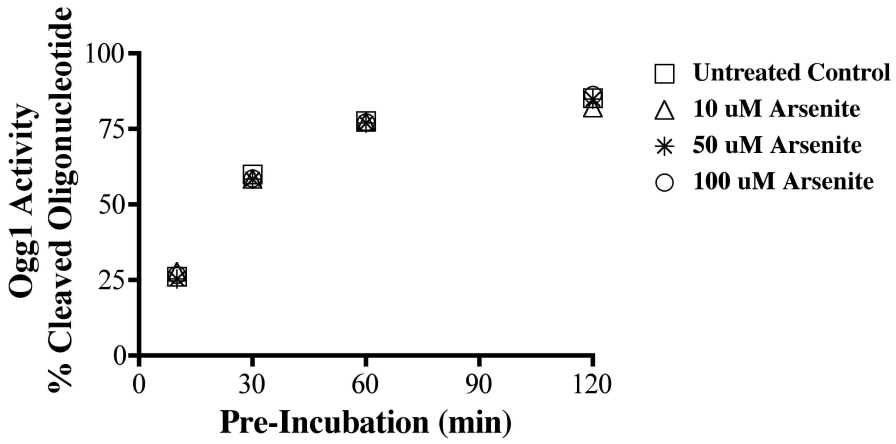
Ogg1 Activity
% Cleaved Oligonucleotide
100
75
50
25
0
0
30
60
90
120
Pre-Incubation (min)
Untreated Control
10 uM Arsenite
50 uM Arsenite
100 uM Arsenite

Figure 20

Ogg1 activity in glycosylase extracts from actively dividing PC12 cells pre-incubated for 30 min with sodium arsenite (0, 10, 50, and 100μM). Samples were run in duplicate at each time point from 0 to 120 min. (n = 2 per dose & time group).

Since there was no direct inhibition by sodium arsenite on Ogg1 activity (Figure 20), and the degree of reduction in enzyme activity was not equivalent between actively dividing and NGF treated PC12 cells (Figure 18), an assessment of Ogg1 mRNA was performed to reveal any transcriptional changes. Figure 21A demonstrates a significant decrease in the levels of Ogg1 mRNA by ~ 30 % in actively dividing PC12 cells. Actively dividing PC12 cells were solely measured for changes in transcription due to the largest reduction in enzyme activity being evident in this group.

FIGURE 21

A.

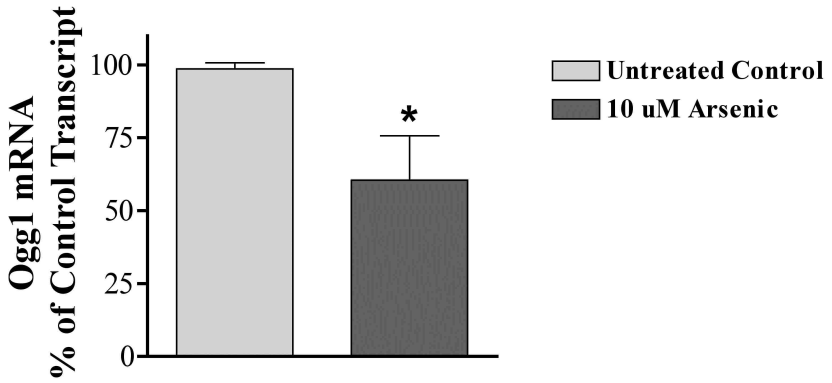
Ogg1 mRNA
% of Control Transcript
100
75
50
25
0
*
Untreated Control
10 uM Arsenic

B.

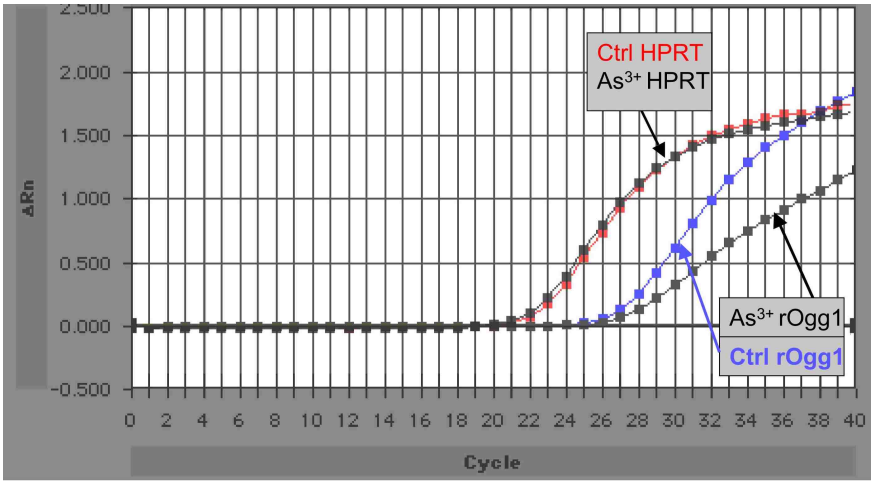
2.500
2.000
1.500
1.000
0.500
0.000
-0.500
ΔRn
0 2 4 6 8 10 12 14 16 18 20 22 24 26 28 30 32 34 36 38 40
Cycle
Ctrl HPRT
As3+ HPRT
As3+ rOgg1
Ctrl rOgg1

Figure 21

(A) Levels of Ogg1 mRNA in actively dividing PC12 cells exposed to 10 μM sodium arsenite for 24 hr as a measure of transcriptional activity. Columns represent mean ± SEM. (n = 8). * Indicates a statistical significant difference from untreated actively dividing PC12 cells $P < 0.05$.

(B) Representative fluorometric plot of real time PCR reactions measuring levels of Ogg1 and HPRT transcripts.

Human Ogg1 has been suggested to be a constitutively expressed housekeeping gene, and the promoter for hOgg1 has been previously sequenced (Dhenaut, Boiteux et al. 2000). Distinct Sp1 binding sites have been identified in the promoter upstream of the transcription initiation site (Figure 4, Chapter 1) and have been validated by gel shift binding analysis (Youn, Kim et al. 2005). Arsenic exposure has been associated with decreased Sp1 binding activities. Decreased Sp1 binding was suggested to be due to protein oxidation occurring at levels of arsenic below 1μM (Chou, Chen et al. 2005). Based on the evidence that arsenite induces oxidative stress, Sp1 binding activities were assessed by EMSA in actively dividing PC12 cells exposed to 10 μM arsenite for 24 hr (Figure 22). Two different double stranded oligonucleotides representing Sp1 binding sites from the hOgg1 promoter were used for binding analysis. The lanes containing extract from untreated PC12 cells exhibited strong binding with a substantial decrease in binding seen in the arsenite treated cells. Co-incubating nuclear extracts with labeled and unlabeled Sp1 oligonucleotides resulted in a complete attenuation of binding, while co-incubation with a non-specific unlabeled oligonucleotide containing a consensus Nrf-2 transcription factor sequence resulted in recovery of binding, showing specificity of protein-DNA interaction at these Sp1 sites.

FIGURE 22

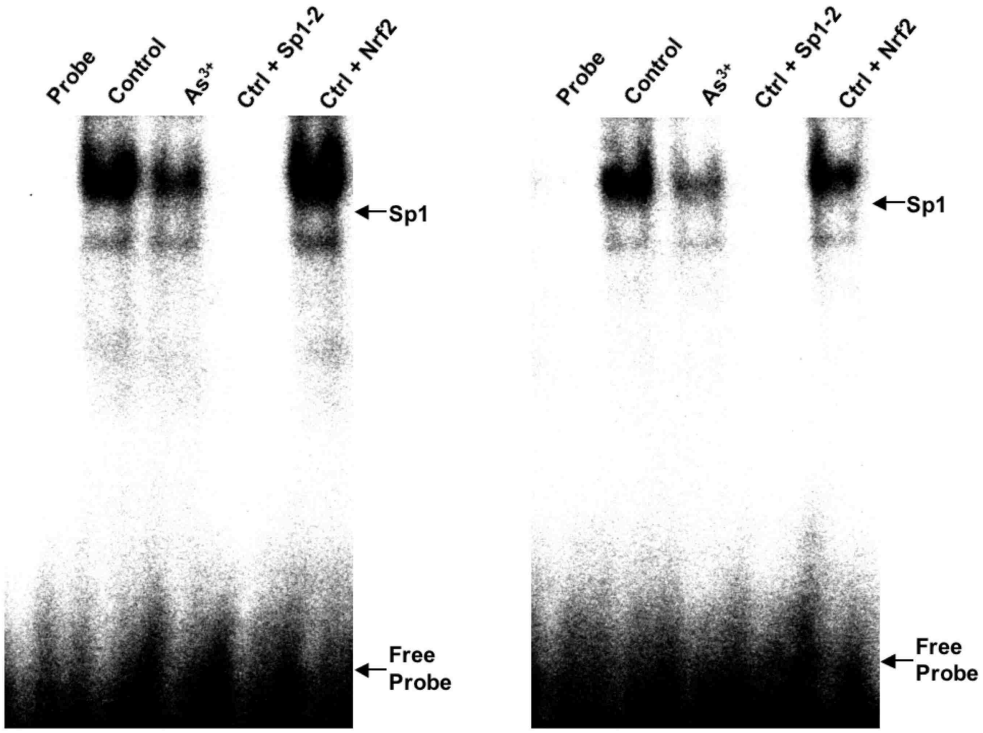

Left Panel **Right Panel**

Figure 22

Representative gel of EMSA analysis of two independent Sp1 sites originating from the hOgg1 promoter. Binding differences were measured from nuclear extracts of untreated and arsenite treated actively dividing PC12 cells. Competition EMSA were performed using γ-^{32}P labeled, double stranded oligonucleotide probes containing the two Sp1 sites. The Sp1 shifted bands and unbound probe are indicated. Competition EMSA using 30 μg nuclear extracts from untreated PC12 cells. Labeled Sp1 probes were co-incubated with either 100X unlabeled Sp1 probe, or unlabeled consensus Nrf2 probe.

Conditions where DNA repair is continually compromised can lead to increased levels of oxo^{8}dG; a situation that can have deleterious effects in both actively dividing and differentiated cells. Although arsenite induced increased levels of GSH (Figure 17), decreased Ogg1 activity and Ogg1 mRNA (Figures 18 and 20), this did not translate into higher levels of oxo^{8}dG in either actively dividing or NGF treated PC12 cells exposed to 10 μM arsenite (Figure 23). Two-way ANOVA analysis showed no significant effect from arsenite or cell status as well as no significant interaction. Basal levels of oxo^{8}dG tend to be higher in NGF treated controls; an observation that can be attributed to the lower Ogg1 activity seen in that group (Figure 18A). It is important to reiterate that non-lethal levels of sodium arsenite were used in these experiments. It is possible that exposure to higher levels of arsenite would result in similar changes in GSH, Ogg1 activity/transcription, and would also yield higher levels of oxo^{8}dG. Longer exposure times, indicative of a chronic exposure to arsenic, would be worthy of consideration to determine if the reduction in Ogg1 activity persists, and ultimately results in greater accumulations of oxo^{8}dG.

FIGURE 23

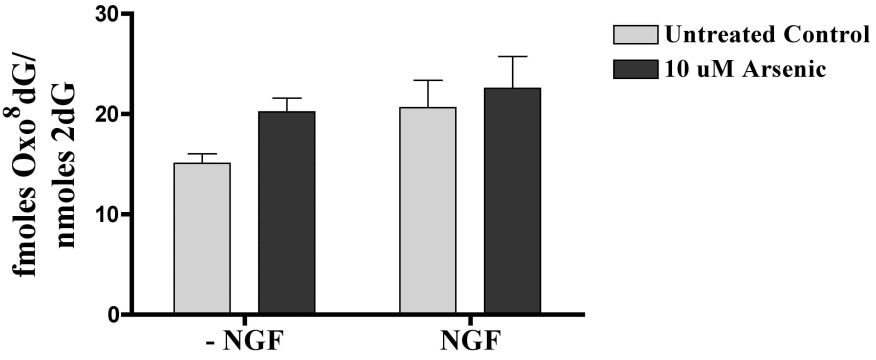
fmoles Oxo8dG/
nmoles 2dG
30
20
10
0
- NGF
NGF
Untreated Control
10 uM Arsenic

Figure 23

Levels of oxo^{8}dG as an indication of DNA damage from exposure to 10μM sodium arsenite for 24 hr were measured in actively dividing and NGF treated PC12 cells. Columns represent mean ± SEM. (n = 6 - 12).

Conclusions

Acute low-level exposure to sodium arsenite facilitates multiple changes in cellular defenses that are both dependent and independent of cell status in PC12 cells; actively dividing or NGF exposed. Susceptibility to sodium arsenite is increased in differentiated cellular populations as shown in the NGF treated PC12 cells when compared to their actively dividing counterparts. Increased susceptibility occurred despite increases in the cellular antioxidants subsequent to both NGF treatment and arsenite exposure. NGF treatment alone led to a decrease in Ogg1 activity implicating a potential role for growth factor signal pathways in Ogg1 regulation. Furthermore arsenite is capable of affecting both antioxidant and DNA repair systems in actively dividing, and NGF treated PC12 cells. Decreased Ogg1 activity is dependent in part, on changes in the transcriptional regulation measured by changes in Ogg1 mRNA. This was further demonstrated in *ex vivo* exposures showing no attenuation of Ogg1 enzymatic activity pre-incubated with sodium arsenite (Figure 20). Gel shift assays further revealed a promising direction for investigation as Sp1 binding was decreased subsequent to arsenite exposure. This suggests an additional component of transcriptional regulation for Ogg1 potentially involved in its arsenic-mediated down regulation. Overall, the decreased repair capacities caused by arsenite exposure suggest a link between attenuated genomic repair DNA and arsenic related health concerns. It also proposes further questions into mechanisms of arsenic toxicity in cellular systems; this is based on the attenuation of both Ogg1 transcription, and activity despite the induction of stress response systems indicated by increases in cellular GSH.

CHAPTER TWO DISCUSSION

Despite the description of a putative Nrf2 recognition site in the promoter region of Ogg1, no association has been made between Nrf2 and the regulation of Ogg1. Mice lacking Nrf-2 (Nrf2 -/-) have basal levels of oxo^{8}dG in the liver and kidney that are higher than wild type littermates (Li 2004). Furthermore, accumulation of oxo^{8}dG in Nrf-2 -/- mice was higher after exposure to both diesel exhaust particles and cigarette smoke (Aoki, Sato et al. 2001; Rangasamy, Cho et al. 2004). However, in both studies the transcription and activity of Ogg1 were not measured making it difficult in determining a role for Ogg1 in those studies. It has been reported that Nrf-2 is highly regulated by the redox status of the cell and its ability to alter gene expression is therefore highly sensitive to intracellular levels of GSH (Dinkova-Kostova, Holtzclaw et al. 2002; Hyun, Jung et al. 2003; Hansen, Watson et al. 2004). An attenuation of GSH can cause shifts in the cellular redox state to more oxidizing conditions, and activate cytoprotective transcriptional pathways.

As a compensatory mechanism for oxidative stress, Nrf2 can be released from a cytosolic inhibitory protein, KEAP1, and translocate to the nucleus (Itoh, Wakabayashi et al. 1999). Once in the nucleus, Nrf2 interacts with its cognate binding sequence or sequences on promoters of Nrf2 regulated genes including ones involved in GSH synthesis and homeostasis; most notably glutamate cysteine ligase, GSH synthase, GSH reductase. Also included are free radical scavenging enzymes such as NADPH quinone oxidoreductase, manganese superoxide dismutase, and GSH peroxidase (Venugopal and Jaiswal; Lee, Calkins et al. 2003). This response has been further characterized by work showing activation of Nrf-2 after exposure to agents known to modulate levels of GSH

including tBHQ, sulforaphane (GST-mediated) and GSH itself (Lee, Moehlenkamp et al. 2001; Kim, Park et al. 2003; Hansen, Watson et al. 2004). The use of these compounds as pharmacologic tools provides a link between the modulation of the cellular redox state and a subsequent induction of cytoprotective genes. Ogg1 has been reported to be responsive to redox changes (Cardozo-Pelaez, Stedeford et al. 2002); a finding further supported by the presence of inducible elements in the promoter of the human Ogg1 gene including binding sites for p53 and NF-YA transcription factors (Lee, Kim et al. 2004; Chatterjee, Mambo et al. 2006). A putative binding site for Nrf2 has also been identified yet still remains unverified (Dhenaut, Boiteux et al. 2000). The putative Nrf2 site is important for basal transcription of hOgg1 as site-directed deletion experiments resulted in a loss of GFP reporter gene expression under the regulation of the altered hOgg1 promoter (Figure 7A and B). PCR analysis of these cultures revealed an equivalent efficiency for transfection demonstrating that an alteration to the hOgg1 promoter sequence (deleting Nrf2 binding site) is facilitating the changes in GFP expression (Figure 7C). In addition, the identification of protein interaction at this binding site that is inducible by tBHQ (Figure 8), lends support that Nrf2 is interacting with this region of the hOgg1 promoter.

Changes in GSH have also been associated with increased Ogg1 transcription, expression, and activity in both *in vivo* and *in vitro* studies (Table 3). In one study, a six hr treatment with DEM increased the activity of Ogg1 in the cerebellum, cortex and pons medulla of C57BL/J6 mice; however no mRNA or transcriptional changes were measured. In addition, a 24 hr exposure to 100 μM BSO caused increases in both the activity and transcription of Ogg1 in PC12 cells that plateau between 12 - 18 hr (data not

shown). It was shown that decreased Ogg1 activity in extracts from cadmium treated human lymphoblastoid cells was attributed to protein oxidation bringing another level of redox regulation for Ogg1, via direct thiol modifications (Bravard, Vacher et al. 2006). It was found in our lab that addition of GSH directly to glycosylase extracts caused an increase in Ogg1 activity compared to untreated extracts derived from the same source (data not shown). The two previous statements suggest that the enzymatic activity of Ogg1 is dependent on a non-oxidizing environment. However, administration of GSH-mee decreased hOgg1 regulated luciferase activities (Figures 12C and 13) bringing forth the question of how increases in cellular GSH are attenuating hOgg1 transcription. It implies the presence of additional factors involved in the transcriptional down-regulation of hOgg1. Changes in hOgg1-regulated reporter gene activity were evident in Figures 10 and 11 (tBHQ and DEM respectively) strengthening the argument that transcriptional regulation of hOgg1 is a major cellular component of cellular defense. Taken together, previous and current data also suggest that Ogg1 is modulated in a manner similar to genes under the regulation of Nrf2 as both compounds have been used as inducers of Nrf2 mediated transcription. Figure 24 illustrates a proposed pathway of hOgg1 transcriptional regulation by Nrf2. This includes how modulation of promoter activity can occur via modulation of intracellular GSH using the compounds tBHQ, DEM, and GSH-mee. Compounds that induce Nrf2 activation (DEM, tBHQ) facilitate the release of Nrf2 from its inhibitory partner KEAP1 and allow translocation of Nrf2 into the nucleus and increase the transcriptional activity of Ogg1. Compounds that stabilize Nrf2/KEAP1 complexes (GSH-mee) via stabilization of sulfhydryl groups on KEAP1 keep Nrf2 sequestered in the cytosol and reduce the transcriptional activity of Ogg1.

FIGURE 24

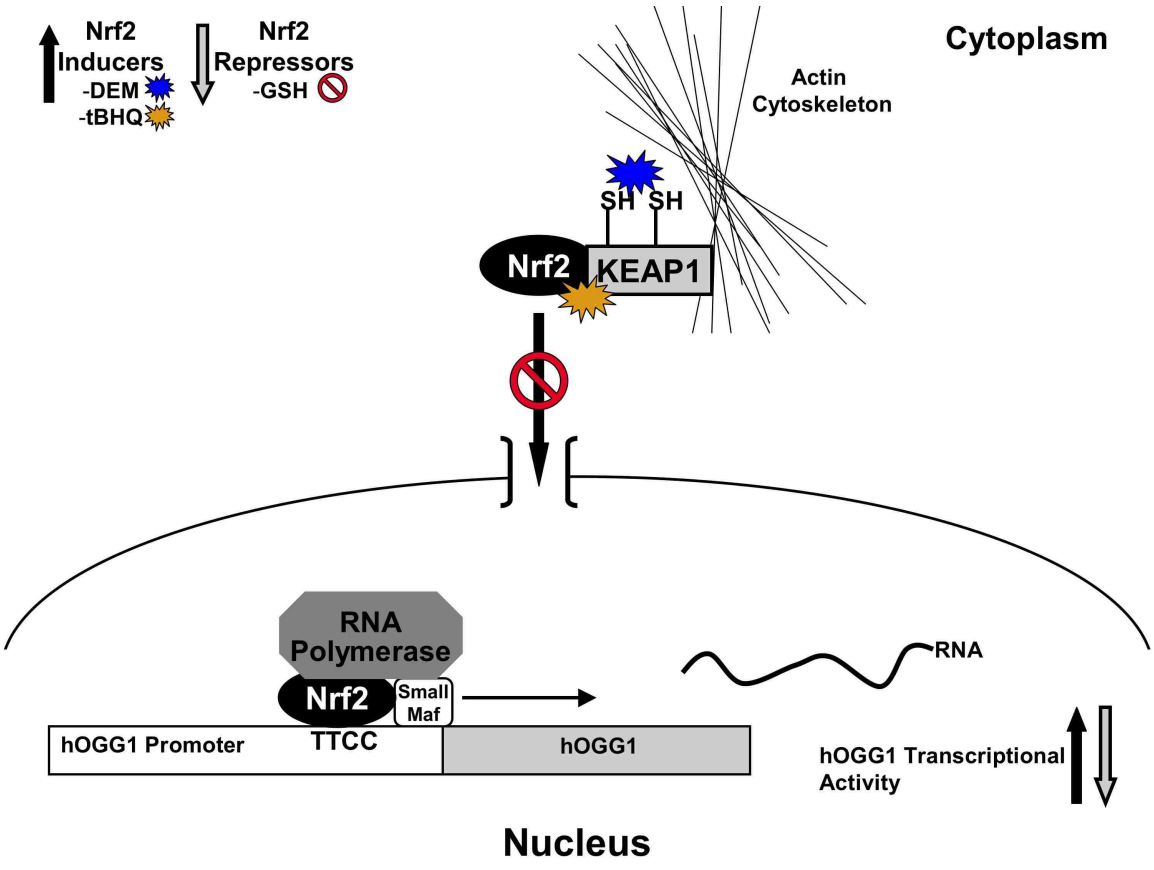
Nrf2
Inducers
-DEM
-tBHQ
Nrf2
Repressors
-GSH
Cytoplasm
Actin
Cytoskeleton
SH SH
Nrf2
KEAP1
RNA
Polymerase
Nrf2
Small
Maf
TTCC
hOGG1 Promoter
hOGG1
RNA
hOGG1 Transcriptional
Activity
Nucleus

Figure 24

Proposed model pathway for transcriptional regulation of hOgg1 by glutathione modulating agents and the transcription factor Nrf2.

In this study we have explored the promoter of the hOgg1 gene originally sequenced and characterized by Dhenaut and colleagues (Dhenaut, Boiteux et al. 2000). We have presented evidence indicating that modulation of the hOgg1 promoter is sensitive to levels of intracellular GSH, and that activation/translocation of the transcription factor Nrf2 is an integral component of this pathway. By characterizing different transcriptional regulators of Ogg1, a better understanding can be gleaned as to how transcriptional changes in Ogg1 can participate in pathologies associated with aging, carcinogenesis, and neurodegenerative disease. It can also aid in understanding the mechanisms of toxicity associated with increased levels of oxo^8dG.

Linking Ogg1 to Nrf2 mediated regulation can allow the investigation of different therapies designed to prevent oxidative damage to DNA (oxo^8dG) by boosting repair capacity (Ogg1). This is due largely to the vast amount of published data pertaining to Nrf2 and its upstream regulatory pathways such as map kinases (Yu, Chen et al. 2000) and phosphatidylinositol 3 kinase (Martin, Rojo et al. 2004); two well characterized protein kinases involved in signal transduction pathways. In addition, compounds capable of inducing an antioxidant response via Nrf2 can also be investigated as potential therapies for limiting oxidative damage to DNA (Kim, Hu et al. 2003; Suh, Shenvi et al. 2004; Chen, Jang et al. 2005). By linking Ogg1 transcriptional regulation to the transcription factor Nrf2 we can advance our understanding of the relationship between the cellular redox state and DNA repair.

CHAPTER THREE DISCUSSION

Cultures of actively dividing and NGF treated PC12 cells were exposed to sodium arsenite for 24 hr. Analysis established a statistical difference between the two plots shown in Figure 16, indicating that NGF treated PC12 cells are more susceptible to increasing concentrations of sodium arsenite. Differential susceptibility is a phenomenon seen in a variety of tissues that contain actively dividing and differentiated cellular populations. A recent study suggested H_2O_2 induced apoptosis was dependent on cell status in human keratinocytes with the differentiated suprabasal cells containing greater resistance to H_2O_2 (Zuliani, Denis et al. 2005). It has been established that neurons are more susceptible than astrocytes to a variety of insults and furthermore astrocytes have been shown to provide a protective response for neurons during oxidative stress (Desagher, Glowinski et al. 1996; Shih, Johnson et al. 2003). This sets up a symbiotic relationship for neuroprotection because of the diminished ability for neurons to elicit an antioxidant response in comparison to astrocytes (Murphy, Yu et al. 2001). NGF has the ability to stop PC12 cells from actively dividing and differentiates them into a neuronal phenotype, including the formation of neurite extensions (Greene and Tischler 1976). A differential stress response can account for actively dividing PC12 cells having a greater resistance to arsenite versus their NGF treated counterparts similar to the relationship between neurons and astrocytes. Ultimately it is unclear what signaling pathways are affected following NGF-induced differentiation in PC12 cells that ultimately contribute to an increased susceptibility to arsenite.

Other studies looking at differences between actively dividing and NGF treated PC12 cells have produced varied results. NGF treated PC12 cells were shown to have an

increased resistance to the peroxide compounds H_2O_2 (Sung, Cheng et al. 2003), and t-butyl hydroperoxide (TBH) (Ekshyyan and Aw 2005) whereas others have shown a decreased resistance to tumor necrosis factor-α (TNF-α) and ROS including lipid- and hydroperoxides including TBH (Sasaki, Baba et al. 2001). In the context of this study, sodium arsenite was able to elicit a decrease in cell viability in the NGF treated PC12 population (Figure 16). A basis for the variation in results can be the culture conditions in which PC12 cells are grown and differentiated. The aforementioned studies have differences in base media used, concentration of growth serum, and in the amount and time used for NGF-induced differentiation. It is difficult to compare results between studies where the culture conditions are so diverse, regardless of common exposure regiments and measured endpoints. Regardless of response capacities between actively dividing and NGF treated PC12 cells, it is evident from the viability plot (Figure 16) that NGF treated PC12 cells are more susceptible to increasing concentrations of sodium arsenite than their actively dividing counterparts.

Glutathione (GSH) is regarded as the first line of cellular defense against free radicals and changes in cellular GSH can be utilized as a marker for oxidative stress, and an indicator of the cellular redox state (Griffith 1999; Sies 1999). Trivalent arsenic has been reported to have a high affinity for vicinal sulfhydryl groups on various macromolecules (Scott, Hatlelid et al. 1993) and there have been in vitro studies showing a direct conjugation of methylated arsenic (III) species with GSH in both rat liver, and rat endothelial cell lines (Hirano, Kobayashi et al. 2004; Sakurai, Ochiai et al. 2004). In the present study, basal levels of GSH were approximately twice as high in the NGF treated PC12 cells (Figure 17). This elevation has been previously reported in PC12 cells

exposed to 50 ng/mL of NGF and it was suggested that the elevation was due to increased uptake of the GSH precursors *L*-cystine and *L*-cysteine, and an increase in the activity of glutamate-cysteine ligase (GCL); the enzyme responsible for glutathione synthesis (Pan and Perez-Polo 1996). Treatment of PC12 cells with NGF has been previously reported to have cytoprotective effects. Pre-treatment of PC12 cells for 24 hr with 50 ng/mL NGF resulted in a recovery of cell viability from H_2O_2 generated by a glucose oxidase based assay, an event that was suggested by the authors to be due to the induction of GSH (Pan and Perez-Polo 1996). Dugan et. al. reported a cytoprotective response initiated by NGF to be a result of map kinase (MAPK) activation via the TrkA/NGF receptor the endogenous receptor for NGF (Dugan, Creedon et al. 1997). A cytoprotective mechanism can be further corroborated by the ability of NGF to decrease the level of superoxide in PC12 cells (Mills, Takeda et al. 1998). The study utilized both a dominant negative Ras, and MEK inhibitors to attenuate the protective effects of NGF, suggesting that activation of MAPK pathways have a cytoprotective role in PC12 cells (Mills, Takeda et al. 1998). Additional evidence implicates the role of interleukin-6 in the recovery of cell viability in PC12 cells exposed to 50μM 4-hydroxynonenal (HNE). This demonstrates a cytoprotective response via increases in GSH (Nakajima, Yamada et al. 2002) as HNE has been shown to elicit a strong induction of GSH synthesis by activation of map kinase pathways (Forman and Dickinson 2003).

The promoter regions for both the catalytic (GCLC), and modulatory (GCLM) sub-units of the GCL genes contain AP-1 and Nrf2 binding sites (Dickinson, Levonen et al. 2004). It is likely that NGF is acting via MAPK pathways to facilitate an AP-1 mediated induction of GCL as one of the pathways for stress response. The transcription

factor Nrf-2 has been reported to induce antioxidant response element (ARE) regulated genes via MAPK's (Yu, Lei et al. 1999) and could also be responsible for increased GSH in PC12 cells exposed to NGF yet no definitive evidence has shown Nrf-2 activation and translocation subsequent to NGF exposure.

An acute exposure to sodium arsenite also caused an increase in intracellular GSH in both actively dividing and NGF treated PC12 cells. Biochemical analysis in actively dividing PC12 cells revealed a 5-fold increase in GSH while the NGF treated PC12 cells had approximately a 2-fold increase (Figure 17). Similar reports of GSH induction subsequent to arsenite exposure have been demonstrated in different cell lines. This includes increased cystine uptake, cysteine utilization in Chinese hamster V79 cells, and increased GCL activity and mRNA in human keratinocyte cell lines at 5 and 10μM arsenite respectively; (Ochi 1997; Schuliga, Chouchane et al. 2002) concentrations also similar to those used in this study. Arsenite was reported to have no effect on the ratio of reduced to oxidized glutathione (GSH/GSSG). However, both glutathione reductase mRNA and activity increased as a consequence of arsenite exposure revealing a plausible explanation for the lack of change seen in the GSH/GSSG ratio (Schuliga, Chouchane et al. 2002). The previous examples demonstrate that a multitude of redundant systems exist to maintain the homeostasis of cellular GSH despite arsenic exposure.

Another explanation for increased GSH from arsenite exposure can be due to the activation of cellular stress pathways similar to the induction seen after NGF treatment. PC12 cells exposed to higher levels of arsenite revealed a transient yet differential increase in map kinase activities for p38, JNK1, and ERK2; listed from highest to lowest induction respectively (Liu, Guyton et al. 1996). Furthermore the activation of all three

MAPK's was attenuated by a 45 min pre-incubation of 20mM NAC thereby associating levels of GSH, or non-protein thiols in general, as probable mediators for stress pathway activation subsequent to arsenite exposure.

Studies have implicated arsenic as a causative agent of oxidative stress (Barchowsky, Klei et al. 1999; Flora 1999) with increased GSH being an event associated with a cellular stress response. In this study, PC12 cells were able to elicit an acute response to sodium arsenite by dramatically increasing intracellular glutathione (Figure 17). Initially, increased GSH appears to be a protective mechanism in acute arsenite exposures. However, chronic exposures can present an alternative scenario with the depletion of GSH resulting in persistent oxidative insult to the cell (Flora 1999; Pi, Yamauchi et al. 2002). This is an important distinction to make when comparing cellular stress response, as it is clear that exposure duration is producing a varied cellular response.

Cells have additional antioxidant defenses to remove free radicals produced during oxidative stress. Catalase and glutathione peroxidase remove H_2O_2 while the precursor for H_2O_2, superoxide is handled primarily by two enzymes; copper/zinc and manganese superoxide dismutase (Cu/Zn SOD & Mn SOD respectively). SOD's are responsible for the enzymatic dismutation of superoxide into H_2O_2 and are important mediators of oxidative stress. Mn SOD is the mitochondrial isoform and studies have reported the deleterious effects of arsenic in mitochondria including disruption of both organelle membrane potential, and enzymatic activities. Sodium arsenite was previously shown as having an inhibitory effect on pyruvate dehydrogenase; an integral mitochondrial enzyme involved in glucose metabolism and energy production in the cell

(Petrick, Ayala-Fierro et al. 2000). Furthermore arsenic (III) oxide was capable of disrupting the mitochondrial membrane potential in a variety of lymphoid cell lines (Rojewski, Korper et al. 2004). These studies demonstrate the diverse effects and toxicity that trivalent arsenic can have on mitochondrial function. A two-fold increase in Mn SOD activity was seen in actively dividing PC12 cells exposed to arsenite while the NGF treated cells remained unchanged. The increased Mn SOD activity demonstrated in Table 4 corresponds to increased Mn SOD expression seen in cases where oxidative stress was present (Blaauwgeers, Vianney de Jong et al. 1996; Warner, Stuart et al. 1996). MnSOD has been reported as inducible via Nrf2 and NF-κB transcription factor pathways (Xu, Krishnan et al. 1999). The increased MnSOD activity seen in actively dividing PC12 (Table 4) cells is consistent with the increased synthesis of GSH (Figure 17) as an indicator of stress response subsequent to arsenite exposure. The GCLC and GCLM subunits also contain regulatory elements similar to MnSOD and are inducible via arsenite exposure (Dickinson, Levonen et al. 2004; Kann, Estes et al. 2005). This also can occur via Nrf2 activation and translocation, as current literature has not identified any definitive NF-κB binding sites in the promoter regions of either GCL subunit (Dickinson, Levonen et al. 2004).

A cross-sectional study of people chronically exposed to arsenic in drinking water found that total SOD activities were unchanged (Pi, Yamauchi et al. 2002) which is consistent with the data presented in Table 4. The inconsistency in Cu/Zn SOD activities among control groups is difficult to explain as others have shown an induction of Cu/Zn SOD expression in non-transformed human epidermal keratinocytes subsequent to a 24-hour exposure to 5 μM arsenite (Hamadeh, Trouba et al. 2002). Analysis of SOD

activities at earlier time points could reveal changes in Cu/Zn SOD activity that were unobservable at 24 hr in this study (Table 4). A caveat in study comparison is that data involving different species is difficult to equate to the changes in SOD activities seen here; a difficulty further compounded by comparing the effects seen in acute versus chronic exposures to arsenite.

Despite the induction of GSH, increasing concentrations of arsenite resulted in decreased cell viability (Figure 16). In addition, arsenite did not change SOD activities in a negative manner. This sets up a role for other cellular defense systems as potential targets for arsenic mediated mechanisms of toxicity. As discussed in chapter one, DNA repair systems are an additional component of cellular defense. Ogg1 is the main enzyme involved in removal of oxo^{8}dG from DNA and plays an integral role in genomic maintenence. Differences in basal Ogg1 activity were identified between actively dividing and NGF treated control groups. The exposure to sodium arsenite lowered the activity to equivalent levels in both the actively dividing and NGF treated PC12 cells (Figure 18A). This could indicate that although NGF treated PC12 cells have a lower basal repair capacity their ability to maintain a minimal level of activity remains equivalent to actively dividing PC12 cells (Figure 18A). It is also plausible that the decrease in Ogg1 activity after arsenite exposure could be due to an additive effect of arsenic-induced changes to both the transcription and activity of Ogg1 and any direct or pharmacological effect from arsenite is playing a minor role. This can be supported by the equivalent reductions in activity of Ogg1 in both the actively dividing and NGF treated PC12 cells (Figure 18A). It is reported that 10μM arsenite decreased DNA ligase activities by 50% in human osteosarcoma cells, although the concentrations required to

inhibit enzyme activity in this study were too high to be physiologically relevant (Hu, Su et al. 1998). An additional *ex vivo* experiment using the DNA repair enzyme formamidopyrimidine DNA glycosylase (Fpg), a bacterial homologue of Ogg1, showed no direct inhibition via arsenite at concentrations as low as 1μM (Asmuss, Mullenders et al. 2000). These studies suggest that decreased Ogg1 activities subsequent to arsenite exposure in actively dividing and NGF treated PC12 cells are not occurring as a consequence of any direct effect from arsenite. Figure 20 also demonstrates that pre-incubation of arsenite with glycosylase extracts has no direct effect on Ogg1 enzyme activity. In a study exposing rats to arsenite, or arsenite in combination with benzo(a)pyrene (BP), showed similar results to the data in Figure 18. An exposure of 2.5 μM sodium arsenite from 1 to 27 days resulted in no significant DNA adduct formation. However, when arsenite was co-administered with BP, the level of DNA adducts remained elevated compared to BP alone suggesting an attenuation of the DNA repair systems because of arsenite (Tran, Prakash et al. 2002). In addition, levels of oxo^{8}dG were increased when Ogg1 activity was attenuated post BP exposure (Stedeford, Cardozo-Pelaez et al. 2001). This study further suggests that arsenite may act through a subtle mechanism that is not evident until an additional exposure is introduced.

A lack of data demonstrating a direct effect of arsenite on Ogg1 activity suggests that alterations are due to some effect on the levels of the enzyme potentially due to changes in gene transcription or translation. The changes seen in Ogg1 activity can be a result of changes in gene transcription. To verify this, levels of Ogg1 mRNA were assessed by quantitative RT-PCR revealing a decrease in Ogg1 transcript in actively dividing PC12 cells exposed to arsenite. Ogg1 mRNA was decreased by 30% in actively

dividing PC12 cells exposed to arsenite. Additional evidence for decreased Ogg1 transcription is demonstrated in Figure 18C. Ogg1 activity remained consistently lower despite increasing the amount of glycosylase protein used in the incision assay (Figure 18C) suggesting that the levels of Ogg1 were decreased as a consequence of arsenite exposure; an event that can be attributed to decreased transcription of Ogg1. Pre-treating nuclear extracts with sodium arsenite also revealed no direct effect of arsenite on Ogg1 enzyme activity (Figure 20). These findings further corroborate the idea that transcriptional changes are facilitating decreased Ogg1 activities. Acute exposure to arsenic in previous work has demonstrated increased transcription of both NQO1 and GCL; genes involved in antioxidant defense. The transcript levels of both genes recovered close to control levels 24 hr post-exposure (Schuliga, Chouchane et al. 2002; Pi, Qu et al. 2003). Temporal changes in gene transcription could account for the disparity between the changes in Ogg1 mRNA (Figure 20) and more drastic decreases shown in Ogg1 excision activity (Figure 18) suggesting a recovery of Ogg1 mRNA could be occurring earlier. Data collected at earlier time points could determine if the transcriptional changes are more representative of enzyme activity. Western blots of Ogg1 protein levels could help corroborate the reductions seen in Ogg1 activity and mRNA however, to date no reliable antibody has been found for Ogg1 by this laboratory as validated by assays using protein extracts from Ogg1 knockout mice.

It has been suggested that the expression of Ogg1 can be modulated by the redox status of the cell, a statement supported by the presence of the putative Nrf2 binding site in the promoter of the human Ogg1 (Dhenaut, Boiteux et al. 2000). Whether arsenic-induced changes to cell redox status of PC12 cells are responsible for alterations in Ogg1

expression remains uncertain, however the data presented indicate concomitant changes in antioxidant systems (GSH), Ogg1 activity, and expression due to sodium arsenite exposure. Ogg1 is the only enzyme to date known to initiate the repair of oxo8dG (Klungland, Rosewell et al. 1999; Minowa, Arai et al. 2000). Conditions where DNA repair is continually compromised can lead to increased levels of oxo^{8}dG; a situation that can have deleterious effects in both actively dividing and differentiated cells. Hyun et. al. found that increased oxo^{8}dG in an Ogg1 deficient human leukemia cell line (KG-1), resulted in the induction of multiple apoptotic pathways despite the administration of NAC. In the same study, the induction of apoptotic pathways was dramatically reduced in Ogg1 proficient cell lines suggesting that diminished DNA repair can result in the induction of apoptotic pathways (Hyun, Jung et al. 2003). Attenuated DNA repair can also lead to the formation of oxo^{8}dG and subsequently cause mutations by incorporating adenine across from the oxidized guanine during DNA replication(Cheng, Jungst et al. 2002) (Figure 15). Increased oxo^{8}dG can also preclude cellular transformation having been identified in the p53 tumor suppressor gene in lung and liver cancers (Hollstein, Peri et al. 1991; Yu, Berlin et al. 2002). Genomic maintenance becomes more relevant in differentiated cellular populations that no longer have the capacity to initiate the repair of DNA during cell cycle progression and replication. The options for genomic maintenance become limited to basal repair systems including constitutive, inducible, and transcription-coupled repair; the latter being a process not associated with the removal of oxo^{8}dG from promoter regions. This type of scenario can underscore the importance of Ogg1 in maintaining not only genomic integrity, but the integrity of regulatory regions as well. The consequences of oxo^{8}dG accumulation in post mitotic cells, such as neurons,

could result in increased damage to promoter regions leading to the reduced transcription of essential cellular proteins (Ghosh and Mitchell 1999; Lu, Pan et al. 2004). Other reports have suggested that activation of the cell cycle occurs as a response to DNA damage and ultimately leads to apoptosis in primary cortical neurons (Kruman, Wersto et al. 2004). NGF treated PC12 showed an increasing trend for oxo^{8}dG in both the control and arsenite treated groups (Figure 23). As stated earlier NGF causes the terminal differentiation of PC12 cells giving them neuronal attributes. In conjunction with a trend in increased levels of DNA damage seen in Figure 23, the NGF treated PC12 cells may undergo a similar mechanism of apoptosis suggested by Kruman et. al. (Kruman, Wersto et al. 2004) thereby explaining their decreased resistance to sodium arsenite (Figure 16).

It is clear that a fundamental difference exists in antioxidants, DNA repair, and DNA damage between actively dividing and NGF treated PC12 cells; a difference that could account for the increased susceptibility in NGF treated PC12 cells exposed to sodium arsenite. Attenuated DNA repair in differentiated cellular populations can lead to the accumulation of oxo^{8}dG, an end result commonly found in correlation with neurodegenerative disease (Sanchez-Ramos 1994; Gabbita, Lovell et al. 1998). The underlying question is whether oxo^{8}dG is a precursor for cellular dysfunction, or a product of the cellular dysfunction itself.

SUMMARY

Using different structural and biochemical analyses, this study investigated two unique mechanisms: (i) the role of transcription factor Nrf2 in the inducible transcription of Ogg1 and (ii) the ability of sodium arsenite to disrupt the response capacity of Ogg1 in an acute exposure model. Results from structural analysis of the hOgg1 promoter reveal that the putative Nrf2 binding site is an integral component of hOgg1 transcriptional regulation. This was confirmed by site-directed deletion of the binding site and subsequent loss of transcription activity.

Binding analysis further showed a physical interaction occurred at this site that was increased subsequent to treatments using *tert*-butylhydroquinone, a frequently used chemical inducer of Nrf2. Results from competitive binding revealed that binding to this region of the hOgg1 promoter could be disrupted by a consensus Nrf2 sequence. This competition was unique as no competition was demonstrated between Sp1 and Nrf2 oligonucleotide sequences. Results using reporter gene constructs revealed hOgg1 transcription is sensitive to Nrf2 modulating compounds and cellular redox changes. Sensitivity to redox changes could be reversed with the over expression of mammalian Nrf2.

Taken together, the results suggest the existence of an Nrf2 binding site in the hOgg1 promoter. Our proposed model in Figure 24 further suggests that hOgg1 transcription can be induced via Nrf2 as a consequence of cellular oxidative stress. Nrf2 activation occurs via two main mechanisms: (1) changes in intracellular GSH, and (2) direct interaction of electrophiles with Nrf2-KEAP1 complexes. The model provides an

additional transcription component for hOgg1 regulation for utilization in environmental and/ or therapeutic studies.

Results from sodium arsenite exposure revealed changes in Ogg1 transcription similar to the proposed model that can be best explained by increases in GSH. The model suggests that Ogg1 transcription can be down regulated in the presence of excess intracellular GSH. This was evident subsequent to arsenite exposure as GSH increased, and Ogg1 mRNA and activities decreased.

REFERENCES

Achanta, G. and P. Huang (2004). "Role of p53 in sensing oxidative DNA damage in response to reactive oxygen species-generating agents." Cancer Res **64**(17): 6233-9.

Agarwal, S. and R. S. Sohal (1994). "DNA oxidative damage and life expectancy in houseflies." Proc Natl Acad Sci U S A **91**(25): 12332-5.

Alam, J., D. Stewart, et al. (1999). "Nrf2, a Cap'n'Collar transcription factor, regulates induction of the heme oxygenase-1 gene." J Biol Chem **274**(37): 26071-8.

Andrew, A. S., M. R. Karagas, et al. (2003). "Decreased DNA repair gene expression among individuals exposed to arsenic in United States drinking water." Int J Cancer **104**(3): 263-8.

Aoki, Y., H. Sato, et al. (2001). "Accelerated DNA adduct formation in the lung of the Nrf2 knockout mouse exposed to diesel exhaust." Toxicol Appl Pharmacol **173**(3): 154-60.

Aposhian, H. V., R. A. Zakharyan, et al. (2004). "A review of the enzymology of arsenic metabolism and a new potential role of hydrogen peroxide in the detoxication of the trivalent arsenic species." Toxicol Appl Pharmacol **198**(3): 327-35.

Asmuss, M., L. H. Mullenders, et al. (2000). "Interference by toxic metal compounds with isolated zinc finger DNA repair proteins." Toxicol Lett **112-113**: 227-31.

Aspinwall, R., D. G. Rothwell, et al. (1997). "Cloning and characterization of a functional human homolog of Escherichia coli endonuclease III." Proc Natl Acad Sci U S A **94**(1): 109-14.

Barber, T., E. Borras, et al. (2000). "Vitamin A deficiency causes oxidative damage to liver mitochondria in rats." Free Radic Biol Med **29**(1): 1-7.

Barchowsky, A., L. R. Klei, et al. (1999). "Stimulation of reactive oxygen, but not reactive nitrogen species, in vascular endothelial cells exposed to low levels of arsenite." Free Radic Biol Med **27**(11-12): 1405-12.

Barchowsky, A., R. R. Roussel, et al. (1999). "Low levels of arsenic trioxide stimulate proliferative signals in primary vascular cells without activating stress effector pathways." Toxicol Appl Pharmacol **159**(1): 65-75.

Barja, G. and A. Herrero (2000). "Oxidative damage to mitochondrial DNA is inversely related to maximum life span in the heart and brain of mammals." Faseb J **14**(2): 312-8.

Basha, M. R., W. Wei, et al. (2005). "The fetal basis of amyloidogenesis: exposure to lead and latent overexpression of amyloid precursor protein and beta-amyloid in the aging brain." J Neurosci **25**(4): 823-9.

Bates, M. N., A. H. Smith, et al. (1992). "Arsenic ingestion and internal cancers: a review." Am J Epidemiol **135**(5): 462-76.

Bau, D. T., T. S. Wang, et al. (2002). "Oxidative DNA adducts and DNA-protein cross-links are the major DNA lesions induced by arsenite." Environ Health Perspect **110 Suppl 5**: 753-6.

Beckman, J. S. and W. H. Koppenol (1996). "Nitric oxide, superoxide, and peroxynitrite: the good, the bad, and ugly." Am J Physiol **271**(5 Pt 1): C1424-37.

Berg, M., H. C. Tran, et al. (2001). "Arsenic contamination of groundwater and drinking water in Vietnam: a human health threat." Environ Sci Technol **35**(13): 2621-6.

Bhakat, K. K., S. K. Mokkapati, et al. (2006). "Acetylation of human 8-oxoguanine-DNA glycosylase by p300 and its role in 8-oxoguanine repair in vivo." Mol Cell Biol **26**(5): 1654-65.

Blaauwgeers, H. G., J. M. Vianney de Jong, et al. (1996). "Enhanced superoxide dismutase-2 immunoreactivity of astrocytes and occasional neurons in amyotrophic lateral sclerosis." J Neurol Sci **140**(1-2): 21-9.

Bloom, D. A. and A. K. Jaiswal (2003). "Phosphorylation of Nrf2 at Ser40 by protein kinase C in response to antioxidants leads to the release of Nrf2 from INrf2, but is not required for Nrf2 stabilization/accumulation in the nucleus and transcriptional activation of antioxidant response element-mediated NAD(P)H:quinone oxidoreductase-1 gene expression." J Biol Chem **278**(45): 44675-82.

Bogdanov, M., R. H. Brown, et al. (2000). "Increased oxidative damage to DNA in ALS patients." Free Radic Biol Med **29**(7): 652-8.

Bohr, V. A. (2002). "Repair of oxidative DNA damage in nuclear and mitochondrial DNA, and some changes with aging in mammalian cells." Free Radic Biol Med **32**(9): 804-12.

Boiteux, S. and J. P. Radicella (2000). "The human OGG1 gene: structure, functions, and its implication in the process of carcinogenesis." Arch Biochem Biophys **377**(1): 1-8.

Bolin, C. M., R. Basha, et al. (2006). "Exposure to lead and the developmental origin of oxidative DNA damage in the aging brain." Faseb J **20**(6): 788-90.

Bravard, A., M. Vacher, et al. (2006). "Redox regulation of human OGG1 activity in response to cellular oxidative stress." Mol Cell Biol **26**(20): 7430-6.

Breen, A. P. and J. A. Murphy (1995). "Reactions of oxyl radicals with DNA." Free Radic Biol Med **18**(6): 1033-77.

Brown, K. G. and G. L. Ross (2002). "Arsenic, drinking water, and health: a position paper of the American Council on Science and Health." Regul Toxicol Pharmacol **36**(2): 162-74.

Bunderson, M., D. M. Brooks, et al. (2004). "Arsenic exposure exacerbates atherosclerotic plaque formation and increases nitrotyrosine and leukotriene biosynthesis." Toxicol Appl Pharmacol **201**(1): 32-9.

Cadenas, E. and K. J. Davies (2000). "Mitochondrial free radical generation, oxidative stress, and aging." Free Radic Biol Med **29**(3-4): 222-30.

Cadenas, S. and G. Barja (1999). "Resveratrol, melatonin, vitamin E, and PBN protect against renal oxidative DNA damage induced by the kidney carcinogen KBrO3." Free Radic Biol Med **26**(11-12): 1531-7.

Cardozo-Pelaez, F., P. J. Brooks, et al. (2000). "DNA damage, repair, and antioxidant systems in brain regions: a correlative study." Free Radic Biol Med **28**(5): 779-85.

Cardozo-Pelaez, F., D. P. Cox, et al. (2005). "Lack of the DNA repair enzyme OGG1 sensitizes dopamine neurons to manganese toxicity during development." Gene Expr **12**(4-6): 315-23.

Cardozo-Pelaez, F., S. Song, et al. (1998). "Attenuation of age-dependent oxidative damage to DNA and protein in brainstem of Tg Cu/Zn SOD mice." Neurobiol Aging **19**(4): 311-6.

Cardozo-Pelaez, F., S. Song, et al. (1999). "Oxidative DNA damage in the aging mouse brain." Mov Disord **14**(6): 972-80.

Cardozo-Pelaez, F., T. J. Stedeford, et al. (2002). "Effects of diethylmaleate on DNA damage and repair in the mouse brain." Free Radic Biol Med **33**(2): 292-8.
Chan, J. Y. and M. Kwong (2000). "Impaired expression of glutathione synthetic enzyme genes in mice with targeted deletion of the Nrf2 basic-leucine zipper protein." Biochim Biophys Acta **1517**(1): 19-26.
Chance, B., H. Sies, et al. (1979). "Hydroperoxide metabolism in mammalian organs." Physiol Rev **59**(3): 527-605.
Chatterjee, A., E. Mambo, et al. (2006). "The effect of p53-RNAi and p53 knockout on human 8-oxoguanine DNA glycosylase (hOgg1) activity." Faseb J **20**(1): 112-4.
Chen, C. Y., J. H. Jang, et al. (2005). "Resveratrol upregulates heme oxygenase-1 expression via activation of NF-E2-related factor 2 in PC12 cells." Biochem Biophys Res Commun **331**(4): 993-1000.
Chen, Q., J. Marsh, et al. (1996). "Detection of 8-oxo-2'-deoxyguanosine, a marker of oxidative DNA damage, in culture medium from human mesothelial cells exposed to crocidolite asbestos." Carcinogenesis **17**(11): 2525-7.
Cheng, B., C. Jungst, et al. (2002). "[Potential role of human DNA-repair enzymes hMTH1, hOGG1 and hMYHalpha in the hepatocarcinogenesis]." J Huazhong Univ Sci Technolog Med Sci **22**(3): 206-11, 215.
Chou, W. C., H. Y. Chen, et al. (2005). "Arsenic suppresses gene expression in promyelocytic leukemia cells partly through Sp1 oxidation." Blood **106**(1): 304-10.
Cox, D. P., Cardozo-Pelaez, F. (2007). "High Throughput Method for Assessment of Cellular Reduced Glutathione in Mammalian Cells." Journal of Environmental Protection Science **1**: 23-28.
Crespo-Hernandez, C. E., D. M. Close, et al. (2007). "Determination of Redox Potentials for the Watson-Crick Base Pairs, DNA Nucleosides, and Relevant Nucleoside Analogues." J Phys Chem B.
Dalton, T. P., H. G. Shertzer, et al. (1999). "Regulation of gene expression by reactive oxygen." Annu Rev Pharmacol Toxicol **39**: 67-101.
Dantzer, F., L. Luna, et al. (2002). "Human OGG1 undergoes serine phosphorylation and associates with the nuclear matrix and mitotic chromatin in vivo." Nucleic Acids Res **30**(11): 2349-57.
de Souza-Pinto, N. C., L. Eide, et al. (2001). "Repair of 8-oxodeoxyguanosine lesions in mitochondrial dna depends on the oxoguanine dna glycosylase (OGG1) gene and 8-oxoguanine accumulates in the mitochondrial dna of OGG1-defective mice." Cancer Res **61**(14): 5378-81.
Desagher, S., J. Glowinski, et al. (1996). "Astrocytes protect neurons from hydrogen peroxide toxicity." J Neurosci **16**(8): 2553-62.
Devasagayam, T. P., S. Steenken, et al. (1991). "Formation of 8-hydroxy(deoxy)guanosine and generation of strand breaks at guanine residues in DNA by singlet oxygen." Biochemistry **30**(25): 6283-9.
Dhenaut, A., S. Boiteux, et al. (2000). "Characterization of the hOGG1 promoter and its expression during the cell cycle." Mutat Res **461**(2): 109-18.
Dickinson, D. A., A. L. Levonen, et al. (2004). "Human glutamate cysteine ligase gene regulation through the electrophile response element." Free Radic Biol Med **37**(8): 1152-9.

Dinkova-Kostova, A. T., W. D. Holtzclaw, et al. (2002). "Direct evidence that sulfhydryl groups of Keap1 are the sensors regulating induction of phase 2 enzymes that protect against carcinogens and oxidants." Proc Natl Acad Sci U S A **99**(18): 11908-13.

Dinkova-Kostova, A. T., W. D. Holtzclaw, et al. (2005). "Keap1, the sensor for electrophiles and oxidants that regulates the phase 2 response, is a zinc metalloprotein." Biochemistry **44**(18): 6889-99.

Dizdaroglu, M., P. Jaruga, et al. (2002). "Free radical-induced damage to DNA: mechanisms and measurement." Free Radic Biol Med **32**(11): 1102-15.

Dugan, L. L., D. J. Creedon, et al. (1997). "Rapid suppression of free radical formation by nerve growth factor involves the mitogen-activated protein kinase pathway." Proc Natl Acad Sci U S A **94**(8): 4086-91.

Eftekharpour, E., A. Holmgren, et al. (2000). "Thioredoxin reductase and glutathione synthesis is upregulated by t-butylhydroquinone in cortical astrocytes but not in cortical neurons." Glia **31**(3): 241-8.

Ekshyyan, O. and T. Y. Aw (2005). "Decreased susceptibility of differentiated PC12 cells to oxidative challenge: relationship to cellular redox and expression of apoptotic protease activator factor-1." Cell Death Differ **12**(8): 1066-77.

Engel, R. R. and A. H. Smith (1994). "Arsenic in drinking water and mortality from vascular disease: an ecologic analysis in 30 counties in the United States." Arch Environ Health **49**(5): 418-27.

Flora, S. J. (1999). "Arsenic-induced oxidative stress and its reversibility following combined administration of N-acetylcysteine and meso 2,3-dimercaptosuccinic acid in rats." Clin Exp Pharmacol Physiol **26**(11): 865-9.

Forman, H. J. and D. A. Dickinson (2003). "Oxidative signaling and glutathione synthesis." Biofactors **17**(1-4): 1-12.

Fraga, C. G., M. K. Shigenaga, et al. (1990). "Oxidative damage to DNA during aging: 8-hydroxy-2'-deoxyguanosine in rat organ DNA and urine." Proc Natl Acad Sci U S A **87**(12): 4533-7.

Fridovich, I. (1995). "Superoxide radical and superoxide dismutases." Annu Rev Biochem **64**: 97-112.

Fukae, J., M. Takanashi, et al. (2005). "Expression of 8-oxoguanine DNA glycosylase (OGG1) in Parkinson's disease and related neurodegenerative disorders." Acta Neuropathol (Berl) **109**(3): 256-62.

Gabbita, S. P., M. A. Lovell, et al. (1998). "Increased nuclear DNA oxidation in the brain in Alzheimer's disease." J Neurochem **71**(5): 2034-40.

Gabelova, A., Z. Valovicova, et al. (2007). "Assessment of oxidative DNA damage formation by organic complex mixtures from airborne particles PM(10)." Mutat Res.

Germolec, D. R., J. Spalding, et al. (1998). "Arsenic enhancement of skin neoplasia by chronic stimulation of growth factors." Am J Pathol **153**(6): 1775-85.

Ghosh, R. and D. L. Mitchell (1999). "Effect of oxidative DNA damage in promoter elements on transcription factor binding." Nucleic Acids Res **27**(15): 3213-8.

Giulivi, C., A. Boveris, et al. (1995). "Hydroxyl radical generation during mitochondrial electron transfer and the formation of 8-hydroxydesoxyguanosine in mitochondrial DNA." Arch Biochem Biophys **316**(2): 909-16.

Greene, L. A. and A. S. Tischler (1976). "Establishment of a noradrenergic clonal line of rat adrenal pheochromocytoma cells which respond to nerve growth factor." Proc Natl Acad Sci U S A **73**(7): 2424-8.
Griffith, O. W. (1982). "Mechanism of action, metabolism, and toxicity of buthionine sulfoximine and its higher homologs, potent inhibitors of glutathione synthesis." J Biol Chem **257**(22): 13704-12.
Griffith, O. W. (1999). "Biologic and pharmacologic regulation of mammalian glutathione synthesis." Free Radic Biol Med **27**(9-10): 922-35.
Hailer, M. K., P. G. Slade, et al. (2005). "Nei deficient Escherichia coli are sensitive to chromate and accumulate the oxidized guanine lesion spiroiminodihydantoin." Chem Res Toxicol **18**(9): 1378-83.
Halliwell, B., Gutteridge, J.M.C. (1999). Free Radicals in Biology and Medicine. Oxford, NY, Oxford University Press.
Hamadeh, H. K., K. J. Trouba, et al. (2002). "Coordination of altered DNA repair and damage pathways in arsenite-exposed keratinocytes." Toxicol Sci **69**(2): 306-16.
Hamilton, M. L., Z. Guo, et al. (2001). "A reliable assessment of 8-oxo-2-deoxyguanosine levels in nuclear and mitochondrial DNA using the sodium iodide method to isolate DNA." Nucleic Acids Res **29**(10): 2117-26.
Hansen, J. M., W. H. Watson, et al. (2004). "Compartmentation of Nrf-2 redox control: regulation of cytoplasmic activation by glutathione and DNA binding by thioredoxin-1." Toxicol Sci **82**(1): 308-17.
Hartwig, A., H. Blessing, et al. (2003). "Modulation of DNA repair processes by arsenic and selenium compounds." Toxicology **193**(1-2): 161-9.
Hazra, T. K., T. Izumi, et al. (1998). "The presence of two distinct 8-oxoguanine repair enzymes in human cells: their potential complementary roles in preventing mutation." Nucleic Acids Res **26**(22): 5116-22.
Hedley, D. W. and S. Chow (1994). "Evaluation of methods for measuring cellular glutathione content using flow cytometry." Cytometry **15**(4): 349-58.
Helbock, H. J., K. B. Beckman, et al. (1998). "DNA oxidation matters: the HPLC-electrochemical detection assay of 8-oxo-deoxyguanosine and 8-oxo-guanine." Proc Natl Acad Sci U S A **95**(1): 288-93.
Hirano, S., Y. Kobayashi, et al. (2004). "The accumulation and toxicity of methylated arsenicals in endothelial cells: important roles of thiol compounds." Toxicol Appl Pharmacol **198**(3): 458-67.
Hirano, T., R. Yamaguchi, et al. (1996). "8-hydroxyguanine levels in nuclear DNA and its repair activity in rat organs associated with age." J Gerontol A Biol Sci Med Sci **51**(5): B303-7.
Hodges, N. J. and J. K. Chipman (2002). "Down-regulation of the DNA-repair endonuclease 8-oxo-guanine DNA glycosylase 1 (hOGG1) by sodium dichromate in cultured human A549 lung carcinoma cells." Carcinogenesis **23**(1): 55-60.
Hollstein, M., D. Sidransky, et al. (1991). "p53 mutations in human cancers." Science **253**(5015): 49-53.
Hollstein, M. C., L. Peri, et al. (1991). "Genetic analysis of human esophageal tumors from two high incidence geographic areas: frequent p53 base substitutions and absence of ras mutations." Cancer Res **51**(15): 4102-6.

Horan, A. D., C. Y. Chan, et al. (1997). "Analysis of tumor thiol concentrations: comparison of flow cytometric with chemical and biochemical techniques." Cytometry **29**(1): 76-82.
Hu, J., S. Z. Imam, et al. (2005). "Phosphorylation of human oxoguanine DNA glycosylase (alpha-OGG1) modulates its function." Nucleic Acids Res **33**(10): 3271-82.
Hu, Y., X. Jin, et al. (2002). "Effect of arsenic on transcription factor AP-1 and NF-kappaB DNA binding activity and related gene expression." Toxicol Lett **133**(1): 33-45.
Hu, Y., L. Su, et al. (1998). "Arsenic toxicity is enzyme specific and its affects on ligation are not caused by the direct inhibition of DNA repair enzymes." Mutat Res **408**(3): 203-18.
Huang, C. S., M. E. Anderson, et al. (1993). "Amino acid sequence and function of the light subunit of rat kidney gamma-glutamylcysteine synthetase." J Biol Chem **268**(27): 20578-83.
Hyun, J. W., Y. C. Jung, et al. (2003). "8-hydroxydeoxyguanosine causes death of human leukemia cells deficient in 8-oxoguanine glycosylase 1 activity by inducing apoptosis." Mol Cancer Res **1**(4): 290-9.
Itoh, K., T. Chiba, et al. (1997). "An Nrf2/small Maf heterodimer mediates the induction of phase II detoxifying enzyme genes through antioxidant response elements." Biochem Biophys Res Commun **236**(2): 313-22.
Itoh, K., K. I. Tong, et al. (2004). "Molecular mechanism activating Nrf2-Keap1 pathway in regulation of adaptive response to electrophiles." Free Radic Biol Med **36**(10): 1208-13.
Itoh, K., N. Wakabayashi, et al. (1999). "Keap1 represses nuclear activation of antioxidant responsive elements by Nrf2 through binding to the amino-terminal Neh2 domain." Genes Dev **13**(1): 76-86.
Jeong, H. G., C. K. Youn, et al. (2004). "Metallothionein-III prevents gamma-ray-induced 8-oxoguanine accumulation in normal and hOGG1-depleted cells." J Biol Chem **279**(33): 34138-49.
Kalyanaraman, B., H. Karoui, et al. (1996). "Detection of thiyl radical adducts formed during hydroxyl radical- and peroxynitrite-mediated oxidation of thiols--a high resolution ESR spin-trapping study at Q-band (35 GHz)." Anal Biochem **241**(1): 75-81.
Kamendulis, L. M., J. Jiang, et al. (1999). "Induction of oxidative stress and oxidative damage in rat glial cells by acrylonitrile." Carcinogenesis **20**(8): 1555-60.
Kann, S., C. Estes, et al. (2005). "Butylhydroquinone protects cells genetically deficient in glutathione biosynthesis from arsenite-induced apoptosis without significantly changing their prooxidant status." Toxicol Sci **87**(2): 365-84.
Kasai, H., P. F. Crain, et al. (1986). "Formation of 8-hydroxyguanine moiety in cellular DNA by agents producing oxygen radicals and evidence for its repair." Carcinogenesis **7**(11): 1849-51.
Kaur, P., S. Kalia, et al. (2006). "Effect of diethyl maleate induced oxidative stress on male reproductive activity in mice: redox active enzymes and transcription factors expression." Mol Cell Biochem **291**(1-2): 55-61.

Kehrer, J. P. (2000). "The Haber-Weiss reaction and mechanisms of toxicity." Toxicology **149**(1): 43-50.
Kehrer, J. P. and L. G. Lund (1994). "Cellular reducing equivalents and oxidative stress." Free Radic Biol Med **17**(1): 65-75.
Ketterer, B. (1988). "Protective role of glutathione and glutathione transferases in mutagenesis and carcinogenesis." Mutat Res **202**(2): 343-61.
Kim, B. R., R. Hu, et al. (2003). "Effects of glutathione on antioxidant response element-mediated gene expression and apoptosis elicited by sulforaphane." Cancer Res **63**(21): 7520-5.
Kim, H. N., Y. Morimoto, et al. (2001). "Changes in DNA 8-hydroxyguanine levels, 8-hydroxyguanine repair activity, and hOGG1 and hMTH1 mRNA expression in human lung alveolar epithelial cells induced by crocidolite asbestos." Carcinogenesis **22**(2): 265-9.
Kim, J. I., Y. J. Park, et al. (2003). "hOGG1 Ser326Cys polymorphism modifies the significance of the environmental risk factor for colon cancer." World J Gastroenterol **9**(5): 956-60.
Klungland, A. and S. Bjelland (2007). "Oxidative damage to purines in DNA: role of mammalian Ogg1." DNA Repair (Amst) **6**(4): 481-8.
Klungland, A., I. Rosewell, et al. (1999). "Accumulation of premutagenic DNA lesions in mice defective in removal of oxidative base damage." Proc Natl Acad Sci U S A **96**(23): 13300-5.
Kruman, II, R. P. Wersto, et al. (2004). "Cell cycle activation linked to neuronal cell death initiated by DNA damage." Neuron **41**(4): 549-61.
Lan, J., W. Li, et al. (2003). "Inducible repair of oxidative DNA lesions in the rat brain after transient focal ischemia and reperfusion." J Cereb Blood Flow Metab **23**(11): 1324-39.
Lardinois, O. M. (1995). "Reactions of bovine liver catalase with superoxide radicals and hydrogen peroxide." Free Radic Res **22**(3): 251-74.
Lee, J. M., M. J. Calkins, et al. (2003). "Identification of the NF-E2-related factor-2-dependent genes conferring protection against oxidative stress in primary cortical astrocytes using oligonucleotide microarray analysis." J Biol Chem **278**(14): 12029-38.
Lee, J. M. and J. A. Johnson (2004). "An important role of Nrf2-ARE pathway in the cellular defense mechanism." J Biochem Mol Biol **37**(2): 139-43.
Lee, J. M., J. D. Moehlenkamp, et al. (2001). "Nrf2-dependent activation of the antioxidant responsive element by tert-butylhydroquinone is independent of oxidative stress in IMR-32 human neuroblastoma cells." Biochem Biophys Res Commun **280**(1): 286-92.
Lee, M. R., S. H. Kim, et al. (2004). "Transcription factors NF-YA regulate the induction of human OGG1 following DNA-alkylating agent methylmethane sulfonate (MMS) treatment." J Biol Chem **279**(11): 9857-66.
Lewis, D. R., J. W. Southwick, et al. (1999). "Drinking water arsenic in Utah: A cohort mortality study." Environ Health Perspect **107**(5): 359-65.
Li, J., Stein, T.D., Johnson, J.A. (2004). "Genetic dissection of systemic autoimmune disease in Nrf2-deficient mice." Physiol Genomics **18**: 261-272.

Lin, L. H., S. Cao, et al. (2000). "Up-regulation of base excision repair activity for 8-hydroxy-2'-deoxyguanosine in the mouse brain after forebrain ischemia-reperfusion." J Neurochem **74**(3): 1098-105.
Liu, F. and K. Y. Jan (2000). "DNA damage in arsenite- and cadmium-treated bovine aortic endothelial cells." Free Radic Biol Med **28**(1): 55-63.
Liu, Y., K. Z. Guyton, et al. (1996). "Differential activation of ERK, JNK/SAPK and P38/CSBP/RK map kinase family members during the cellular response to arsenite." Free Radic Biol Med **21**(6): 771-81.
Liu, Z., J. Shen, et al. (2002). "Arsenite transport by mammalian aquaglyceroporins AQP7 and AQP9." Proc Natl Acad Sci U S A **99**(9): 6053-8.
Lu, T., Y. Pan, et al. (2004). "Gene regulation and DNA damage in the ageing human brain." Nature **429**(6994): 883-91.
Lyras, L., N. J. Cairns, et al. (1997). "An assessment of oxidative damage to proteins, lipids, and DNA in brain from patients with Alzheimer's disease." J Neurochem **68**(5): 2061-9.
Martin, D., A. I. Rojo, et al. (2004). "Regulation of heme oxygenase-1 expression through the phosphatidylinositol 3-kinase/Akt pathway and the Nrf2 transcription factor in response to the antioxidant phytochemical carnosol." J Biol Chem **279**(10): 8919-29.
Martin, J. and I. N. White (1991). "Fluorimetric determination of oxidised and reduced glutathione in cells and tissues by high-performance liquid chromatography following derivatization with dansyl chloride." J Chromatogr **568**(1): 219-25.
Matsui, M., C. Nishigori, et al. (1999). "The role of oxidative DNA damage in human arsenic carcinogenesis: detection of 8-hydroxy-2'-deoxyguanosine in arsenic-related Bowen's disease." J Invest Dermatol **113**(1): 26-31.
McMahon, M., N. Thomas, et al. (2004). "Redox-regulated turnover of Nrf2 is determined by at least two separate protein domains, the redox-sensitive Neh2 degron and the redox-insensitive Neh6 degron." J Biol Chem **279**(30): 31556-67.
Mecocci, P., U. MacGarvey, et al. (1993). "Oxidative damage to mitochondrial DNA shows marked age-dependent increases in human brain." Ann Neurol **34**(4): 609-16.
Meister, A. and M. E. Anderson (1983). "Glutathione." Annu Rev Biochem **52**: 711-60.
Merrill, C. L., H. Ni, et al. (2002). "Etomoxir-induced oxidative stress in HepG2 cells detected by differential gene expression is confirmed biochemically." Toxicol Sci **68**(1): 93-101.
Mills, E. M., K. Takeda, et al. (1998). "Nerve growth factor treatment prevents the increase in superoxide produced by epidermal growth factor in PC12 cells." J Biol Chem **273**(35): 22165-8.
Minowa, O., T. Arai, et al. (2000). "Mmh/Ogg1 gene inactivation results in accumulation of 8-hydroxyguanine in mice." Proc Natl Acad Sci U S A **97**(8): 4156-61.
Mo, J., Y. Xia, et al. (2006). "Chronic arsenic exposure and oxidative stress: OGG1 expression and arsenic exposure, nail selenium, and skin hyperkeratosis in inner mongolia." Environ Health Perspect **114**(6): 835-41.
Moi, P., K. Chan, et al. (1994). "Isolation of NF-E2-related factor 2 (Nrf2), a NF-E2-like basic leucine zipper transcriptional activator that binds to the tandem NF-E2/AP1

repeat of the beta-globin locus control region." Proc Natl Acad Sci U S A **91**(21): 9926-30.
Murphy, T. H., J. Yu, et al. (2001). "Preferential expression of antioxidant response element mediated gene expression in astrocytes." J Neurochem **76**(6): 1670-8.
Nakajima, A., K. Yamada, et al. (2002). "Interleukin-6 protects PC12 cells from 4-hydroxynonenal-induced cytotoxicity by increasing intracellular glutathione levels." Free Radic Biol Med **32**(12): 1324-32.
Nguyen, T., P. J. Sherratt, et al. (2003). "Increased protein stability as a mechanism that enhances Nrf2-mediated transcriptional activation of the antioxidant response element. Degradation of Nrf2 by the 26 S proteasome." J Biol Chem **278**(7): 4536-41.
Nguyen, T., C. S. Yang, et al. (2004). "The pathways and molecular mechanisms regulating Nrf2 activation in response to chemical stress." Free Radic Biol Med **37**(4): 433-41.
Nishioka, K., T. Ohtsubo, et al. (1999). "Expression and differential intracellular localization of two major forms of human 8-oxoguanine DNA glycosylase encoded by alternatively spliced OGG1 mRNAs." Mol Biol Cell **10**(5): 1637-52.
Nordstrom, D. K. (2002). "Public health. Worldwide occurrences of arsenic in ground water." Science **296**(5576): 2143-5.
Ochi, T. (1997). "Arsenic compound-induced increases in glutathione levels in cultured Chinese hamster V79 cells and mechanisms associated with changes in gamma-glutamylcysteine synthetase activity, cystine uptake and utilization of cysteine." Arch Toxicol **71**(12): 730-40.
Ongwijitwat, S. and M. T. Wong-Riley (2004). "Functional analysis of the rat cytochrome c oxidase subunit 6A1 promoter in primary neurons." Gene **337**: 163-71.
Pan, Z. and R. Perez-Polo (1996). "Increased uptake of L-cysteine and L-cystine by nerve growth factor in rat pheochromocytoma cells." Brain Res **740**(1-2): 21-6.
Pan, Z. and R. Perez-Polo (1996). "Regulation of gamma-glutamylcysteine synthetase activity by nerve growth factor." Int J Dev Neurosci **14**(5): 559-66.
Parrish, A. R., X. H. Zheng, et al. (1999). "Enhanced transcription factor DNA binding and gene expression induced by arsenite or arsenate in renal slices." Toxicol Sci **50**(1): 98-105.
Petrick, J. S., F. Ayala-Fierro, et al. (2000). "Monomethylarsonous acid (MMA(III)) is more toxic than arsenite in Chang human hepatocytes." Toxicol Appl Pharmacol **163**(2): 203-7.
Pi, J., W. Qu, et al. (2003). "Transcription factor Nrf2 activation by inorganic arsenic in cultured keratinocytes: involvement of hydrogen peroxide." Exp Cell Res **290**(2): 234-45.
Pi, J., H. Yamauchi, et al. (2002). "Evidence for induction of oxidative stress caused by chronic exposure of Chinese residents to arsenic contained in drinking water." Environ Health Perspect **110**(4): 331-6.
Piao, F., N. Ma, et al. (2005). "Oxidative DNA damage in relation to neurotoxicity in the brain of mice exposed to arsenic at environmentally relevant levels." J Occup Health **47**(5): 445-9.

Potts, R. J., R. D. Watkin, et al. (2003). "Cadmium exposure down-regulates 8-oxoguanine DNA glycosylase expression in rat lung and alveolar epithelial cells." Toxicology **184**(2-3): 189-202.

Prosperi, M. T., D. Ferbus, et al. (1998). "The pag gene product, a physiological inhibitor of c-abl tyrosine kinase, is overexpressed in cells entering S phase and by contact with agents inducing oxidative stress." FEBS Lett **423**(1): 39-44.

Pu, Y. S., K. Y. Jan, et al. (2007). "8-Oxoguanine DNA glycosylase and MutY homolog are involved in the incision of arsenite-induced DNA adducts." Toxicol Sci **95**(2): 376-82.

Qi, W., R. J. Reiter, et al. (2000). "Chromium(III)-induced 8-hydroxydeoxyguanosine in DNA and its reduction by antioxidants: comparative effects of melatonin, ascorbate, and vitamin E." Environ Health Perspect **108**(5): 399-402.

Rahman, M., M. Tondel, et al. (1999). "Hypertension and arsenic exposure in Bangladesh." Hypertension **33**(1): 74-8.

Ramanathan, K., B. S. Balakumar, et al. (2002). "Effects of ascorbic acid and alpha-tocopherol on arsenic-induced oxidative stress." Hum Exp Toxicol **21**(12): 675-80.

Rangasamy, T., C. Y. Cho, et al. (2004). "Genetic ablation of Nrf2 enhances susceptibility to cigarette smoke-induced emphysema in mice." J Clin Invest **114**(9): 1248-59.

Remiao, F., H. Carmo, et al. (2000). "Simultaneous determination of reduced and oxidized glutathione in freshly isolated rat hepatocytes and cardiomyocytes by HPLC with electrochemical detection." Biomed Chromatogr **14**(7): 468-73.

Rojewski, M. T., S. Korper, et al. (2004). "Depolarization of mitochondria and activation of caspases are common features of arsenic(III)-induced apoptosis in myelogenic and lymphatic cell lines." Chem Res Toxicol **17**(1): 119-28.

Rosenquist, T. A., D. O. Zharkov, et al. (1997). "Cloning and characterization of a mammalian 8-oxoguanine DNA glycosylase." Proc Natl Acad Sci U S A **94**(14): 7429-34.

Rushmore, T. H. and C. B. Pickett (1990). "Transcriptional regulation of the rat glutathione S-transferase Ya subunit gene. Characterization of a xenobiotic-responsive element controlling inducible expression by phenolic antioxidants." J Biol Chem **265**(24): 14648-53.

Sakurai, T., M. Ochiai, et al. (2004). "Role of glutathione in dimethylarsinic acid-induced apoptosis." Toxicol Appl Pharmacol **198**(3): 354-65.

Salinas, M., R. Diaz, et al. (2003). "Nerve growth factor protects against 6-hydroxydopamine-induced oxidative stress by increasing expression of heme oxygenase-1 in a phosphatidylinositol 3-kinase-dependent manner." J Biol Chem **278**(16): 13898-904.

Sanchez-Ramos, J., Overvik, Eva., Ames, B. (1994). "A Marker of Oxyradical-Mediated DNA Damage (8-Hydroxy-2'-Deoxyguanosine) is Increased in Nigro-Striatum of Parkinson's Disease Brain." Neurodegeneration **3**: 197-204.

Sasaki, H., H. Sato, et al. (2002). "Electrophile response element-mediated induction of the cystine/glutamate exchange transporter gene expression." J Biol Chem **277**(47): 44765-71.

Sasaki, N., N. Baba, et al. (2001). "Cytotoxicity of reactive oxygen species and related agents toward undifferentiated and differentiated rat phenochromocytoma PC12 cells." Biol Pharm Bull **24**(5): 515-9.
Schuliga, M., S. Chouchane, et al. (2002). "Upregulation of glutathione-related genes and enzyme activities in cultured human cells by sublethal concentrations of inorganic arsenic." Toxicol Sci **70**(2): 183-92.
Scott, N., K. M. Hatlelid, et al. (1993). "Reactions of arsenic(III) and arsenic(V) species with glutathione." Chem Res Toxicol **6**(1): 102-6.
Sebastia, J., R. Cristofol, et al. (2003). "Evaluation of fluorescent dyes for measuring intracellular glutathione content in primary cultures of human neurons and neuroblastoma SH-SY5Y." Cytometry A **51**(1): 16-25.
Senft, A. P., T. P. Dalton, et al. (2000). "Determining glutathione and glutathione disulfide using the fluorescence probe o-phthalaldehyde." Anal Biochem **280**(1): 80-6.
Shibutani, S., M. Takeshita, et al. (1991). "Insertion of specific bases during DNA synthesis past the oxidation-damaged base 8-oxodG." Nature **349**(6308): 431-4.
Shih, A. Y., D. A. Johnson, et al. (2003). "Coordinate regulation of glutathione biosynthesis and release by Nrf2-expressing glia potently protects neurons from oxidative stress." J Neurosci **23**(8): 3394-406.
Sies, H. (1999). "Glutathione and its role in cellular functions." Free Radic Biol Med **27**(9-10): 916-21.
Slade, P. G., M. K. Hailer, et al. (2005). "Guanine-specific oxidation of double-stranded DNA by Cr(VI) and ascorbic acid forms spiroiminodihydantoin and 8-oxo-2'-deoxyguanosine." Chem Res Toxicol **18**(7): 1140-9.
Smith, K. R., L. R. Klei, et al. (2001). "Arsenite stimulates plasma membrane NADPH oxidase in vascular endothelial cells." Am J Physiol Lung Cell Mol Physiol **280**(3): L442-9.
Stedeford, T., F. Cardozo-Pelaez, et al. (2001). "Organ-specific differences in 8-oxoguanosine glycosylase (OGG1) repair following acute treatment with benzo[a]pyrene." Res Commun Mol Pathol Pharmacol **109**(1-2): 73-85.
Suh, J. H., S. V. Shenvi, et al. (2004). "Decline in transcriptional activity of Nrf2 causes age-related loss of glutathione synthesis, which is reversible with lipoic acid." Proc Natl Acad Sci U S A **101**(10): 3381-6.
Sung, Y. J., C. L. Cheng, et al. (2003). "Distinct mechanisms account for beta-amyloid toxicity in PC12 and differentiated PC12 neuronal cells." J Biomed Sci **10**(4): 379-88.
Tauskela, J. S., K. Hewitt, et al. (2000). "Evaluation of glutathione-sensitive fluorescent dyes in cortical culture." Glia **30**(4): 329-41.
Tietze, F. (1969). "Enzymic method for quantitative determination of nanogram amounts of total and oxidized glutathione: applications to mammalian blood and other tissues." Anal Biochem **27**(3): 502-22.
Tran, H. P., A. S. Prakash, et al. (2002). "Arsenic inhibits the repair of DNA damage induced by benzo(a)pyrene." Toxicol Lett **133**(1): 59-67.
Tsurudome, Y., T. Hirano, et al. (1999). "Changes in levels of 8-hydroxyguanine in DNA, its repair and OGG1 mRNA in rat lungs after intratracheal administration of diesel exhaust particles." Carcinogenesis **20**(8): 1573-6.

Upadhyay, S., A. Chatterjee, et al. (2007). "TAp63gamma regulates hOGG1 and repair of oxidative damage in cancer cell lines." Biochem Biophys Res Commun.
Venugopal, R. and A. K. Jaiswal (1996). "Nrf1 and Nrf2 positively and c-Fos and Fra1 negatively regulate the human antioxidant response element-mediated expression of NAD(P)H:quinone oxidoreductase1 gene." Proc Natl Acad Sci U S A **93**(25): 14960-5.
Venugopal, R. and A. K. Jaiswal (1998). "Nrf2 and Nrf1 in association with Jun proteins regulate antioxidant response element-mediated expression and coordinated induction of genes encoding detoxifying enzymes." Oncogene **17**(24): 3145-56.
Wallace, S. S. (1998). "Enzymatic processing of radiation-induced free radical damage in DNA." Radiat Res **150**(5 Suppl): S60-79.
Wanibuchi, H., E. I. Salim, et al. (2004). "Understanding arsenic carcinogenicity by the use of animal models." Toxicol Appl Pharmacol **198**(3): 366-76.
Warner, B. B., L. Stuart, et al. (1996). "Redox regulation of manganese superoxide dismutase." Am J Physiol **271**(1 Pt 1): L150-8.
Welch, K. D., T. Z. Davis, et al. (2002). "Deleterious iron-mediated oxidation of biomolecules." Free Radic Biol Med **32**(7): 577-83.
Wilson, D. M., 3rd and L. H. Thompson (1997). "Life without DNA repair." Proc Natl Acad Sci U S A **94**(24): 12754-7.
Xu, Y., A. Krishnan, et al. (1999). "Mutations in the promoter reveal a cause for the reduced expression of the human manganese superoxide dismutase gene in cancer cells." Oncogene **18**(1): 93-102.
Yamanaka, K., F. Takabayashi, et al. (2001). "Oral exposure of dimethylarsinic acid, a main metabolite of inorganic arsenics, in mice leads to an increase in 8-Oxo-2'-deoxyguanosine level, specifically in the target organs for arsenic carcinogenesis." Biochem Biophys Res Commun **287**(1): 66-70.
Youn, C. K., S. H. Kim, et al. (2005). "Cadmium down-regulates human OGG1 through suppression of Sp1 activity." J Biol Chem **280**(26): 25185-95.
Yu, D., J. A. Berlin, et al. (2002). "Reactive oxygen species generated by PAH o-quinones cause change-in-function mutations in p53." Chem Res Toxicol **15**(6): 832-42.
Yu, R., C. Chen, et al. (2000). "Activation of mitogen-activated protein kinase pathways induces antioxidant response element-mediated gene expression via a Nrf2-dependent mechanism." J Biol Chem **275**(51): 39907-13.
Yu, R., W. Lei, et al. (1999). "Role of a mitogen-activated protein kinase pathway in the induction of phase II detoxifying enzymes by chemicals." J Biol Chem **274**(39): 27545-52.
Zharkov, D. O. and T. A. Rosenquist (2002). "Inactivation of mammalian 8-oxoguanine-DNA glycosylase by cadmium(II): implications for cadmium genotoxicity." DNA Repair (Amst) **1**(8): 661-70.
Zuliani, T., V. Denis, et al. (2005). "Hydrogen peroxide-induced cell death in normal human keratinocytes is differentiation dependent." Free Radic Biol Med **38**(3): 307-16.

APPENDICES

APPENDIX A

Molecular Biology Appendix

SECTION I: Oligonucleotide Sequences for RT-PCR Primers and Probes

I.i Rat Ogg1 RT-PCR Primer and Probe Set

Transcript Target GENBank #	Oligonucleotide Sequence 5′ – 3′ Forward Primer; Fluorescent Probe; Reverse Primer
Rat Ogg1 NM_030870	GGC CTC TAT TCC GTG TCC AC FAM/TCT GAG CTG CGT CTG GAC CTG GTT T/TAMTph CGG AAG GAC TGT CCA GAA GC
Rat HPRT XM_343829	GCT CGA GAT GTC ATG AAG GAG A HEX/CAT CAC ATT GTG GCC CTC TGT GTG CT/BHQ2 AGG TCA GCA AAG AAC TTA TAG CCC

I.ii Mouse Ogg1 RT-PCR Primer and Probe Set

Transcript Target GENBank #	Oligonucleotide Sequence 5′ – 3′ Forward Primer; Fluorescent Probe; Reverse Primer
Mouse Ogg1 U96711	GCC CAA GCA GTG CTG TTC A FAM/TGC TGA CCT TCG CCA ACC AAG CC/TAMTph GCT GGT GGC TCC CGA AA
Mouse HPRT BC004686	GCT CGA GAT GTC ATG AAG GAG A HEX/CAT CAC ATT GTG GCC CTC TGT GTG CT/BHQ2 AGG TCA GCA AAG AAC TTA TAG CCC

SECTION II: Oligonucleotide Sequences for EMSA Probe Sets

II.i Consensus Nrf2 and hOgg1 Nrf2 EMSA Probes

Transcription Factor Binding Site	Oligonucleotide Sequence 5′ – 3′ Sense; Anti-sense
Consensus Nrf2	GAA ATG ACA TTG CTA ATG GTG ACA AAG CAA C GTT GCT TTG TCA CCA TTA GCA ATG TCA TTT C
hOgg1-Nrf2	TGA GCC CTA CTT CCG GTG GTG CTG CAG CAC CAC CGG AAG TAG GGC TCA

II.ii Sp1 EMSA Probes

Transcription Factor Binding Site	Oligonucleotide Sequence 5′ – 3′ Sense; Anti-sense
Sp1 Oligo Set 1	GCA AGG AGG GGG CGG GAC CTA CAC GTG TAG GTC CCG CCC CCT CCT TGC
Sp1 Oligo Set 2	TCC TTG TCT GGG CGG GGT CTT TGG CCA AAG ACC CCG CCC AGA CAA GGA

SECTION III: Oligonucleotide Sequences of PCR Primers Used for Reporter Gene Expression Vector Construction

III.i Human Ogg1 Promoter PCR Primer Oligonucleotides

PCR Product (Size)	Oligonucleotide Sequence 5′ – 3′ Forward, Reverse	5′ Restriction Site
hOgg1 Promoter (2.1 Kb)	GGT ACC TTT ACT GCT GTG CAT GCT ACA TT GGA TCC TTT AGA ACC AGG CCT CGT CGA C	Asp718 BamHI

SECTION IV: Oligonucleotide Sequences of PCR Primers Used for Site Directed Deletion of Nrf2

IV.i Primer Sequences of Oligonucleotides Used in Site Directed Deletion of the Putative Nrf2 Binding Site in the Human Ogg1 Promoter

Deletion Target	Oligonucleotide Sequence 5′ – 3′ Forward, Reverse
Putative Nrf2 Site	GGT TGA GCC CTA CGG TGG TGC TGT CCA CAG CAC CAC CGT AGG GCT CAA CC

SECTION V. Vector Maps of Reporter Gene and Mammalian Expression Vectors

Figure I. Vector Map of pAM/CAG-*hr*GFP-WPRE-BGH-polyA

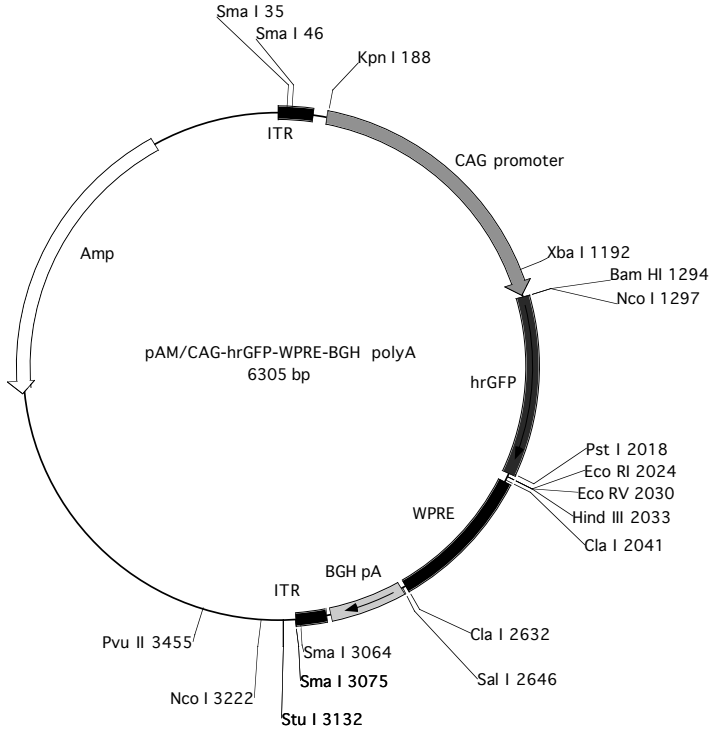

Figure II. Vector Map of pAM/hOgg1-*hr*GFP-WPRE-BGH-polyA

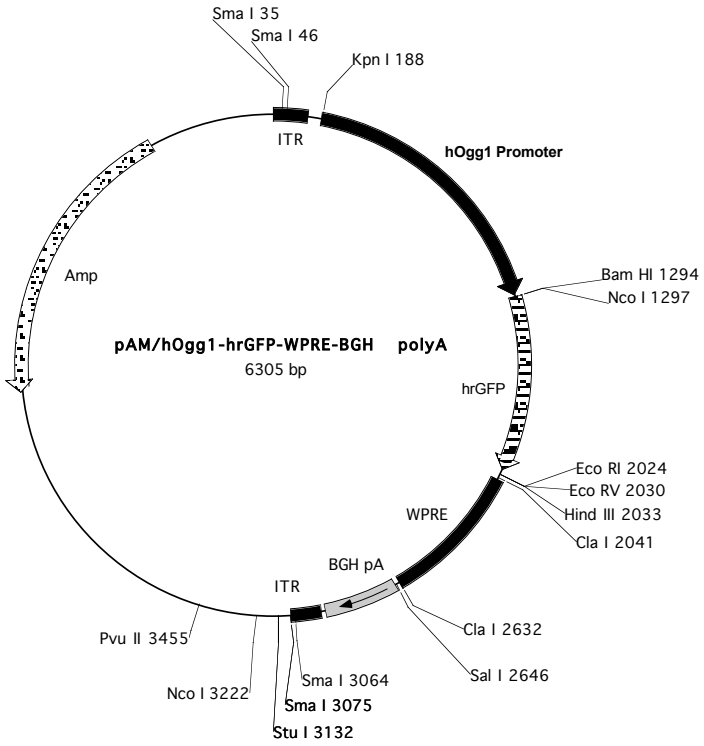

Figure III. Vector Map of pGL3/hOgg1-Luc+

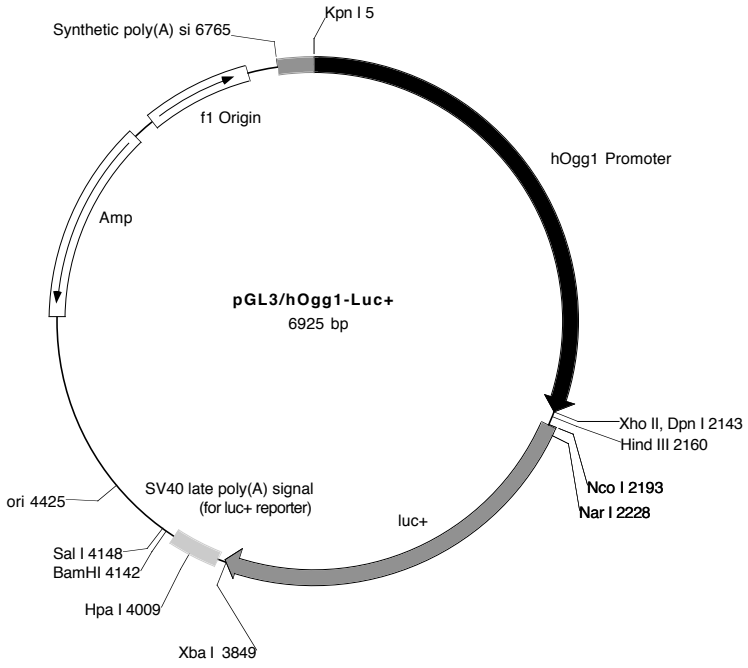

Figure IV. Vector Map of pEF(Blue)-Basic

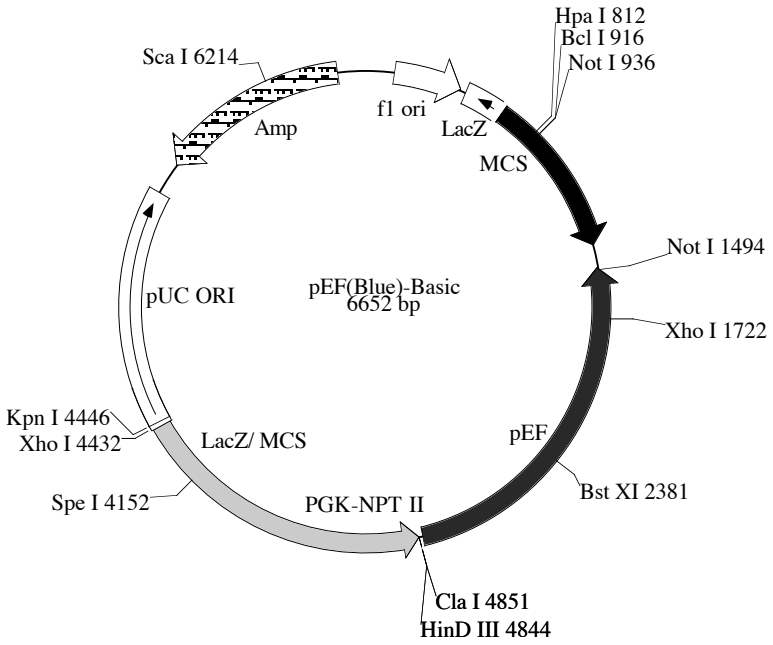

Figure V. Vector Map of pEF(Blue)-Nrf2

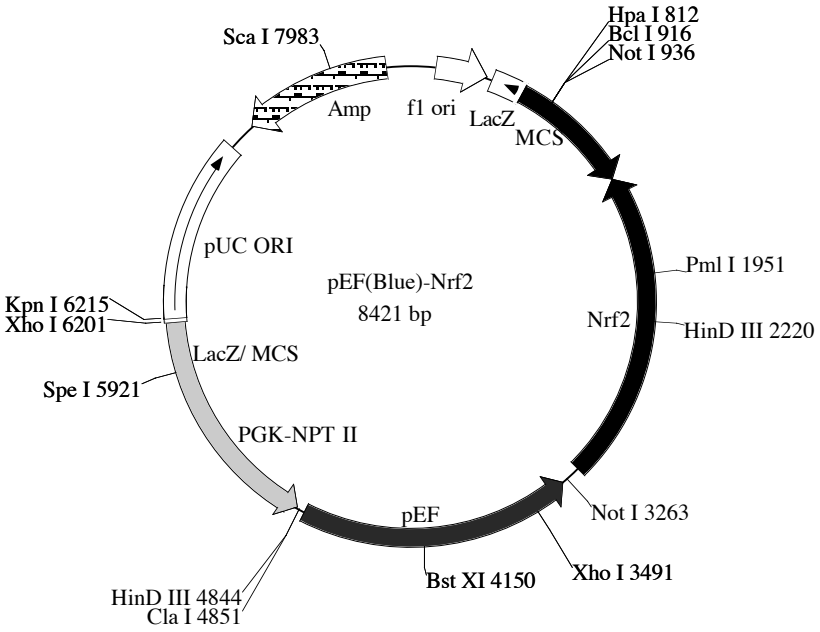

Appendix B

High Throughput Method for Assessment of Cellular Reduced Glutathione in Mammalian Cells

Abstract

Reduced glutathione (GSH) is an intracellular molecule essential for many aspects of cell physiology and defense. Determination of GSH has been used to identify potential anti-cancer drugs and for the assessment of drug toxicity via generation of oxidative stress. The described protocol was designed to modify existing protocols for the fluorescent detection of intracellular GSH in a high throughput 96-well microplate format. Dibromobimane was used to label intracellular GSH, and an additional dye, Hoechst 33342 was used to measure cell density for data normalization. Cell density curves were performed using HEK 293T cells to determine the optimal starting cell density, ($< 8.0 \times 10^4$ cells/well) for fluorescent analysis. Fluorescent dyes were also analyzed for compatibility and spectral overlap. The method was further validated by exposing HEK 293T cells to GSH modulating agents; tert-butylhydroquinone a potent inducer of GSH, and L-buthionine-(SR)-sulfoximine a potent inhibitor of GSH. This study provides a fast, simple method for the high throughput screening of GSH in a widely available 96-well format. It also addresses the pitfalls associated with fluorescent compounds in cell culture and proper data normalization.

Introduction

Glutathione (GSH) is a low molecular weight molecule considered to be the first line of cellular defense in mammalian cells (Ketterer 1988). Composed of three amino acids, cysteine is the moiety capable of reacting with oxygen radicals and other electrophilic compounds. In addition to its antioxidant activities GSH also participates in other processes including xenobiotic metabolism, gene regulation, intracellular signal transduction, and homeostasis of the cellular redox state (Dalton, Shertzer et al. 1999; Sies 1999). GSH is the most abundant intracellular non-protein thiol followed by cysteine; a substrate in the GSH synthetic pathway. Ultimately, changes in GSH can indicate a global antioxidant, or redox status in cells and has led researchers to monitor its levels; particularly in the context of induction of antioxidant systems, or assessment of oxidative stress.

Traditional methods for measuring GSH have involved biochemical assays dependent on the reaction of compounds with GSH such as 5,5′-dithio-*bis*-2-nitrobenzoic acid (Tietze 1969), or o-phthalaldehyde (Senft, Dalton et al. 2000) that readily form chromophoric or fluorescent compounds respectively, measurable by ultra-violet/visible or fluorescent spectroscopy. This method is considered reliable and highly quantitative, however, the preparation of tissue or cellular samples requires an investment of time and effort before measurement of GSH can be accomplished.

High performance liquid chromatography (HPLC) is an additional method for measuring GSH and is considered the most specific. HPLC utilizes a variety of systems including electrochemical detection (Remiao, Carmo et al. 2000) or a lengthier process using fluorescent detection requiring derivatization prior to analysis (Martin and White

1991). Despite the quantitative aspect of HPLC, there is a large reliance on sample preparation to account for, and in some cases depending on sample size and run times, analysis can take 12 to 24 h to complete. In addition, analysis by HPLC will require increased costs for the startup, and for running and maintaining the instrument.

An alternatively accepted method for GSH measurement is to label intracellular thiols with fluorescent bimane compounds and analyze cells via fluorescent activated cell sorting (FACS) (Hedley and Chow 1994; Horan, Chan et al. 1997). FACS analysis of GSH does not demand as much time and can be simpler than biochemical methods; however, there are limitations. Sample preparation can require fewer steps than the aforementioned assays yet ultimately the preparation requires the extraction and resuspension of cells before analysis can occur. Similar to HPLC, the availability of FACS instrumentation can also be problematic due to the initial costs and maintenance required for operation of the instrument. The sensitivity of FACS is another limitation to consider if the instrument is not equipped with the proper excitation or emission filters. Accurate measurement at optimal wavelengths is essential for FACS especially if you are using compounds with similar emission spectra.

Micro-plate readers are another technique for measuring fluorescent signals and can offer high throughput sample analysis by using a 96 or 384-well format. A large advantage of high throughput assays is the screening of several compounds, or conditions in the same plate can be performed, thereby decreasing the variable conditions that can occur between separate cell culture dishes. Fluorescent bimane dyes have also been previously characterized for use in the microplate format however an inherent problem with cell culture in the micro-plate format is that loss of cells can occur as a consequence

of physical stressors such as media addition or removal. Thus, accuracy of the signal obtained could be skewed as a result of cell loss. The presence of an additional dye can be used in order to normalize each well to the cellular density actually contained therein, and allow a more accurate assessment of your target endpoint.

This work describes a modification to previously published protocols for measuring GSH. It is a method designed for a high throughput assay to measure cellular GSH levels using 96-well microplates and a bimane compound, dibromobimane that is fluorescently activated upon conjugation with thiol groups. The method is performed in combination with a viable nuclear stain, Hoechst 33342. Hoechst 33342 staining allows GSH levels to be normalized to the cell density contained in the well, and therefore report a more accurate value. Along with the high throughput capacity of this assay there is the benefit of a short time interval between addition of target and reference compounds, and subsequent fluorescent measurement. By reducing time intervals there is a decreased chance of non-specific labeling to occur, thereby decreasing the potential for increased signal artifacts.

Materials & Methods

Cell Culture

HEK 293T cells purchased from American Type Culture Collection were grown in flat bottomed, tissue culture treated 96-well microplates (Costar, Corning Inc., Corning, NY, USA) at 37° C, 5% CO_2 under the following media conditions; 1X Dulbecco's Modification of Eagle's Medium with 4.5 g/L glucose and L-glutamine, 10% fetal bovine serum, 1 mM sodium pyruvate, 1X non-essential amino acids, 1000 international units penicillin – 1 mg/mL streptomycin, 50 μg/mL gentamicin sulfate; all media reagents were purchased from CellGro® technologies (Mediatec Inc., Herndon, VA, USA). HEK 293T cells were plated at starting densities between $5.0 \times 10^4 - 2.0 \times 10^5$ per well, (n = 6 wells per cell density) in a final volume of 200 μL media and grown for a period of 16 hr.

Nuclear & Glutathione Fluorescent Labeling

Media containing 1.5 μg/mL Hoechst 33342 (Molecular Probes, Carlsbad, CA, USA) was gently added at a volume of 100 μL to each well yielding a final concentration of 0.5 μg/mL Hoechst 33342/well and incubated for 30 min at 37° C. Plates were then drained of media by inversion and gentle shaking; any residual media at this point was removed by blotting the plate on bench paper. A stock solution of 4 mM dibromobimane (CAS # 68654-25-1; Sigma-Aldrich, St. Louis, MO, USA) suspended in 100% sterile-filtered dimethyl sulphoxide (Sigma-Aldrich, St. Louis, MO, USA) was made immediately prior to Hoechst 33342 media removal and diluted to a final concentration of 40 μM in sterile phosphate buffered saline, pre-warmed to 37° C. The dibromobimane was gently added to a final volume of 200 μL/well and incubated at 37° C for 30 min. (Horan, Chan et al. 1997; Sebastia, Cristofol et al. 2003).

Fluorescent Measurement

Fluorescence was measured using a SPECTRAmax© Gemini XS fluorescent plate reader (Molecular Devices, Sunnyvale, CA, USA) at the following wavelengths: [Hoechst 33342 Ex_{λ} = 340, Em_{λ} = 450], [dibromobimane Ex_{λ} = 393, Em_{λ} = 477]. Fluorescent values were quantified using SOFTmax® PRO version 3.1.2 software (Molecular Devices, Sunnyvale, CA, USA).

Raw fluorescent results reported as fluorescent arbitrary units (F.A.U.) were obtained by first subtracting the mean blank value from all wells [$F.A.U._{.experimental} - F.A.U._{.blank}$]. Final results for GSH levels were reported as the ratio of dibromobimane normalized to Hoechst 33342 [dibromobimane F.A.U./ Hoechst 33342 F.A.U.]. For the validation studies cells were grown as described above and exposed to GSH modulating compounds. Following a 24 hr exposure of either 25μM tert-butylhydroquinone (tBHQ) or 100 μM L-buthionine-(SR)-sulfoximine (BSO), cells were stained and measured for GSH content as described above.

Statistical Analysis

Statistical analysis involved the use of one-way ANOVA with student Newman-Keuls post-test for GSH modulating agents; Dunnet's post-test was used for assessment of signal overlap between dibromobimane and Hoechst 33342.

Results and Discussion

Cultures of HEK 293T cells were set up in 96-well microplates in a range between $5.0 \times 10^3 - 2.0 \times 10^5$ cells/well. The objective was to determine the response of Hoechst 33342 over a range of starting cell densities. As seen in Figure 1A and Table 1,

the Hoechst 33342 signal showed a linear response up to 8.0 x 10^4 cells/well. Cultures started at densities above that value had both an increase in their standard error of the mean (SEM, Figure 1A), and a decrease in the r^2 value of the linear response (Table 1). Increasing the starting density from 8.0 x 10^4 to 1.0 x 10^5 cells/well results in an attenuation of r^2 value from 0.9948 down to 0.7880, a trend that continued to yield a lower r^2 with increased starting cell density.

Table 1. Linear Regression Summaries of Cell Density and Hoechst 33342 Response in HEK 293T cells

Hoechst 33342 Response to Cell Density
Ex 340nm; Em 450nm

Cell Density Range	Slope	r2
5 to 20,000	1.37E-02	0.9986
5 to 40,000	1.07E-02	0.9846
5 to 60,000	1.05E-02	0.9943
5 to 80,000	1.00E-02	0.9948
5 to 100,000	6.87E-03	0.7880
5 to 125,000	5.26E-03	0.7127
5 to 150,000	3.85E-03	0.5904
5 to 200,000	4.08E-03	0.7366

n = 6 wells per density

This experiment sets up some important parameters for both cell type and assay conditions; (a) optimizing the starting cell density for the experiment (b) determining the response of the experimental and reference stains and, (c) determining if any signal overlap exists between the experimental and reference stains.

As shown in Figure 1A and Table 1 the Hoechst 33342 dye is only effective up to a starting cell density of 8.0×10^4 cells/well for HEK 293T cells as indicated by the loss of linearity with higher starting cell densities. Cultures were then analyzed using the excitation wavelength for dibromobimane (393nm) and the emission wavelength for Hoechst 33342 (450nm). Hoechst 33342 showed no signal when exposed to the dibromobimane excitation wavelength (393nm) thereby ensuring no signal overlap was occurring between the two stains at that particular excitation wavelength (Figure 1A). A similar scan was performed on the dibromobimane by using the excitation wavelength for Hoechst 33342 (340nm) and scanning at the emission wavelength for dibromobimane (477nm) to determine if the dibromobimane is creating a signal overlap while measuring the Hoechst 33342 dye (Figure 1B). As seen in figure 1B there is some response of dibromobimane at the Hoechst 33342 excitation wavelength (340nm). When analyzed in comparison to the mean value for the blank wells, the dibromobimane signal excited at the Hoechst 33342 wavelength (340nm) does not differ statistically until the cell density is higher than 8.0×10^4 cells/well as determined by one-way ANOVA using a Dunnet's post-hoc test. This finding further supports the idea that the maximum starting cell density should be no greater than 8.0×10^4 cells/well for this particular cell type based on (i) the loss of linearity of the Hoechst 33342 signal (Figure 1A, Ex. λ = 340 nm plot) and (ii) the increase in signal overlap between dyes at the higher cell densities (Figure 1B, Ex.

λ = 340 nm plot).

FIGURE 1

A.

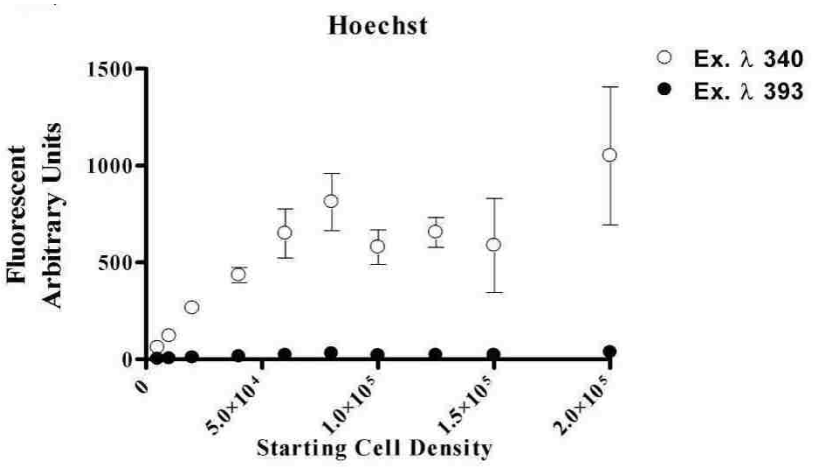
Hoechst
Ex. λ 340
Ex. λ 393
Fluorescent Arbitrary Units
1500
1000
500
0
0
5.0×10⁴
1.0×10⁵
1.5×10⁵
2.0×10⁵
Starting Cell Density

B.

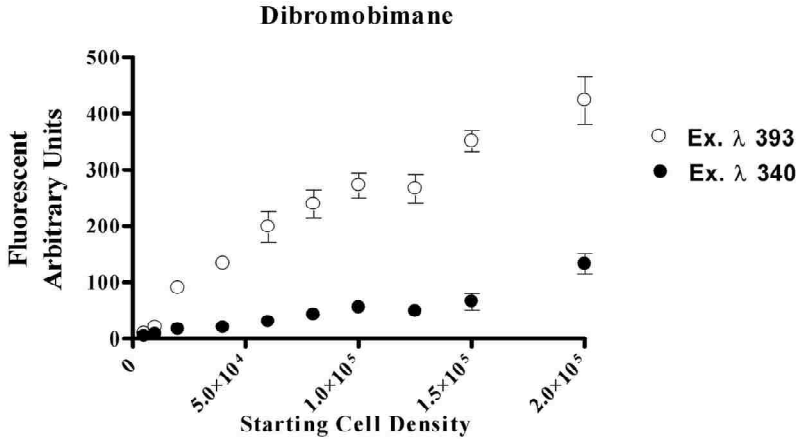
Dibromobimane
Ex. λ 393
Ex. λ 340
Fluorescent Arbitrary Units
500
400
300
200
100
0
0
5.0×10⁴
1.0×10⁵
1.5×10⁵
2.0×10⁵
Starting Cell Density

Figure 1

Measurement of fluorescent signal for Hoechst 33342 and dibromobimane in HEK 293T cells as a function of increased starting cell density. (A) Hoechst 33342 signal at [λ_{ex}340 nm, λ_{em}450 nm; open circles O], and at [λ_{ex} 393 nm, λ_{em}450 nm; closed circles ●] in HEK 293T cells (B) Dibromobimane signal at [λ_{ex} 393 nm, λ_{em} 477 nm; open circles O], and at [λ_{ex}340 nm, λ_{em} 477 nm; closed circles ●] in HEK 293T cells. Values are reported as fluorescent arbitrary units (F.A.U.) and are reported as mean ± SEM.

Contrary to the Hoechst 33342 in Figure 1A, dibromobimane is linear up to the maximum starting cell density of 2.0 x 10^5 cells/well (Figure 1B). This reinforces the importance of normalizing your data as demonstrated by the linear response of the dibromobimane. By measuring dibromobimane alone, it is possible that the results could yield inaccurate values if the cell density in the well does not remain constant throughout the experiment. Previous publications demonstrate the use of GSH probes in a 96-well format, however it is unclear what type of normalization if any was performed (Sebastia, Cristofol et al. 2003). During these types of assays the opportunity exists for loss of cell density due to cell death, or physical agitation during media addition or removal. Figure 1C shows the dibromobimane signal normalized by the Hoechst 33342 signal over increased starting cell densities (values calculated as F.A.U. dibromobimane/ F.A.U. Hoechst 33342). The range of starting cell densities between 6.0 x 10^4 cells/well and 1.5 x 10^5 cells/well yields a balanced measurement of GSH levels. However, taking into account the Hoechst 33342 plot in Figure 1A, and the change in the r^2 values indicated in Table 1, starting cell densities greater than 8.0 x 10^4 cells/well could be problematic.

FIGURE 1

C.

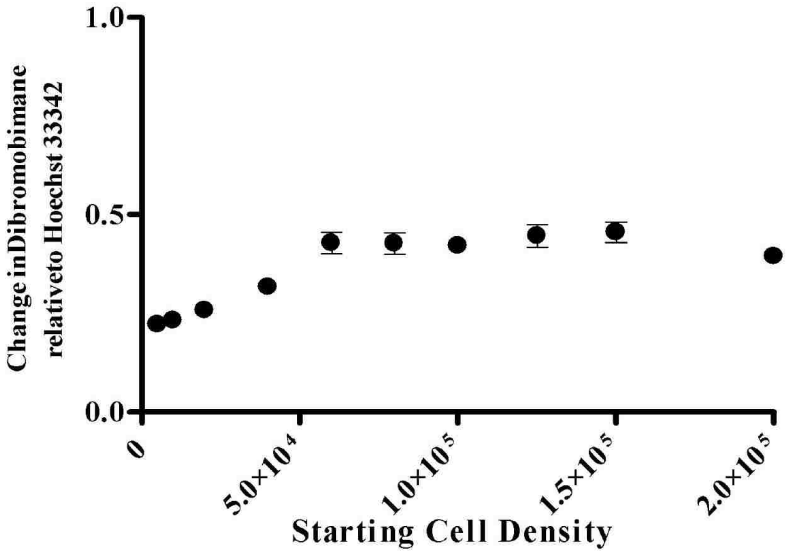
1.0
0.5
0.0
Change in Dibromobimane relativeto Hoechst 33342
0
5.0×10^4
1.0×10^5
1.5×10^5
2.0×10^5
Starting Cell Density

Figure 1C

Measurement of fluorescent signal for Hoechst 33342 and dibromobimane in HEK 293T cells as a function of increased starting cell density. (C) Changes in dibromobimane fluorescence normalized to the Hoechst 33342 as a function of increasing cell density in HEK 293T cells; dibromobimane F.A.U. were normalized by the Hoechst 33342 F.A.U. of the same well. Values were calculated by the following formula; [dibromobimane F.A.U./ Hoechst 33342 F.A.U.] and reported as mean ± SEM.

To further scrutinize this assay, cell cultures were set up at a starting density of 7.0×10^4 cells/well. Sixteen hr later, cells were exposed to compounds shown to modulate cellular GSH levels; 25 μM tBHQ an inducer of GSH synthesis (Hansen, Watson et al. 2004), and 100 μM BSO an inhibitor of GSH synthesis (Griffith 1982). Figure 2 demonstrates the importance of normalizing the dibromobimane fluorescent signal rather than assuming equal cell density.

Figure 2A shows the changes in dibromobimane signal in control, and cells exposed to BSO for 24 hr. The data is displayed prior to Hoechst 33342 normalization and carries the assumption of equal starting cell density (Figure 2A). Although the results of this experiment display the expected outcome, (reduced GSH), the degree of reduction is less than levels reported using biochemical or HPLC methods (Griffith 1982; Horan, Chan et al. 1997). Normalization of the dibromobimane signal with the Hoechst 33342 signal yields values more in accord with the published effects of BSO (Figure 2C). Treatment of cells with tBHQ has been reported to lead to an increase in levels of GSH however, Figure 2B shows a reduction in GSH levels in the cells exposed to 25 μM tBHQ for 24 hr. Once normalized to the Hoechst 33342 dye, the data shows an increase in GSH levels (Figure 2C); changes that are comparable with previous publications using tBHQ (Eftekharpour, Holmgren et al. 2000; Hansen, Watson et al. 2004).

FIGURE 2

A.

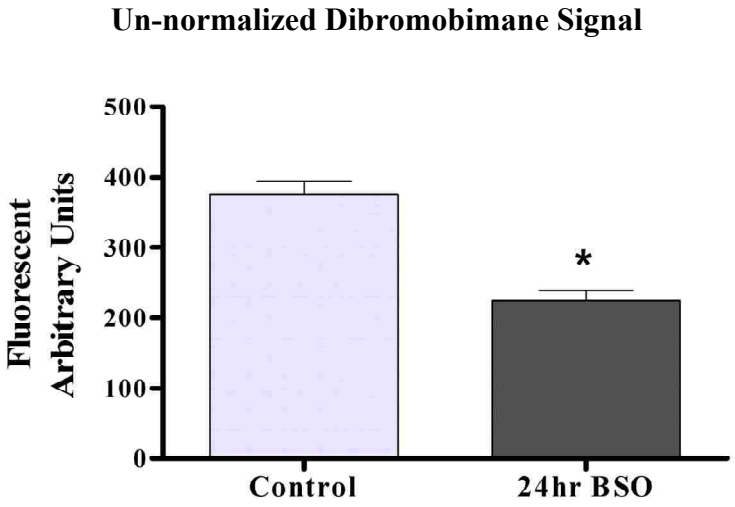
Un-normalized Dibromobimane Signal
Fluorescent Arbitrary Units
500
400
300
200
100
0
*
Control
24hr BSO

B.

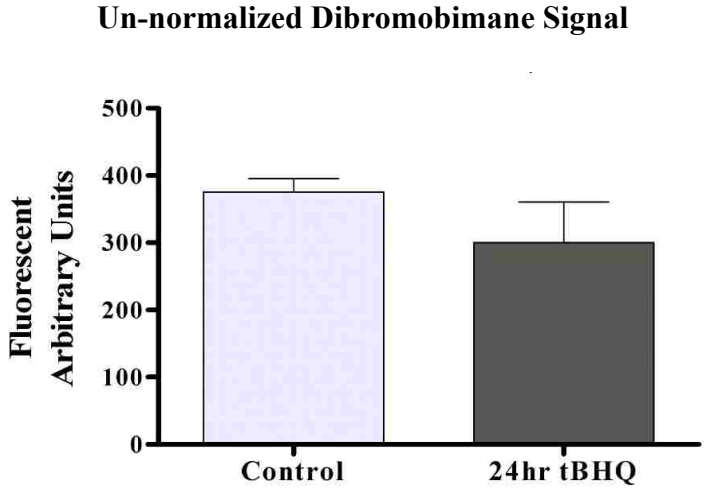
Un-normalized Dibromobimane Signal
Fluorescent Arbitrary Units
500
400
300
200
100
0
Control
24hr tBHQ

FIGURE 2

Changes in GSH status of HEK 293T cells exposed to GSH modulating agents. A) HEK 293T cells exposed to 100 μM BSO or B) 25 μM tBHQ for 24 hr. All values are reported as mean ± SEM. * Indicates a significant fluorescent difference from untreated control at $p < 0.05$.

FIGURE 2

C.

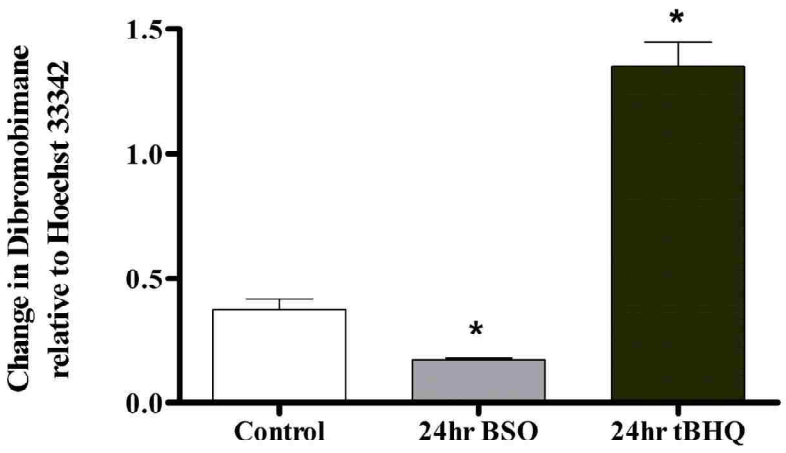
Change in Dibromobimane relative to Hoechst 33342
1.5
1.0
0.5
0.0
*
*
Control
24hr BSO
24hr tBHQ

Figure 2. Changes in GSH status of HEK 293T cells exposed to GSH modulating agents. (C) Normalized values of dibromobimane from Figure 2A and 2B, indicative of the GSH levels in the cells. All values are reported as mean ± SEM. * Indicates a significant fluorescent difference from control at $p < 0.05$.

Conclusions

This method demonstrates a high throughput assay for determining changes in cellular GSH in a semi-quantitative manner. It combines the use of well-characterized fluorescent dyes, ultimately allowing the measurement of target endpoint (GSH) and cell density in the same well of a standard microplate. This technique can be useful in screening compounds capable of modulating GSH; a strategy often used in the identification of potential chemotherapeutic compounds. It can also be used in the assessment of cytotoxicity for multiple compounds in one plate, as decreased GSH is often associated with conditions of oxidative stress and can therefore serve as a reliable marker of compromised cell status.

The assay can be utilized with immortalized cell lines and more importantly, primary cell cultures (Tauskela, Hewitt et al. 2000) where oftentimes there is a limitation on the starting tissue and or cell number. The high throughput format allows for the screening of multiple fluorescent compounds, however proper dye selection is an important parameter to consider due to signal overlap being a potential confounder for this type of assay. This assay also addresses the pitfalls that can occur in 96-well microplate assays if the normalization to cell density is not performed.

REFERENCES

Dalton, T. P., H. G. Shertzer, et al. (1999). "Regulation of gene expression by reactive oxygen." Annu Rev Pharmacol Toxicol **39**: 67-101.

Eftekharpour, E., A. Holmgren, et al. (2000). "Thioredoxin reductase and glutathione synthesis is upregulated by t-butylhydroquinone in cortical astrocytes but not in cortical neurons." Glia **31**(3): 241-8.

Griffith, O. W. (1982). "Mechanism of action, metabolism, and toxicity of buthionine sulfoximine and its higher homologs, potent inhibitors of glutathione synthesis." J Biol Chem **257**(22): 13704-12.

Hansen, J. M., W. H. Watson, et al. (2004). "Compartmentation of Nrf-2 redox control: regulation of cytoplasmic activation by glutathione and DNA binding by thioredoxin-1." Toxicol Sci **82**(1): 308-17.

Hedley, D. W. and S. Chow (1994). "Evaluation of methods for measuring cellular glutathione content using flow cytometry." Cytometry **15**(4): 349-58.

Horan, A. D., C. Y. Chan, et al. (1997). "Analysis of tumor thiol concentrations: comparison of flow cytometric with chemical and biochemical techniques." Cytometry **29**(1): 76-82.

Ketterer, B. (1988). "Protective role of glutathione and glutathione transferases in mutagenesis and carcinogenesis." Mutat Res **202**(2): 343-61.

Martin, J. and I. N. White (1991). "Fluorimetric determination of oxidised and reduced glutathione in cells and tissues by high-performance liquid chromatography following derivatization with dansyl chloride." J Chromatogr **568**(1): 219-25.

Remiao, F., H. Carmo, et al. (2000). "Simultaneous determination of reduced and oxidized glutathione in freshly isolated rat hepatocytes and cardiomyocytes by HPLC with electrochemical detection." Biomed Chromatogr **14**(7): 468-73.

Sebastia, J., R. Cristofol, et al. (2003). "Evaluation of fluorescent dyes for measuring intracellular glutathione content in primary cultures of human neurons and neuroblastoma SH-SY5Y." Cytometry A **51**(1): 16-25.

Senft, A. P., T. P. Dalton, et al. (2000). "Determining glutathione and glutathione disulfide
using the fluorescence probe o-phthalaldehyde." Anal Biochem **280**(1): 80-6.

Sies, H. (1999). "Glutathione and its role in cellular functions." Free Radic Biol Med **27**(9-10): 916-21.

Tauskela, J. S., K. Hewitt, et al. (2000). "Evaluation of glutathione-sensitive fluorescent dyes in cortical culture." Glia **30**(4): 329-41.

Tietze, F. (1969). "Enzymic method for quantitative determination of nanogram amounts of total and oxidized glutathione: applications to mammalian blood and other tissues." Anal Biochem **27**(3): 502-22.